DOKLADY PHYSICAL CHEMISTRY
VOLUME 112 NUMBERS 1 - 6
JANUARY - FEBRUARY 1957

PROCEEDINGS OF THE ACADEMY OF SCIENCES OF THE USSR

(Doklady Akademy Nauk SSSR)

Section: PHYSICAL CHEMISTRY

Volume 112, Issues 1-6

January-February, 1957

Editorial Board:

Acad. L. A. Artsimovich, Acad. A. G. Betekhtin, Acad. S. A. Vekshinsky,
Acad. A. N. Kolmogorov (Asst. to Editor in Chief), Acad. A. L. Kursanov,
Acad. S. A. Lebedev, Acad. I. N. Nazarov, Acad. A. I. Nekrasov,
Acad. A. I. Oparin (Editor in Chief), Acad. E. N. Pavlovsky, Acad. L. I. Sedov,
Acad. N. M. Strakhov, Acad. A. N. Frumkin (Asst. to Editor in Chief)

(A Publication of the Academy of Sciences of the USSR)

IN ENGLISH TRANSLATION

Copyright, 1958

CONSULTANTS BUREAU, INC.
227 West 17th Street
New York 11, N. Y.

Printed in the United States

Annual Subscription	$160.00
Single Issue	35.00

Note: The sale of photostatic copies of any portion of this copyright translation is expressly prohibited by the copyright owners. A complete copy of any article in this issue may be purchased from the publisher for $5.00.

SIGNIFICANCE OF ABBREVIATIONS MOST FREQUENTLY ENCOUNTERED IN SOVIET PHYSICS PERIODICALS

AN SSSR	*Academy of Sciences, USSR*
FIAN	*Physics Institute, Academy of Sciences USSR*
GITI	*State Scientific and Technical Press*
GITTL	*State Press for Technical and Theoretical Literature*
GOI	*State Optical Institute*
GONTI	*State United Scientific and Technical Press*
Gosenergoizdat	*State Power Press*
Gosfizkhimizdat	*State Physical Chemistry Press*
Gozkhimizdat	*State Chemistry Press*
GOST	*All-Union State Standard*
Goztekhizdat	*State Technical Press*
GTTI	*State Technical and Theoretical Press*
GUPIAE	*State Office for Utilization of Atomic Energy*
IF KhI	*Institute of Physical Chemistry Research*
IFP	*Institute of Physical Problems*
IL	*Foreign Literature Press*
IPF	*Institute of Applied Physics*
IPM	*Institute of Applied Mathematics*
IREA	*Institute of Chemical Reagents*
ISN (Izd. Sov. Nauk)	*Soviet Science Press*
I YaP	*Institute of Nuclear Studies*
Izd	*Press (publishing house)*
KISO	*Solar Research Commission*
LETI	*Leningrad Electrotechnical Institute*
LFTI	*Leningrad Institute of Physics and Technology*
LIM	*Leningrad Institute of Metals*
LITMiO	*Leningrad Institute of Precision Instruments and Optics*
Mashgiz	*State Scientific-Technical Press for Machine Construction Literature*
MATI	*Moscow Aviation Technology Institute*
MGU	*Moscow State University*
Metallurgizdat	*Metallurgy Press*
MOPI	*Moscow Regional Institute of Physics*
NIAFIZ	*Scientific Research Association for Physics*
NIFI	*Scientific Research Institute of Physics*
NIIMM	*Scientific Research Institute of Mathematics and Mechanics*
NII ZVUKSZAPIOI	*Scientific Research Institute of Sound Recording*
NIKFI	*Scientific Institute of Motion Picture Photography*
OIYaI	*Joint Institute of Nuclear Studies*
ONTI	*United Scientific and Technical Press*
OTI	*Division of Technical Information*
OTN	*Division of Technical Science*
RIAN	*Radium Institute, Academy of Sciences of the USSR*
SPB	*All-Union Special Planning Office*
Stroiizdat	*Construction Press*
URALFTI	*Ural Institute of Physics and Technology*

NOTE: Abbreviations not on this list and not explained in the translation have been transliterated, no further information about their significance being available to us.—*Publisher.*

THE LIMITS OF STABLE PROPAGATION OF FLAMES IN GASES UNDER CHANGING PRESSURES

D. I. Abugov

(Presented by Academician N. N. Semenov on July 9, 1956)

1. In investigating a combustion mechanism by the methods of heat theory, the role of heat transfer in exothermic reactions [1-3] is given substantial importance. But if there are rapid changes in the state of the gas with a large amount of specific work, the heat interaction (heat transfer) of the thermodynamic system with the surrounding medium is of secondary importance relative to mechanical interaction (exchange of mechanical work). This is the state of affairs in engines of the pulsating type including piston engines and, in general, under conditions of changing pressure and volume.

The mechanism of the cessation of flame propagation (cessation of combustion) is similar to the mechanism of ignition: of fundamental importance in both cases are the conditions of energy exchange between the reacting gas and the medium surrounding it,* which determine the transition from a stationary reaction state to an essentially nonstationary one (on ignition – from a stationary reaction accompanied by an insignificant evolution of heat, to a progressively downward reaction; on cessation of combustion – from a stationary fast reaction to a progressively downward reaction).

The problem of ignition under various forms of energy exchange with the surroundings has been studied before [4].

2. Let us set up the energy equation for the element of the flame zone where the reacting gases and the products of the reaction occur, assuming the following simplifications to hold: a) pressure p is constant throughout the chamber, b) the kinetic energy of the gases is small relative to their enthalpy and hence the changes in the kinetic energy are not considered, c) the gas is considered to be ideal and its physical parameters (specific heat, coefficient of heat conductivity, etc.) constant (average values within the interval considered), d) the combustion (chemical reaction) is considered as the heat source, e) the change in the number of moles due to chemical reactions and thermal dissociations at high temperatures, is not considered, f) the case is one-dimensional, i.e., the state of the gas (temperature T, density ρ, velocity, u) depends on the x-coordinate, the direction of which coincides with the direction of flame propagation, and on time τ.

The differential equation expressing the principle of conservation of energy (first law of thermodynamics) we will write in the following form (considering a unit volume in unit time):

$$c_v \rho \frac{dT}{d\tau} = \rho \frac{dQ}{d\tau} + \frac{dp}{d\tau}. \qquad (1)$$

Let us take a system of coordinates related to the flame zone. In this coordinate system the flame zone

* It is possible to treat analogously the conditions for detonational collapse i.e., transition from a slow flame propagation to a detonation.

is stationary and the initial gas moves along the direction of the x-coordinate with a velocity u_{fl}. According to the conditions of the problem $T = f(\tau, x)$ and hence $\frac{dT}{d\tau} = \frac{\partial T}{\partial \tau} + u_{fl} \frac{\partial T}{\partial x}$.

The expression for the quantity of heat for a unit volume and a unit time, including the heat evolved during the chemical reaction, the heat conducted away (in the direction of the flame propagation) and the heat lost to the wall, will be

$$\rho \frac{dQ}{d\tau} = H_{mix} w + \lambda \frac{\partial^2 T}{\partial x^2} - \Phi_{st}.$$

Here w is the velocity of the chemical reaction, H_{mix} the heat effect of the reaction, $\Phi_{st} = \frac{\pi}{F} \alpha (T - T_{st})$ is the heat given off to the wall where α is the transmission coefficient between the wall and the gas, π is the perimeter of the flame zone and F its cross section.

Substituting into equation (1) the appropriate expressions, dividing by $C_r \rho$ and transforming we will obtain the following:

$$\frac{\partial T}{\partial \tau} + u_{fl} \frac{\partial T}{\partial x} - a \frac{\partial^2 T}{\partial x^2} = \frac{H_{mix}}{c_r} \frac{w}{\rho} + A, \qquad (2)$$

where $A = \frac{k-1}{k} \frac{T}{p} \left[-\alpha \frac{\Pi}{F} (T - T_{st}) + \frac{dp}{d\tau} \right]$ is the term representing the energy interaction of the reacting gas with the surroundings, and $a = \frac{\lambda}{C_r \rho}$ is the coefficient of heat conductivity.

3. The propagation of a flame in a turbulent gaseous mixture is of interest in the application to engines. Let us make some assumptions concerning the structure of the flame zone and its propagation in the turbulent mixture.

According to contemporary representations [5] a small-scale turbulence influences the propagation of the flame by intensifying the processes of heat transfer (and transfer of matter) in the flame zone which leads to an increase in the propagation of the flame and corresponding increase in the width of the flame zone ($\delta \sim u_{fl}$). Hence equation (2) can be applied to the turbulent flame zone with complete confidence for the case of a small-scale turbulence.

To determine the conditions for the cessation of the propagation of the flame let us use approximate methods of solution. Let us consider the limiting case where the rate of the chemical reaction is strongly dependent on temperature (i.e., $E/RT >> 1$) and where we can consider [2] that the reaction is occurring at a temperature near to the maximum combustion temperature.

Let us denote the left-hand side of equation (2) by $D(T, x)$. If $A = 0$ (i.e., if $p = \text{const}$ and $\Phi_{st} = 0$) we will have from equation (2) $D_\theta = \frac{H_{mix}}{c_r} \frac{w}{\rho}$. Let us denote the maximum flame temperature for the case $A=0$ by $T_{fl\ theor}$, whereupon $\frac{H_{mix}}{c_r} = T_{fl\ theor} - T_0$. Let us introduce the characteristic reaction time $\tau_r = \rho / w$ (time taken for the complete combustion of all the reacting material present, at constant rate). In the case $A=0$, $\tau_r = \tau_{r\ theor}$, where $\tau_{r\ theor} \sim \exp(E/RT_{theor})$.

Now the previous equation can be written in the form $D_\theta = \frac{T_{fl\ theor} - T_0}{\tau_{r\ theor}}$, where D_θ is the average rate of temperature increase in the flame zone which would occur if the reaction proceeded at constant rate without any transfer of heat or matter, in the case $A=0$.

For flame propagation under variable pressure and with transfer of heat and matter $A \neq 0$. Depending on the actual conditions either $A < 0$ and $D < D_0$ is possible or $A > 0$ and $D > D_0$. Here $D = \frac{T_\Pi - T_0}{\tau_r}$, T_Π is the maximum flame temperature for the case $A \neq 0$ and τ_r is the characteristic reaction time corresponding to T_Π ($\tau_r \sim e^{E/RT_\Pi}$).

For the case $A \neq 0$ Equation (2) can be written in the form $\frac{T_\Pi - T_0}{\tau_r} = \frac{T_{\Pi\ theor} - T_0}{\tau_r} + A$, from which we will obtain

$$\Delta T_\Pi = A\tau_r. \qquad (3)$$

where $\Delta T_\Pi = T_\Pi - T_{\Pi\ theor}$. Breaking down the exponential [3] we find approximately $\tau_r = \tau_{r,\ theor} \exp(-\Delta T_\Pi E/RT^2_{\Pi\ theor})$. Using this expression and dividing both sides of Equation (3) by $RT^2_{\Pi\ theor}/E$, we obtain

$$\theta = \psi \exp(-\theta), \qquad (4)$$

where $\theta = \frac{\Delta T_\Pi E}{RT^2_{\Pi\ theor}}$; $\psi = \frac{AE}{RT^2_{\Pi\ theor}} \tau_{r,\ theor}$.

From Equation (4) we find (in considering Equation (4) we can neglect the weak dependence of ψ on temperature relative to the exponential factor): at $A = 0$, $\theta = 0$, i.e., $\Delta T_\Pi = 0$ or $T_\Pi = T_{\Pi\ theor}$; at $A > 0$, $\theta > 0$, i.e., $T_\Pi > T_{\Pi\ theor}$.

Whereupon two types of conditions leading to detonational collapse are possible: 1) ignition of the mixture* due to compression (in front of the flame limit) which causes the formation of shock waves, 2) formation of shock waves due to the processes of combustion within the propagating flame limit.

With $A < 0$ we have $\theta < 0$, i.e., $T_\Pi < T_{\Pi\ theor}$. Solving Equation (4) it is possible to determine that the limiting value of ψ corresponds to $\theta = -1$, i.e., the flame temperature as a consequence of energy transfer can decrease by no more than $RT^2_{\Pi\ theor}/E$. It must be noted that such a fall in temperature at the boundary occurs in laminary combustion at constant pressure and in the presence of heat losses [2].

With $\theta \rightarrow -1$ we have $\partial\theta/\partial\psi \rightarrow \infty$ – a nonstationary state accompanied by a fall in temperature and decrease in the reaction rate, i.e., the limit of the flame propagation is reached and collapse of combustion occurs.

Modifying Equation (4) we obtain at the boundary of the collapse the approximate relation $\frac{[A]}{D_0} = \frac{1}{e} \frac{RT_{\Pi\ theor}}{E}$, i.e., the ratio of [A] (rate of decrease of temperature due to decrease in pressure and loss of heat to the wall) to D_0 (the average rate of temperature increase in the flame zone with $A = 0$) has a certain critical value at the propagation boundary. The presence of the term $RT_{\Pi\ theor}/E$ in the latter expression is due to the fact that the width of the flame zone (where losses occur) is approximately $E/RT_{\Pi\ theor}$ times larger than that of the chemical reaction zone.

* Local ignition, taking into consideration the temperature nonuniformity of the mixture under real conditions.

If one introduces the characteristic loss time $\tau_{loss} = RT^2 / n_{theor} / E[A]$ (time taken for the gas temperature to decrease by one characteristic interval due to change in pressure and heat loss to the wall), then we will obtain at the flame propagation boundary from equation (4) $\frac{\tau_{r\ theor}}{\tau_{loss}} = \frac{1}{e}$, i.e., the ratio of the characteristic reaction time to the characteristic loss time, is constant.

4. In the case of large-scale turbulence there occurs an increase in the surface of combustion due to its deformation by the turbulent pulsations; a comparatively large combustion zone is formed on propagation of the flame. This zone does not have a homogeneous structure and looks like a folded flame front (a layer of burning gas is divided by layers of initial gas).

Turbulence by itself does not affect the occurrence of the chemical reaction. In the case of large-scale turbulence the reaction also occurs at temperatures near to the maximum flame temperatures. Hence, the constant ratio of the time of temperature decrease because of heat exchange, to the time of temperature increase due to the chemical reaction ($\tau_{r\ theor}/\tau_{loss} = const.$), obtained as the condition for combustion collapse for a small-scale turbulence should hold for the case of a large-scale turbulence.

5. The limits of stable flame propagation depend strongly on the magnitude of $dp/d\tau$. In the case of periodic combustion engines with one end of the chamber open (gas turbines, reaction turbines), besides the law of heat evolution, the conditions of gaseous flow play a very important role in determining the magnitude of $dp/d\tau$[6-8].

In the case of piston engines $p = f(V,z)$, where $V(\tau)$ is the volume of the chamber and $z(\tau)$ is the fraction of burned material. Hence,

$$\frac{dp}{d\tau} = \left(\frac{\partial p}{\partial V}\right)_z \frac{dV}{d\tau} + \left(\frac{\partial p}{\partial z}\right)_V \frac{dz}{d\tau}.$$

or, since

$$\left(\frac{\partial p}{\partial V}\right)_z = -k\frac{p}{V}, \quad \frac{1}{p}\frac{dp}{d\tau} = -k\frac{d\ln V}{d\tau} + \frac{1}{p}\left(\frac{\partial p}{\partial z}\right)_V \frac{dz}{d\tau}.$$

In this equation the first term which takes into account the change in the volume of the chamber (motion of the piston), depends strongly on the position of the piston relative to the upper dead point; the second term which takes into account the burning out depends on the heat properties of the mixture ($H_{mix}/C_V T_0$) and on the rate of flame propagation.

Many experimental facts about combustion in engines, in particular the problem of stable work by a piston engine with spark ignition and using poor mixtures, can be explained on the basis of above considerations.

I take this opportunity to thank Ya. B. Zeldovich and O. M. Todes for their valuable advice and remarks on this work.

Received July 9, 1956

LITERATURE CITED

[1] N. N. Semenov, Prog. Phys. Sci. 23, 3, 251 (1940); 24, 4, 433 (1940).

[2] Ya. B. Zeldovich, Theory of Combustion and Detonation of Gases (Acad. Sci. USSR Press. 1947).

[3] D. A. Frank-Kamenetsky, Diffusion and Heat Transfer in Chemical Kinetics (Acad. Sci. USSR Press, 1947).

[4] D. L. Abugov, Proc. Acad. Sci. USSR 100, No. 2, 291 (1955).

[5] K. I. Shchelkin, J. Tech. Phys. (USSR) 13, 9-10 (1943); Bull. Acad. Sci. USSR, Div. Tech. Sci. 1953, No. 3.

[6] V. V. Uvarov, Characteristics of the Aviation Gas Turbine (1946).

[7] K. P. Stanyukovich, Elementary Applied Theory of Irregular Gas Movements (1953).

[8] A. Kahane and L. Lees, Third Symposium on Combustion and Flame and Explosions Phenomena, (1949), pp. 222-229.

DEPENDENCE OF ABSORPTION SPECTRA OF SOLUTIONS AND ISOMORPHOUS ALUM CRYSTALS ON THEIR CHROMIUM CONTENT

I. I. Antipova-Karataeva

(Presented by Academician A. V. Shubnikov July 18, 1956)

Theoretical works dedicated to the investigation of light absorption by admixtures in dielectrics [1-3], consider only those cases where the "absorption centers" are independent of each other. However, it is known that Beer's law which is based on such an assumption, is not always obeyed. In those cases where deviation from Beer's law cannot be explained chemically, one must, apparently, look for an explanation in the interaction between the "absorption centers." It seems to be of interest to determine the conditions under which this interaction becomes appreciable enough to manifest itself through the absorption spectra.

We investigated the absorption spectra of mixed crystals and solutions of aluminum-potassium and chromium-potassium alums. In the latter the chromium ions replace isomorphously the Al^{+3} ions and are the coloring admixture. An analogous but less complete investigation has been performed earlier by Ritschl and Müller [4], on crystals of corundum Al_2O_3, colored by an isomorphous admixture of Cr^{+3}. It was of interest to determine the behavior of wide bands in the spectra of structurally different crystals as a function of the concentration of the same coloring species.

The absorption spectra of alum crystals and solutions were measured in the wavelength region 250-700 mμ at room temperature. In the visible part of the spectrum the measurements were performed using a monochromator UM-2 (YM-2) and a photoelectric method. In the ultraviolet region the spectrograph Q-12 was used. The concentration of the chromium in crystals varied from 2.9 to 100 mole% and in the solutions from $7 \cdot 10^{-3}$ to $5.6 \cdot 10^{-1}$ mole %.

The absorption spectra of alum crystals exhibit three wide absorption bands ν_{max} = 17700, 24600 and 38750 cm^{-1} of which the latter is so near the continuum that it was not possible to investigate it completely. The position of the maxima of the other two absorption bands and their half-widths do not depend on the concentration of the chromium (Fig. 1). The areas bounded by the spectral absorption curve and the frequency axis, and the extinction coefficients at the maximum absorptions, are proportional to the concentration of the chromium. Beer's law was strictly followed (Fig. 2). The shape of the absorption bands approximates to the Gaussian error curve. The oscillator strengths are equal: $f_{17700} = 2.25 \cdot 10^{-5}$ and $f_{24600} = 2.16 \cdot 10^{-5}$.

Investigation of the positions of the maxima of the corresponding wide bands in the absorption spectra of corundums colored with chromium showed that the bands shifted to lower frequencies on increase in the chromium concentration, with a strong shift occurring in the concentration interval 8.4 to 100 mole%, while for smaller concentrations the position of the bands remains practically constant. According to Thilo [5] the magnetic and thermochemical properties of these crystals, as well as their lattice parameters, specific gravities and luminescence thresholds, all exhibit analogous changes on variation in the chromium concentration. Thilo and Sauer [6] investigated the dependence of coloration, lattice parameter, density and thermochemical properties on the chromium concentration in mixed crystals of spinel $MgO \cdot Al_2O_3$–$MgO \cdot Cr_2O_3$. The curves of the dependences of the properties of corundums and spinels on the chromium concentration were found to be similar but the limiting concentration in spinels was 15%. Thilo explains the phenomena described by assuming that the chromium ions

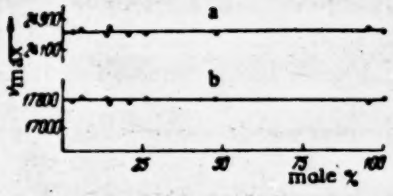

Fig. 1. Dependence of the position of the maxima of the absorption bands of alum crystals on the chromium concentration.
a) $\nu_{max} = 24600\ cm^{-1}$, b) $\nu_{max} = 17700\ cm^{-1}$.

in these crystals are bonded in two different ways: at low concentrations when they exist independently of each other and at large concentrations when each ion has at least one other ion as its nearest neighbor. A rough calculation shows that such a limiting concentration would be 8.4 mole% for corundums and 15 mole % for spinels. The chromium ions in mixed alum crystals behave independently of their concentration. The reason for such a difference lies in the difference between the structures of the crystal studied. In corundum the chromium ion occurs in the center of the octahedron, in spinels in the center of a tetrahedron of oxygen ions whereupon the shortest distance in corundum between the metallic ions is about 2 A. In alum crystals the chromium occurs in the center of an octahedron of H_2O molecules which are at 1.98 A from it.

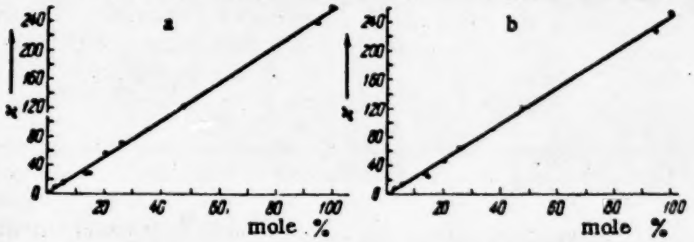

Fig. 2. The fulfillment of Beer's law in the case of mixed alum crystals.
a) $\nu_{max} = 17700\ cm^{-1}$, b) $\nu_{max} = 24600\ cm^{-1}$.

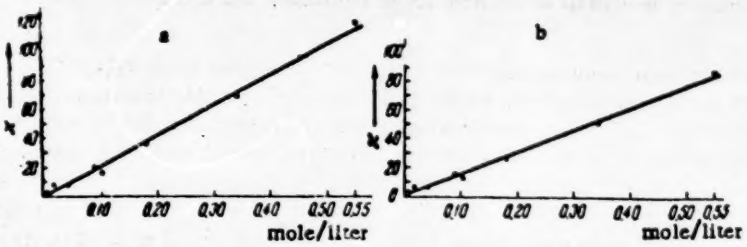

Fig. 3. The fulfillment of Beer's law in the case of mixed solutions of alums.
a) $\nu_{max} = 17300\ cm^{-1}$, b) $\nu_{max} = 24300\ cm^{-1}$.

Chromium belongs to the transition elements. The electronic transitions corresponding to the wide absorption bands in the absorption spectra of the crystals examined, occur, apparently within the unfilled 3-d shell, since the oscillator strengths are small – of the order of 10^{-4}-10^{-5}. On absorption of light there occurs a redistribution of electrons within the 3-d shell; hence, the electric field of the ion changes but very slightly at large distances away from it and a strong interaction can occur only with the nearest neighbors of the ion.

As shown above the distance to the nearest neighbors must be of the order of 2 A. The chromium ions in alum crystals are shielded by a sheath of six water molecules; hence change in the chromium concentration is not reflected in their absorption spectra.

This supposition is supported by the investigation of the absorption spectra of mixed alum solutions. It is known that on solution of alums the chromium ion passes into solution as the complex $[Cr(H_2O)_6]^{+3}$ retaining its water sheath. The absorption spectra of the solutions are very similar to those of the crystals: the half-widths of the corresponding bands are nearly equal and the bands in the spectra of the solutions are slightly displaced toward lower frequencies. Beer's law is strictly followed (Fig. 3). The position of the band maxima and their half-widths do not depend on the chromium concentration. The shape of the absorption bands approximates to that of the Gaussian curve. The oscillator strengths are $f_{17300} = 6.2 \cdot 10^{-5}$ and $f_{24500} = 4.0 \cdot 10^{-5}$. Therefore, change in neighbors far removed from the chromium ion affects but little the absorption spectrum of chromium ions. The fundamental role is played by the nearest neighbors and any substitution among them leads to considerable change in the spectrum. As was shown by an investigation of the absorption spectra of solutions of the green modification of alums – basic complexes of chromium and complexes $[Cr(SO_4)_3]^{-3}$ – there was a strong shift in the band positions and a considerable change in the half-widths of the bands (up to 13%) on going from alum solutions to those solutions than on going to the crystals.

The described peculiarities in the behavior of the wide bands in absorption spectra of solutions and mixed alum crystals show that in this case it is not the chromium ions but the chromium ion complexes $[Cr(H_2O)_6]^{+3}$ which must be considered as "absorption centers" according to the theory of A. S. Davydov and S. I. Pekar.

Institute of Crystallography of the Academy of Sciences of the USSR

Received July 4, 1956

LITERATURE CITED

[1] S. I. Pekar, J. Exptl.-Theoret. Phys. (USSR) 22, 6, 41 (1952).

[2] A. S. Davydov, ibid., 24, 2, 197 (1953).

[3] F. E. Williams, J. Chem. Phys. 19, 57 (1951).

[4] R. Ritschl and R. Müller, Z. Physik. 133, 237 (1952).

[5] E. Thilo, Miscellanea academica berolinesia, 1, 82 (1950).

[6] E. Thilo and R. Sauer, Chemie der Erde, 17, 165 (1955).

THE ROLE OF INTERMEDIATES IN COMPLEX CHAIN REACTIONS

N. S. Enikolopyan

(Presented by Academician V. N. Kondratyev, July 4, 1956)

The kinetics of complex chain reactions which proceed with formation of a number of stable intermediates (I) (e.g., peroxides, aldehydes, alcohols, etc. on oxidation of hydrocarbons) differs from the kinetics of simple chain reactions (reaction of hydrogen with chlorine, oxidation of hydrogen and carbon monoxide at low pressures etc.), in that in complex chain reactions the mechanism of the process changes as the intermediates (I) accumulate. In the beginning of the reaction when the concentration of (I) is small, the active particles (atoms and radicals) react mainly with the initial substances. As (I) accumulates, the active particles react simultaneously with the initial particles and (I) which leads to change in the mechanism of the reaction during its course.

The rate of an unbranched chain process is described by the equation

$$w = a_0 \nu = a_0 \frac{a}{g}, \qquad (1)$$

where a_0 is the rate of conception of active centers, ν is the length of the chain, a is the rate constant for the propagation of the chain and g is the rate constant for destruction.

On quadratic destruction of active centers a_0 and g in equation (1) will have a $^1/_2$ power. This will not introduce substantial changes into our discussion and hence the presentations on the role of (I) developed below will apply fully for the case of quadratic destruction.

In complex chain reactions there occur cases where (I) produces the conception of active centers at a higher rate than the initial substances. This phenomenon became the basis of the degenerate branching theory of N. N. Semenov [1] and was examined by us previously [2]. In this case the rate of the reaction is described by the equation

$$w = (a_0 + hx)\nu = (a_0 + hx)\frac{a}{g}, \qquad (2)$$

where hx is the rate of the degenerate branching, x is the concentration of (I) capable of producing the conception of active centers at a larger rate than the initial substances, h is the constant of the elementary process of degenerate branching.

The theory of degenerate branching is at present widely recognized, however, in complex chain reactions degenerate branching is not the only process through which (I) influence the course of the reaction. In complex chain reactions a case is possible where (I) influence not the process of conception of a_0 but the chain length ν. Whereupon it is necessary to distinguish between two basically different cases: 1) increase, and 2) decrease in the length of the chain ν as (I) accumulates.

1) Increase in Chain Length ν As (I) Accumulates.

Let us consider the scheme

0. $RH + O_2 = \dot{R} + H\dot{O}_2$.
1. $\dot{R} + O_2 = ROO\dot{}$.
2. $ROO\dot{} + RH = ROOH + \dot{R}$.
3. $ROO\dot{} + ROOH = ROOH + \dot{R}'OOH$.
4. $\dot{R}'OOH = A + \dot{O}H$.
5. $\dot{O}H + RH = H_2O + \dot{R}$.
6. $\dot{O}H + ROOH = H_2O + \dot{R}'OOH$.
7. $ROO\dot{} \rightarrow$ termination

This scheme must not be considered as chemically and experimentally proven. We give it only as an illustration.

As can be seen from the scheme the rate for the reaction of consumption of the hydrocarbon is

$$w = a_2[ROO\dot{}] + a_5[\dot{O}H]. \tag{3}$$

Applying the conditions of the stationary state and expressing the concentrations of the radicals $[ROO\dot{}]$ $[\dot{O}H]$ in terms of the concentrations of the initial substances, we obtain for the rate of the reaction

$$w = a_0 \frac{a_2 + k_3[X]}{a_7}, \tag{4}$$

where [X] is the concentration of (I) (in this case the hydroperoxide), reacting with the slightly active radical $ROO\dot{}$, a_2 and a_7 are the constants for propagation and termination of chains, respectively.

As can be seen from equation (4) the length of the chain increases by $\frac{k_3[X]}{a_7}$. Had there not been process 3, the chain length would have been a_2/a_7.

The rate of accumulation of (I) is

$$\frac{d[X]}{dt} = a_2[ROO\dot{}] - k_6[X][\dot{O}H]. \tag{5}$$

Substituting [ROO] and [OH] expressed in the concentrations of the initial substances into equation (5) and solving it with the assumption that at the beginning of the process the concentration [X] is zero, we will obtain:

$$\xi = \frac{e^{2s\tau} - 1}{e^{2s\tau} + 1}, \tag{6}$$

where

$\xi = \frac{[ROOH]}{\left[\frac{a_2 a_5}{k_3 k_6}\right]^{1/2}}$ — unitless concentration

$s = \left[\frac{a_5 k_3}{k_6 a_2}\right]^{1/2}$ — unitless parameter

$\tau = \frac{a_2 k_3}{a_7} t$ — unitless time

Substituting the expressions for [ROȮ], [ȮH] and [X] into equation (3) we will obtain for the unitless rate of reaction

$$\theta = 1 + \varepsilon \frac{e^{2\varepsilon\tau} - 1}{e^{2\varepsilon\tau} + 1}, \qquad (7)$$

where

$$\theta = \frac{wa_7}{a_0 a_2}.$$

As can be seen from equation (7) the rate of the reaction increases with time tending toward the maximum value

$$\theta = 1 + \varepsilon.$$

The unitless parameter ϵ shows the effectiveness of increase in the rate of the reaction (chain length) as a result of participation of (I) in the propagation process.

Fig 1. shows the dependence of the reaction rate on time at different values of ϵ. The calculations were performed using equation (7) and without taking into account the expenditure of the initial substance.

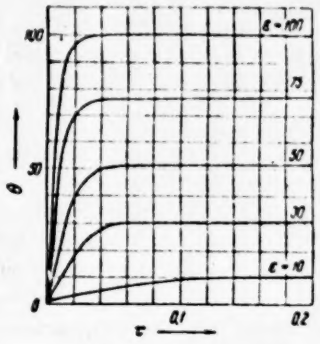

Fig. 1.

As must be expected initially, the reaction rate is unity since we considered the establishment a stationary state as the time origin and determined the unitless rate as the ratio of the actual rate of the reaction to the stationary rate. If $\epsilon = 0$, then there is no acceleration and the reaction proceeds at constant rate equal to unity.

2) Decrease in Chain Length ν as (I) Accumulates.

Let us examine the scheme

0. $RH + O_2 = \dot{R} + HO_2$.
1. $\dot{R} + O_2 = ROȮ$.
2. $ROȮ = A + \dot{R}'Ȯ$.
3. $\dot{R}'Ȯ + RH = B + \dot{R}$.
4. $\dot{R}'O + A \rightarrow B + \dot{R}''$.
5. $\dot{R}'' + B \rightarrow ROȮ$.
6. $ROȮ \rightarrow$ termination

This scheme must also be considered only as illustrative.

According to this scheme as a result of the reaction with the stable intermediates A and B the active radical R'O is transformed into the slightly active radical ROȮ, which leads to a decrease in chain length.

Applying the method of stationary state of active centers, the rate of consumption of hydrocarbons will be:

$$w = a_0 \frac{a_2}{a_6} \frac{a_3}{a_3 + k_4 [X]} \qquad (8)$$

where [X] is the concentration of the intermediate A.

On absence of process 4 the chain length would have been a_3/a_4. Process 4 decreases the chain length by $a_3/(a_3+k_4[X])$ times. As can be seen the larger the accumulation of the intermediate A, the smaller the chain length and hence the smaller the reaction rate. The rate of accumulation of A is given by

$$\frac{d[A]}{dt} = a_3[\dot{ROO}] - k_4[A][\dot{R'O}]. \qquad (9)$$

Expressing the concentrations [ROO] and [R'O] in terms of the concentration of the initial substances and solving equations (8) and (9) with the assumption that at the beginning of the reaction the concentration of intermediate A is zero, we will obtain the dependence of the reaction rate on time:

$$\theta = \frac{2}{1+\sqrt{1+4\epsilon\tau}}, \qquad (10)$$

where

$$\theta = \frac{w a_4}{a_3 a_2},$$

and θ, ϵ and τ have the same meaning as in equation (7).

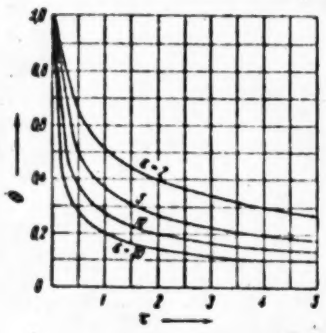

Fig. 2.

Fig. 2 shows the dependence of the reaction rate on time calculated from equation (10) for various values of ϵ and without taking into account the expenditure of the initial substance.

Thus, as can be seen from the examination of schemes 1 and 2, the chain length in complex chain reactions proceeding with formation of stable intermediates, can change in the course of the reaction and in its own turn can lead to a change in the reaction rate. If as a result of the reaction of (I) with the radical a radical is formed which is more active than the initial radical, increase in chain length occurs. In the other case there occurs a decrease in the chain length on accumulation of (I). It must be noted that the laws of acceleration and deceleration can be different depending on the concrete mechanism of the complex process.

The ambiguous action of stable intermediates on complex chain reactions, examined above, allows us to take up the explanation of certain peculiarities in the kinetics of such processes.

The stopping of oxidation of hydrocarbons long before the complete expenditure of the initial substances, the constant reaction rate up to very high values for the conversion (observed for methane, benzene and others), the difference between the orders of the reaction determined during the process and from the initial concentration of the hydrocarbon, autocatalysis by intermediates and final products, the catalysis and inhibition by the same substances in different reactions, can all be satisfactorily explained within the frame of the above representation.

Institute of Chemical Physics of the
Academy of Sciences of the USSR

Received July 2, 1956

LITERATURE CITED

[1] N. N. Semenov, Z. Phys. Chem. 11, 434 (1931).

[2] N. S. Enikolopyan, J. Phys. Chem. 30, No. 1, 769 (1956).

DETERMINATION OF THE ZERO POTENTIAL OF LEAD DIOXIDE ELECTRODES BY THE METHOD OF MEASURING THE HARDNESS

D. I. Leikis and E. K. Venstrem

(Presented by Academician P. A. Rebinder July 8, 1956)

The work of P. A. Rebinder and E. K. Venstrem [1-3] has shown that the electrocapillary curve of lowering of the hardness of a hard metal as a function of the potential jump on the boundary metal-electrolyte is completely analogous to the classical electrocapillary curve for the lowering of the surface tension of the liquid metal. Later, E. K. Venstrem, V. L. Lichtman and P. A. Rebinder [4] have shown for the case of lead that a normal curve with a maximum is obtained on measuring the hardness of the metal by the pendulum method under conditions of sufficiently strong deformation and dispersion of the metal. The curve has a minimum under the limiting condition of friction between the support of the pendulum and the metal. However, independently of this, the extreme points of the curve always lie at the zero potential.

The application of such methods allows the direct determination of the zero potential of the hard metal in concentrated solutions, which is either impossible or very difficult to do using other methods (e.g., method of measurement of the capacity of the double layer, adsorption method).

The method of measurement of the hardness was used by us to determine the zero potential of PbO_2 electrodes. Such a direct determination of the zero potential in a concentrated solution is of particular interest in view of the use of PbO_2 electrodes in lead accumulators. I. G. Kiselev and B. N. Kabanov [5] have shown that irreversible adsorption of sulfuric acid occurs on the PbO_2 electrode, which changes its electrochemical properties (in particular changes the oxygen overvoltage). As a result of such an adsorption, a change in the zero potential is very probable on going from dilute to concentrated solutions.

We performed measurements in 0.1N and 8N H_2SO_4 solutions. The measurements in the dilute acid were done in order to enable us to compare our results with results obtained by other methods.

Measurements have shown that the PbO_2 deposit formed on anodic oxidation of lead in H_2SO_4 (analogously to the preparation of plates for the lead accumulator) possesses physical properties sufficient for measurements of the hardness, by the pendulum method, on dispersion of the surface. The curve of the dependence of hardness on potential exhibits a well-defined maximum. The PbO_2 deposit was obtained on lengthy (several days) anodic oxidation of metallic lead in the same solution in which the measurements were later performed. Figure 1 shows the curves obtained on the PbO_2 electrode. As can be seen from it the maximum for the 0.1N H_2SO_4 curve occurs at the potential $\sim$ 1.9 volts (relative to the hydrogen electrode). We suppose that this value corresponds to the zero potential. Let us point out that B. N. Kabanov, N. T. Kiseleva and D. I. Leikis [6] using the method of measurement of the capacity of the double layer and the adsorption method, obtained for the zero potential the value of 1.8 volts (relative to the hydrogen electrode) in 0.01N and 0.1N H_2SO_4 solutions. The difference of only $\sim$0.1 volt shows the applicability of such methods to electrochemical deposits such as PbO_2, particularly if one considers that in the case of metallic electrodes the difference between the results obtained by various methods reaches 0.2-0.3 volts (e.g., Tl, Cd and others) [7-9].

As can be seen from Fig. 1 the maximum of curve B obtained for 8N H_2SO_4 occurs at 1.7 volts, i.e., by 0.2 volts less than for 0.1N H_2SO_4. The shift in the zero potential on change in the H_2SO_4 concentration is in qualitative agreement with the representations of the surface-active properties of the sulfuric acid anion [5, 10, 11].

As is well known, the specifically adsorbing anions shift the maximum of the electrocapillary curve on mercury toward negative values. Apparently in concentrated solutions of sulfuric acid there is a larger number of anions of the acid adsorbed on the surface than in the dilute solution, and this causes the indicated shift in the zero potential.

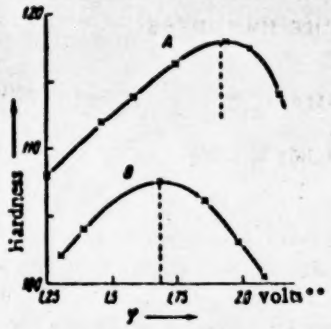

Fig. 1. Curves of the dependence of hardness on potential for PbC_2 electrodes in H_2SO_4.
A) in 0.1N H_2SO_4, B) in 8N H_2SO_4.

On examining curve A in Fig. 1 one notices the asymmetry of the curve which manifests itself by a sharper decrease in hardness in the region of positive potentials than in the region of negative potentials. Basically this effect, as is known from the theory of electrocapillary phenomena, is determined by the fact that a positive potential on the surface helps the adsorption of specifically active anions. This phenomenon can apparently be tied in with the results on the capacity of the double layer on the same electrode [6]. At potentials higher than 1.9 volts a sharp increase in the capacity of the double layer was observed. This was tentatively explained by an increase in the true surface in connection with change in the crystalline structure of the surface. It can be supposed that the sharp decrease in hardness and sharp increase in capacity of the double layer are partly the result of a superficial dispersion caused by adsorption of sulfuric acid anions [12, 13]. Such a supposition is in agreement with the fact that the deposit obtained in concentrated solution (8N H_2SO_4 and which naturally adsorbs more acid, possesses a lower hardness — is more easily dispersed note that in Fig. 1, curve A lies considerably higher than curve B). In the case of the concentrated solution (curve B) there is no noticeable asymmetry. Apparently the total number of specifically adsorbed anions of the acid in the concentrated solution, even in the region of negative potentials on the surface, is so large that it does not change appreciably on transition to the region of positive potentials.* In other words, molecules of sulfuric acid are partly adsorbed.

Thus, it is shown that the method of measuring the hardness can be applied to the determination of zero potentials of oxide electrodes. With this method it is possible to measure the dependence of the zero potential on the electrolyte concentration.

In conclusion we would like to express our gratitude to Prof. B. N. Kabanov for valuable advice which contributed to the success of our investigation.

Received June 21, 1956

LITERATURE CITED

[1] P. A. Rebinder and E. K. Venstrem, J. Phys. Chem. 19, 1 (1945).

[2] P. A. Rebinder and F. K. Venstrem, Proc. Acad. Sci. USSR 68, 329 (1949).

[3] E. K. Venstrem and P. A. Rebinder, J. Phys. Chem. 26, 1847 (1952).

[4] E. K. Venstrem, V. L. Lichtman and P. A. Rebinder, Proc. Acad. Sci. USSR 107, 105 (1956).

[5] L. G. Kiseleva and B. N. Kabanov, ibid. 108, 864 (1956).

[6] B. N. Kabanov, L. G. Kiseleva and D. L. Leikis, ibid. 99, 805 (1954).

[7] A. V. Gorodetskaya and B. N. Kabanov, J. Phys. Chem. 4, 529 (1933).

* May be in connection with simultaneous adsorption of cations.

** Relative to the Hydrogen electrode.

[8] T. L. Borisova, B. V. Ershler and A. N. Frumkin, ibid. 22, 925 (1948); T. L. Borisova and B. V. Ershler, ibid. 24, 337 (1950).

[9] V. S. Ostrovsky and V. I. Lichtman, Proc. Acad. Sci. USSR 96, 319 (1954).

[10] N. A. Balashova, ibid. 103, 639 (1955).

[11] Ya. M. Kolotyrkin and L. A. Medvedeva, J. Phys. Chem. 25, 1355 (1951).

[12] P. A. Rebinder, Jubilee Symposium on the 30th Anniversary of the Great October Socialistic Revolution. (Acad. Sci. USSR Press, 1947) 1.

[13] V. I. Lichtman, P. A. Rebinder and G. V. Karpenko, Influence of a Surface-Active Medium on the Deformation of Metals, Acad. Sci. USSR Press, 1954).

DIFFUSION PRECIPITATION OF AEROSOLS ON A STREAMLINED CYLINDER WITH A SMALL CAPTURE COEFFICIENT

G. L. Natanson

(Presented by Academician A. N. Frumkin July 12, 1956)

1. Langmuir was the first to make an approximate calculation of the number of aerosol particles which precipitate from a viscous stream, due to diffusion, on a cylinder perpendicular to the stream [1]. He assumed that all particles within a volume bounded by a certain flow line ψ_1 (ψ is a function of the flow), passing at $\theta = \pi/2$ and distance $r_0 - a = x_0$ from the cylinder surface (θ and r are polar coordinates, a is the radius of the cylinder), are able to diffuse to the surface of the cylinder. The value of x_0 was calculated from the expression for the average absolute Brownian shift of a particle

$$x = \left(\frac{4}{\pi} Dt\right)^{1/2}, \tag{1}$$

where x was determined as the average quadratic distance from the cylinder surface on motion along the flow line ψ_1 between $\theta = 5\pi/6$ and $\theta = \pi/6$ and where t is the duration of this motion. On substituting into equation (1) the values of x and t expressed in terms of x_0, a and w according to Lamb's equations for velocity distribution at $r-a \ll a$, we obtain $x_0/a = (0.56D/wa)^{1/2}$ where $w = v_0/2(2.00 - \ln \mathrm{Re})$, $\mathrm{Re} = 2av_0/\nu$, and v_0 is the velocity far away from the cylinder. The expression for the capture coefficient ϵ as given by Langmuir, has the form $\epsilon = \psi_1/v_0 a = w/v_0[2(r_0/a)\ln(r_0/a) + a/r_0 - r_0/a]$, where $r_0/a = 1 + x_0/a$. Since x_0 was calculated for the condition $r - a \ll a$, the approximate expression obtained applies only to the region of small capture coefficients; because of $x_0/a \ll 1$ it reduces to

$$\epsilon = 2\frac{w}{v_0}\left(\frac{x_0}{a}\right)^2 = 1.36\left(\frac{w}{v_0}\right)^{1/3}\left(\frac{D}{v_0 a}\right)^{2/3}. \tag{2}$$

It is not difficult to show that for small ϵ expressions for diffusion precipitation can be strictly obtained from the differential equation of diffusion by the method developed by V. G. Levich for solution of similar problems [2].

2. The equation for convective diffusion on a circular cylinder perpendicular to the flow has in polar coordinates the following form

$$\frac{\partial c}{\partial t} + v_r\frac{\partial c}{\partial r} + \frac{v_\theta}{r}\frac{\partial c}{\partial \theta} = D\left(\frac{\partial^2 c}{\partial r^2} + \frac{1}{r}\frac{\partial c}{\partial r} + \frac{1}{r^2}\frac{\partial^2 c}{\partial \theta^2}\right).$$

On establishment of the stationary state, assuming the velocity of diffusion transportation in the direction θ to be much less than in the direction r or than the velocity of the convection transportation, we obtain

$$v_r \frac{\partial c}{\partial r} + \frac{v_\theta}{r} \frac{\partial c}{\partial \theta} = D\left(\frac{\partial^2 c}{\partial r^2} + \frac{1}{r} \frac{\partial c}{\partial r}\right).$$

If we limit ourselves to the region $\frac{r - a}{a} = \varkappa << 1$ i.e., to the case of small capture coefficients, then the diffusion equation will take the form

$$v_r \frac{\partial c}{\partial r} + \frac{v_\theta}{r} \frac{\partial c}{\partial \theta} = D \frac{\partial^2 c}{\partial r^2}.$$

Changing from coordinates (r, θ) to the coordinates $(\psi \beta)$[2] and taking $v_\theta = \partial\psi/\partial r$ and $v_r = (1/r)\partial\psi/\partial\theta$, we will obtain for $r \sim a$,

$$\left(\frac{\partial c}{\partial \theta}\right)_\psi = aD \frac{\partial}{\partial \psi}\left(v_\theta \frac{\partial c}{\partial \psi}\right)_\theta. \tag{3}$$

3. In the case of viscous flow around the cylinder described by Lamb's distribution of velocities, on $\varkappa << 1$, $\psi = 2wa\,\varkappa^2 \sin\theta$ and $v_\theta = -4w\varkappa\sin\theta$. On eliminating $\varkappa$ equation (3) takes the form

$$\frac{\partial c}{\partial \theta} = -(8\,wa\,D^2 \sin\theta)^{1/3} \frac{\partial}{\partial \psi}\left(\psi^{1/3} \frac{\partial c}{\partial \psi}\right). \tag{4}$$

Introducing the variable

$$\varphi = \int_0^{\theta_1} (8wa\,D^2 \sin\theta)^{1/3} d\theta,$$

we will obtain

$$\frac{\partial c}{\partial \varphi} = \frac{\partial}{\partial \psi}\left(\psi^{1/3} \frac{\partial c}{\partial \psi}\right). \tag{5}$$

The solution of equation (5) with the boundary conditions $c = 0$ at $\psi = 0$ (on the surface of the cylinder) and $c = c_0$ at $\psi = \infty$ (far away from the cylinder), has the form [2]

$$c = \frac{3}{\Gamma(1/3)}\left(\frac{4}{9}\right)^{1/3} c_0 \int_0^u e^{-1/3 u^3}\, du, \tag{6}$$

where $\underline{u} = \psi^{1/3} / \varphi^{1/3}$.

The diffusion flow per unit of cylinder length is

$$2J = 2\int_0^{\pi} D\left(\frac{\partial c}{\partial r}\right)_{r=a} a\,d\theta = 2D\int_0^{\pi}\left(\frac{\partial c}{\partial u}\,\frac{\partial u}{\partial \psi}\,\frac{\partial \psi}{\partial r}\right)_{r=a} a\,d\theta. \qquad (7)$$

Taking into consideration that in the incoming flow (at $\theta = \pi$) $c = c_0$, we will obtain from (6): at $\theta = \pi$ $u - \infty$ and $\varphi = 0$, i.e. $\theta_1 = \pi$. Hence from equations (6) and (7) we obtain

$$2J = \frac{6}{\Gamma(1/3)}\left(\frac{4}{9}\right)^{1/3} c_0 (wa D^2)^{1/3} \int_0^{\pi} \frac{\sin^{2/3}\theta\,d\theta}{\left(\int_0^{\pi}\sin^{1/3}\theta\,d\theta\right)^{1/3}}. \qquad (8)$$

The integral in the denominator on the substitution $\sin^{1/2}\theta = z$ becomes for $\theta < \frac{\pi}{2}$, $\int_0^1 \frac{2z^3\,dz}{\sqrt{1-z^4}} + \int_z^1 \frac{2z^3\,dz}{\sqrt{1-z^4}}$, and for $\theta > \frac{\pi}{2}$, $\int_0^1 \frac{2z^3\,dz}{\sqrt{1-z^4}} - \int_z^1 \frac{2z^3\,dz}{\sqrt{1-z^4}}$.

Since $\int_z^1 \frac{z^3\,dz}{\sqrt{1-z^4}} = \int_z^1 \sqrt{\frac{1+z^2}{1-z^2}}\,dz - \int_z^1 \frac{dz}{\sqrt{1-z^4}} = \sqrt{2}\,E\left(\arccos z, \frac{1}{\sqrt{2}}\right) - \frac{1}{\sqrt{2}}\,F\left(\arccos z, \frac{1}{\sqrt{2}}\right)$,

where E and F are elliptic integrals of second and first order respectively. Their values can be obtained from tables. Evaluating the total integral in equation (8) graphically we obtain

$$2J \approx \frac{6}{\Gamma(1/3)}\left(\frac{4}{9}\right)^{1/3} 2.71\, c_0 (wa D^2)^{1/3}.$$

Hence, the capture coefficient will be

$$\varepsilon = \frac{J}{v_0 a c_0} = 2.32\left(\frac{w}{v_0}\right)^{1/3}\left(\frac{D}{v_0 a}\right)^{2/3}, \qquad (9)$$

which differs considerably from Langmuir's equation (2) in the value of the numerical factor.

Equation (9) applies only to point particles, since for particles of finite size the boundary condition on the cylinder surface changes and one must besides, consider the effect of catching (a particle moving in the line of flow precipitates even in the absence of diffusion, when its center approaches the cylinder to a distance $r - a \leq R$ where R is the radius of the particle). In the absence of diffusion the capture coefficient for viscous flow at $R/a = \kappa_0 << 1$ is equal to $2w\kappa_0^2/u_0$ because of the catching effect. Thus equation (9) is correct for

$$\left(\frac{D}{v_0 a}\right)^{2/3} = \frac{1}{\mathrm{Pe}^{2/3}} \ll 1$$

and

$$\left(\frac{R^2}{a^2}\,\frac{v_0 a}{D}\right)^{2/3} \ll 1.$$

where Pe is the Peclε number.

4. In the case of potential flow around the cylinder at $\kappa \ll 1$, $\psi = 2 v_0 a \kappa \sin\theta$ and $v_\theta = -2v_0 \sin\theta$. Equation (3) takes the form

$$\frac{\partial c}{\partial \theta} = -2v_0 a D \sin\theta \frac{\partial^2 c}{\partial \psi^2}.$$

which can be transposed into

$$\frac{\partial c}{\partial (\cos\theta + 1)} = 2v_0 a D \frac{\partial^2 c}{\partial \psi^2}. \tag{10}$$

The boundary conditions for the problem in form (10) are the following: $c = 0$ at $\psi = 0$ and $c = c_0$ at $\cos\theta + 1 = 0$ ($\theta = \pi$). Under these conditions the solution of (10) is

$$c = c_0 \Phi\left(\psi \Big/ \sqrt{8 v_0 a D \cos\theta + 1}\right) \tag{11}$$

where $\Phi(x) = \frac{2}{\sqrt{\pi}} \int_0^x e^{-y^2} dy$ is Cramp's function.

Analogously to (7) we will obtain

$$2J = 2\int_0^\pi D\left(\frac{\partial c}{\partial \psi}\right)_{\psi=0}\left(\frac{\partial \psi}{\partial r}\right)_{r=a} a\, d\theta = c_0 \left(\frac{8 v_0 a D}{\pi}\right)^{1/3} \int_0^\pi \frac{\sin\theta\, d\theta}{(\cos\theta + 1)^{1/3}} = 8 c_0 \left(\frac{v_0 a D}{\pi}\right)^{1/3}.$$

which corresponds to the solution of Bussinesk [3] in an analogous problem on heat transfer.

The capture coefficient will be

$$\varepsilon = \frac{J}{v_0 a c_0} = \frac{4}{\sqrt{\pi}} \left(\frac{D}{v_0 a}\right)^{1/3}. \tag{12}$$

Since the capture coefficient for pure catching on potential flow around the cylinder at $\kappa_0 \ll 1$ is equal to κ_0 then equation (12) is correct under the conditions

$$\left(\frac{D}{v_0 a}\right)^{1/3} = \frac{1}{\mathrm{Pe}^{1/3}} \ll 1, \quad \left(\frac{R^3}{a^3} \frac{v_0 a}{D}\right)^{1/3} \ll 1.$$

The L. Ya. Karpov Physicochemical Institute of Scientific Investigations

Received June 20, 1956

LITERATURE CITED

[1] I. Langmuir, OSRD Rep., No. 865 (1949) (quoted from C. Chen, Chem. Rev. 55, 595 (1955); see Progr. Chem (USSR) 25, No. 3 (1956).

[2] V. G. Levich, Physicochemical Hydrodynamics (Moscow, 1952), ch. 2, pp.13-14.

[3] F. Frank and R. Mizes, Differential and Integral Equations of Mathematical Physics (Leningrad-Moscow, 1937) vol. 2, ch. 14, p. 2.

THE INFLUENCE OF SULFUR ON THE INTERPHASE TENSION AT THE METAL – SLAG BOUNDARY

S. I. Popel, O. A. Esin, G. F. Konovalov and N. S. Smirnov

(Presented by Academician L. P. Bardin on July 17, 1956)

A study of the surface activity of sulfur is of substantial interest in the clarification of the mechanism of desulfurization of liquid steel and in the investigation of the evolution of sulfide inclusions in the crystallization process [1, 2].

However, the influence of sulfur on the interphase tension (σ) at the metal–slag boundary has not been investigated. There is only the work of Kazakevich, et al. [3] where the change in interphase tension was determined during the process of transition of the sulfur from the cast iron into industrial slag. The authors came to the conclusion that σ increases during the process and that under the conditions of the equilibrium the sulfur is inactive in relation to the interphase boundary.

We used mainly the previous method in investigating the behavior of sulfur in relation to the metal–slag boundary [4]. The only difference was the use of x-ray assembly RUP-1 (200 kv) to obtain the diffraction of the melt.

The metallic phase was technically pure iron previously melted with the required proportion of FeS.

The slags were prepared from chemically pure oxides CaO, SiO_2, Al_2O_3 and Fe_2O_3 and contained:

	CaO	SiO_2	Al_2O_3	FeO	MgO
slag No. 1 (ferrous)	34.9	34.6	—	27.2	0.5
slag No. 2 (blast furnace)	47	27	23	1.0	0.1

Experiments with ferrous slag were performed in fused magnesium oxide and those with blast-furnace slag in corundum and graphite crucibles. In the latter case, in order to eliminate carbonization, the drop of metal was placed in an MgO plate. Due to interaction with the crucible material the magnesium oxide content in slags increased during the experiments reaching toward their end 11%. This however, as the experiments showed, did not appreciably influence the interphase tension.

In some experiments the sulfur was introduced only into the slag (as FeS), in others only into the metal and in the rest into both phases, so as to study not only the equilibrium but also the dynamical tension in the process of transition of the sulfur from the metal into the slag and back.

After melting of the metal the drops were photographed every 10 minutes and a sample (2 g) of the slag was taken out simultaneously to determine the sulfur concentration. In all experiments the weight of a drop of the metal was 11 g and the weight of the slag changed from 30 to 50 g.

The establishment of the equilibrium was determined from the constancy of the sulfur concentration in the slag. It was usually reached after 15-20 minutes and coincided with the establishment of a permanent form by the drop. The magnitude of the dynamical tension was determined from single photographs of drops comparing them to the subsequent equilibrium ones. The photographs of the drops were magnified about 6 times and the

true dimensions were determined from them with the help of a micrometric screen (unit division 0.1 mm). The relative error in the determinations did not exceed 3%.

The required values for calculation, of the densities of liquid slag were determined experimentally [6] and those of steel were taken from a handbook [7].

Experiments showed that when the sulfur content in both phases was low the interphase tension at the boundary of iron with the slag No. 1 was 650 ergs/cm^2. With increase in the sulfur concentration the static interphase tension decreased. The photographs of drops shown in Fig. 1 (first and second vertical rows) can serve as qualitative illustrations. The numerical values of σ as a function of the sulfur concentration in the metal are given in Fig. 2. The sulfur concentrations in slag No. 1 were 1.6 times smaller.

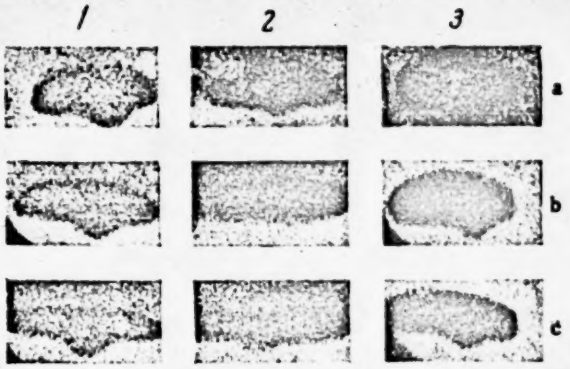

Fig. 1. Change in the shape of the metal drop with increase in sulfur concentration.

	S_{metal}			Slag
	a	b	c	
1	0.025	0.90	3.4	№ 1
2	0.70	2.0	3.0	№ 1
3	0.025	0.17	0.5	№ 2

When the iron oxide content in the slag was small (slag No. 1) the interphase tension at its boundary with the iron ($[S]_{metal} \approx 0.025\%$) was 1015 ergs/cm^2. This differs little from the value obtained earlier for different concentrations of CaO, SiO_2 and Al_2O_3 [5] and is substantially larger than σ for the ferrous slag. On introduction of sulfur the static interphase tension decreased regularly and for blast-furnace slag (see Fig. 1 third row and Fig. 2), with 2% sulfur in the metal ($S_{slag}/S_{metal} \approx 2$) reached the value 500 ergs/cm^2.

Thus, sulfur substantially lowers the interphase tension of iron at the boundary with oxide as well as blast-furnace slag. In our previous work [3] this effect was not detected probably because the sulfur concentration in the cast iron was small and did not change from one experiment to another.

The values of $\sigma_{dynamic}$ in our present and past [3] experiments were found to be lower than the static tensions. For example in one of the experiments on transition of sulfur from slag No. 2 into steel $\sigma_{dynamic}$ = = 470 ergs/cm^2 while at equilibrium σ = 515 ergs/cm^2. In another experiment on transition of sulfur into slag No. 1 $\sigma_{dynamic}$ = 440 ergs/cm^2 while at equilibrium σ = 510 ergs/cm^2.

The lowering in the interphase tension with increase in the sulfur concentration is easily understood if one takes into consideration the fact that sulfur has a high surface activity in relation to the steel-gas boundary [8,9]. Crowding into the surface layer of the metal it forms sufficiently strong bonds with the cations of the slag, to lower σ. The weaker influence of sulfur in the case of ferrous slags is apparently connected with the higher

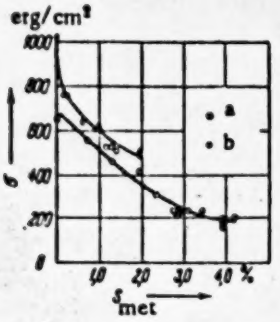

Fig. 2. Influence of sulfur on the interphase tension steel-slag at 1530-1570°.
a) slag No. 1, b) slag No. 2.

oxygen concentration in the metal, the surface activity of oxygen being similar to the activity of the sulfur [8, 10]. Crowding into the surface layer of the metal, the oxygen partly dislodges the sulfur. Moreover, a comparison of the stabilities of sulfides and oxides leads to the supposition that the bond between the oxygen and the cations of the slag is stronger than in the case of the sulfur. The two above-mentioned circumstances, namely crowding of the oxygen into the surface layer of the metal and its stronger bond with the cations of the slag cause a substantial lowering of the interphase tension on presence of oxygen in the metal and a much smaller change in the tension on addition of sulfur.

In the absence of equilibrium the directed transition of the sulfur through the interphase boundary washes it out, and thus the dynamic tension is lower than the static one.

The lowering in the interphase tension with increase in the concentration of sulfur and oxygen points out the greater thermodynamic stability of nonmetallic inclusions in steel if the sulfur and iron oxide content of these inclusions is high. Moreover, adsorption of sulfur and oxygen can substantially change the magnitude of the loosening pressure which hinders the blending of such emulsions [11].

The S. M. Kirov Ural Polytechnic Institute, Sverdlovsk

The Seversk Metallurgical Plant, Polevskoe

Received July 17, 1956

LITERATURE CITED

[1] O. A. Esin and P. V. Geld, The Physical Chemistry of Pyrometallurgic Processes (1954), vol. 2.

[2] S. L. Popel and O. A. Esin, Sbornik Trudov Uralsk. Politekh. Inst. [Coll. Papers Ural Polytech. Inst. 49, 47 (1954)].

[3] P. Kozakevich, G. Urbain and M. Sage, Rev. Met. 52, 161 (1955).

[4] S. L. Popel, O. A. Esin and P. V. Geld, Proc. Acad. Sci. USSR 74, 1097 (1950).

[5] S. L. Popel, O. A. Esin and Yu. P. Nikitin, ibid. 83, 253 (1952).

[6] S. L. Popel and O. A. Esin J. Appl. Chem. 29, 651 (1956).*

[7] C. Mellor, Comprehensive Treatise on Inorganic and Theoretical Chemistry (1934) 14, Part 2.

[8] F. A. Halden and W. D. Kingery, J. Phys. Chem. 59, 557 (1955).

[9] P. Kozakevich, S. Chatel, G. Urbain and M. Sage, Rev. met. 52, 139 (1955).

[10] B. V. Stark and S. I. Filippov, Bull. Acad. Sci. USSR, Div. Tech. Sci. 1949, No. 3, 413.

[11] B. V. Deryagin, ibid., Div. Math. Nat. Sci., Chem. Ser. 1937, No. 5, 1153.

*Original Russian pagination. See C. B. Translation.

THE FORMATION OF NITRIC OXIDE BY THE ADIABATIC COMPRESSION OF COMBUSTIBLE MIXTURES

Yu. N. Ryabinin, A. M. Markevich, I. I. Tamm.

(Presented by Academician N. N. Semenov, July 24, 1956)

We have shown [1] that the thermal reaction of the formation of nitric oxide occurred in air which was subjected to a strong adiabatic compression. However, even with pressures of 9000 kg/cm^2, the yield of nitric oxide in the compression of pure air was comparatively small and did not exceed 1%, despite the high degree of quenching of the products of reaction which was obtained by the use of an adiabatic compressor with a movable piston [2]. This resulted from the fact that the temperatures which were obtained on compression of the air were not sufficiently high. A thermodynamic calculation shows that with an increase of the temperature the point of equilibrium is displaced in the direction of the formation of nitric oxide. In order to obtain higher temperatures, without at the same time having recourse to especially high ratios of compression, there was added to the reacting mixture a quantity of combustible gases and oxygen. Higher temperatures can be attained in such mixtures at the expense of the heat of combustion. This heat is liberated at the time of the reaction during the compression of the mixture and is added to the energy which is set free during the adiabatic compression, thereby considerably increasing the temperature of the mixture.

In the present work there was studied the formation of nitric oxide during the compression of mixtures of nitrogen and oxygen which contained the combustible gases methane, hydrogen and carbon monoxide.

The mixtures which were investigated contained such quantities of nitrogen and of oxygen as would be close to the stoichiometric proportions corresponding to NO in the products of reaction. At the same time, the concentration of the combustible gas was chosen in each case so that the heating value of the mixture was constant and amounted to 470 calories per liter of mixture. These experiments were carried out under exactly the same conditions as those of the preceding work [1]. The apparatus functioned in separate strokes, in the course of which the piston in its cylinder completed one movement forward (compression), and one movement backward (expansion). These conditions were attained in each individual case by a special choice of the parameters of the reverse canal [2]. The analysis for the NO content of the gases was carried out in exactly the same manner as in the earlier work; the sample for analysis was taken not later than 1-2 seconds after the completion of an experiment.

Experiments with mixtures containing methane. Methane was taken directly from the Saratov-Moscow main and was not subjected to any additional purification. It contained as impurities the higher hydrocarbons (2-4%) and nitrogen (3-4%). This natural gas made up 5.5% of the total volume of those investigated mixtures which we, in what is to follow, will designate as "methane."

The results of the analyses for the nitric oxide content of the products of compression, i.e., of those gases which were present in the cylinder of the apparatus after compression had taken place, are shown graphically in Figure 1. Curve 1 indicates the yield of NO which was obtained through the compression of air with 5.5% added methane (piston weight, 41.2 g). Curve 2 was obtained for a mixture which was enriched with oxygen. In this case the mixture had the following composition: methane 5.5%, oxygen 52.7%, nitrogen 41.8% (piston weight, 40.5 g).

It was established in these experiments that nitric oxide is formed during the compression of air with 5.5% added methane when the pressure reaches the value of 250 kg/cm² (compression ratio 41). A further increase in the yield of nitric oxide is brought about by a rise in the pressure and at 1400 kg/cm² (compression ratio 102) the yield of NO in the quenched products amounts to about 1.5%. During the compression of a mixture of the composition: methane 5.5%, oxygen 52.7%, nitrogen 41.8%, the formation of nitric oxide begins at a pressure less than 100 kg/cm² (compression ratio 27). An increase in the pressure of compression raises the yield of NO and at pressures of approximately 2000 kg/cm² (compression ratio 130) the yield in the quenched products exceeds 3%.

Experiments with mixtures containing hydrogen. The mixture which was investigated had the composition: hydrogen 18.3%, oxygen 45.4%, nitrogen 36.3%.

The data from the analysis of the products of reaction for NO are given in Figure 1 (Curve 3). In these experiments it was established that the formation of nitric oxide begins at pressures of compression in the neighborhood of 50 kg/cm² (compression ratio 18). The maximum yield of nitric oxide in the quenched products at a pressure of 770 kg/cm² (compression ratio 88) amounted to 2.91 %.

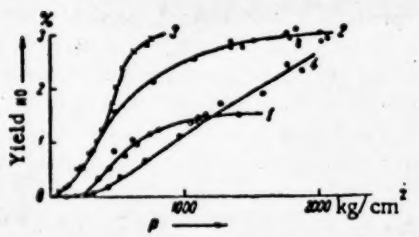

Fig. 1. The dependence of the yield of nitric oxide on the maximum pressure of compression for different variants

Experiments with mixtures containing carbon monoxide. The initial mixture had the composition: carbon monoxide 15.6%, oxygen 46.1%, nitrogen 38.3%. The results of the analysis of the products of compression for NO are represented in Figure 1 (Curve 4). A mixture of this composition lies at the lower ignition limit (the limit of ignition for $CO + O_2$ is at 15.5% CO) [3]. Here is to be found the explanation of the difficulty which was experienced in igniting such mixtures. It is, in all likelihood, for this reason that this curve has a considerably steeper slope than does the curve for either the methane or the hydrogen mixtures. Gas analyses of the products of compression show that for ratios of compression up to 65 the carbon monoxide, for all practical purposes, does not succeed in undergoing combustion and nitric oxide is not formed. The formation of nitric oxide begins at pressures of compression in the neighborhood of 250-300 kg/cm² (compression ratio about 70) when, obviously, the carbon monoxide begins to burn. The maximum yield of nitric oxide for this mixture amounts to 2.41% at a pressure of compression of 1780 kg/cm² and a compression ratio of 142. The experimental data are presented in Table 1 without any correction for the leakage of the gases through the clearance space between the piston and the cylinder walls; they represent the directly measured values. By a conservative estimate this correction would amount to not less than 10-15% in the direction of an increase in the yield of nitric oxide. It should be pointed out that the experimental data are fully reproducible, which makes it possible to obtain clearly expressed relationships.

The data show that the yield of NO varies for the mixtures involving the different combustible gases; the hydrogen mixture requires the smallest pressure of compression, whereas the mixture with carbon monoxide calls for the highest. At the same time, the heats of combustion of the mixtures are equal, as has been pointed out earlier, and are, practically, equal to the heat contents of the products of combustion. Insofar as the formation of NO is a purely thermal reaction [6, 1], this dependence on the nature of the combustion gas must be related to differences in the velocity of the liberation of heat which, in turn, results from differences in the rate of combustion. It is natural that in the case of hydrogen, which has a high rate of combustion and for which the concentration is within the region of ignition, the rate of combustion of the mixture should be greater than it is in the case of carbon monoxide, for which not only is the rate of combustion relatively small but also, the concentration lies at the lower limit of the region of ignition. Thus, the differences which have been noticed in the yield of NO are the result of differences in the kinetics of the processes of combustion. It is possible that in the case of carbon monoxide combustion is incomplete at the moment of the maximum compression and that it can continue even in the process of expansion. Methane occupies an intermediate position between that of H_2 and that of CO, as the experimental data show.

TABLE 1

Compression ratio	Max. pressure compress. (kg/cm²)	Yield of NO (%)	Compression ratio	Max. pressure compress. (kg/cm²)	Yield of NO (%)	Compression ratio	Max. pressure compress. (kg/cm²)	Yield of NO (%)
Methane 5.5%: air 94.5%: piston weight 41.2 g								
38	120	0.00	53	650	0.97	77	1080	1.40
41	240	0.00	53	620	1.06	82	1100	1.43
43	360	0.37	62	750	1.17	86	1140	1.44
46	440	0.50	75	810	1.22	73	1150	1.46
49	550	0.77	75	1060	1.37	102	1410	1.52
44	470	0.82	73	1120	1.39	—	—	—
Methane 5.5%: oxygen 52.7%: nitrogen 41.8%: piston weight 40.5 g								
28	110	0.17	72	1080	2.52	139	2070	2.91
31	132	0.19	100	1340	2.77	95	1520	2.92
32	240	0.56	86	1430	2.77	112	1790	2.92
33	290	0.80	121	1860	2.81	134	2100	2.99
35	315	0.85	101	1340	2.83	105	1760	3.02
40	480	1.59	121	1860	2.84	114	1810	3.08
54	760	2.12	134	2020	2.86	—	—	—
Hydrogen 18.3%: oxygen 45.4%: nitrogen 36.3%: piston weight 40.7 g								
18	65	0.07	38	350	1.01	74	630	2.67
21	110	0.14	41	385	1.24	85	730	2.76
25	150	0.19	48	470	1.75	88	770	2.91
27	200	0.51	55	500	2.01	—	—	—
31	240	0.53	62	550	2.37	—	—	—
Carbon monoxide 15.6%: oxygen 46.1: nitrogen 38.3%: piston weight 40.7 g								
40	130	0.00	75	530	0.37	132	1590	1.89
53	200	0.00	96	720	0.63	154	1880	2.33
77	330	0.05	104	980	1.11	142	1780	2.41
89	440	0.17	120	1280	1.70	—	—	—

The differences in the yield of NO which are observed for the two mixtures containing methane are to be explained by the differences in the nitrogen-oxygen ratio in the products of reaction. It is easy to show, by making use of the Law of Mass Action, that in the case of the mixture which was enriched with respect to oxygen (Figure 1, a; Curve 2) the yield should have been the greater by a factor of 1.6. In actuality, this factor was somewhat larger.

It has long been known that nitric oxide is formed during combustions and explosions and this method of obtaining nitrogen in the combined form has been repeatedly studied. It is only the theoretical work of Ya. B Zeldovich [6] which has shed light on the essence of this process and which has permitted the explanation of those differences in the yield of NO which are observed under different conditions of experimentation. Various methods of investigation have been employed. Yields of NO in the interval 1.4-1.8% have been obtained by compressing combustible mixtures in closed containers with natural quenching [4-6]. In experiments on the combustion of mixtures in various types of continuous-action burners the yield did not exceed 2% [6,7]. An arrangement has also been employed in which forced quenching was obtained by throttling the burned mixture [8]. In these experiments the containers which were employed were of large volume (300 l) and the actual rate of quenching remained low; accordingly the yield of NO did not exceed 0.7%.

At the present time it is known that the velocity of quenching plays an important role in fixing the yield of nitric oxide [6].

With the adiabatic compressor it is possible to obtain high rates of quenching and experiments carried out with it have led to yields of NO up to 3%, which yields considerably exceed those which were realized by the other methods which were cited above. Only Townend and Outridge [9] have succeeded in reaching higher yields and only then because they achieved higher rates of quenching of the mixtures through a method involving a rupture membrane.

It should be pointed out that the method of quenching which is incorporated in the adiabatic compressor is applicable to other processes than those in which the investigated product is a thermodynamically stable substance, as is the case in the reaction of the formation of nitric oxide. This method can also be successfully applied to the study of metastable intermediate compounds, which makes it particularly valuable for the investigation of rapid processes.

LITERATURE CITED

[1] Yu. N. Ryabinin, A. M. Markevich and I. I. Tamm, Proc. Acad. Sci. USSR 95, 111 (1953).

[2] Yu. N. Ryabinin, J. Exptl. Theoret. Phys. (USSR) 23, 461 (1952).

[3] B. Lewis and G. Elbe, Explosions, Flames and Combustion in Gases (Foreign Lit. Press, 1948).

[4] A. G. Ekelbard, R. I. Genkina and M. V. Polyakov, J. Phys. Chem. (USSR) 13, 464 (1939).

[5] M. V. Polyakov and R. I. Genkina, Acta Physicochim. URSS 11, 443 (1939).

[6] Ya. B. Zeldovich, P. Ya. Sadovnikov and D. A. Frank-Kamenetsky, The Oxidation of Nitrogen During Combustion (Acad. Sci. USSR Press, 1947).

[7] D. M. Newitt and F. G. Lamont, Proc. Roy. Soc. (London) 139, 83 (1933).

[8] T. Hausser, J. Soc. Chem. Ind. 41, 253 (1922).

[9] D. A. Townend, L. E. Outridge, Proc. Roy. Soc. (London) 139, 75 (1933).

Received July 23, 1956

The Institute of Chemical Physics
The Academy of Sciences of the USSR

THE MECHANISM OF VULCANIZATION IN THE PRESENCE OF 2-MERCAPTOBENZOTHIAZOLE

B. A. Dogadkin, I. A. Tutorsky and D. M. Pevzner

(Presented by Academician L. N. Nazarov, September 3, 1956)

The mechanism of the action of 2-mercaptobenzothiazole (Kaptax, MBT) one of the most commonly employed accelerators of vulcanization, remains unclear. L. Wistinghausen [1] and B. A. Dogadkin and D. M. Pevzner (1951, published) showed that MBT is consumed in the vulcanization, but these authors, because of the crudity of their methods, did not obtain quantitative relationships.

In the present work there has been employed a preparation of the MBT which was tagged in the thiazole ring by the radioisotope S^{35}. The synthesis of this compound was carried out in the following manner. MBT, tagged in both of its sulfur atoms, was first synthesized from phenyl isothiocyanate and elementary S^{35} [2]. The resulting MBT was then heated in a sealed ampule with an excess of inactive elementary sulfur for six hours at a temperature of 140°. Under these conditions the exchange reaction between the elementary sulfur and the sulfur of the mercapto group of the MBT reaches equilibrium [3]. The activity of the resulting MBT fell to one-half of the original value. In this way the benzothiazole radical was tagged, by the introduction into the molecule of MBT of the radio-isotope S^{35} which does not exchange with elementary sulfur, under the conditions of vulcanization, and it thus became possible to measure simultaneously the velocity of the addition of the sulfur and the velocity of addition of the accelerator to the rubber.

Vulcanization was investigated in a mixture containing natural rubber (NR) which had been extracted from a benzene solution and dried, and also, in a mixture containing a sodium-butadiene rubber (SKB). The compositions of the mixtures are indicated in Table 1. The combined sulfur (the elementary sulfur and also that which enters into the structure of the accelerator) was determined in the vulcanizate, after extraction with acetone, by means of oxidation with a mixture of HNO_3 and Br_2 in the presence of MgO [4]. The MBT which was combined with the rubber was determined by a radiometric method [5]. From the maxima of the swelling of the vulcanizate in acid solution there was calculated the number of cross-linkages, using the equation of Flory and Rehner [6].

In Figure 1 data are given concerning the kinetics of the addition of sulfur and MBT during the process of vulcanization of NR at 121°. The reaction of addition of the sulfur to the rubber and that of addition of the accelerator proceed in a similar fashion. In the presence of the activator ZnO there is observed a more intensive combination of the accelerator, whereas this activator does not influence the velocity of the combination of the sulfur.

A small quantity of the MBT combines with the rubber even in the roller during the preparation of the mixture. In order to interpret the mechanism of this combination of the MBT during the rolling, purified natural rubber* with an addition of one part by weight of MBT was subjected to a 20 minute rolling in the absence of atmospheric oxygen. The masticated rubber was then separated into fractions in a binary benzene-methyl alcohol solvent by the reduction of the temperature. The viscosity was determined for each fraction in benzene

* The rubber was purified by a 20 hour extraction with cold acetone in an atmosphere of pure nitrogen.

TABLE 1

Composition of mixture	Temperature of vulcanization (°C)	Time of vulcanization (min)	Combined elementary S (g-atoms/g) · 10⁴	Combined MBT (moles/g) · 10⁵	Number of cross linkages (moles/g) · 10⁴	Number of molecules of MBT reacted per cross linkage
NR-100	121	0	—	1.00	—	—
S - 4		20	3.52	2.84	6.27	0.29
MBT - 2		40	5.10	3.16	8.97	0.24
		60	5.65	3.72	10.80	0.25
Neozon D-1*		80	6.22	4.11	10.26	0.30
ZnO - 5		100	7.16	4.12	10.88	0.28
Stearic acid - 2		120	8.38	4.22	14.0	0.23
SKB - 100	140	0	—	0.37	—	—
S - 2		5	3.88	0.47	0.45	0.20
MBT - 1		10	5.04	0.56	0.91	0.20
Neozon D - 1		20	5.97	0.92	1.20	0.45
		30	5.95	1.38	1.69	0.63
		40	5.95	1.36	1.66	0.59
		60	6.11	1.66	2.19	0.58

* (Phenyl beta-naphthylamine).

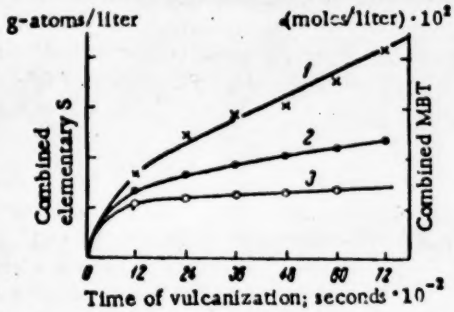

Fig. 1. The kinetics of the addition of sulfur (1) and MBT during the vulcanization of natural rubber in a mixture with ZnO (2) and without ZnO (3).

TABLE 2

Number of fraction	Mn	Amount of combined MBT (moles/liter) · 10³	[η]
Unfractionated	—	—	12.0
1	0.053	3.21	27.0
2	0.091	5.45	24.5
3	0.110	6.22	9.2
4	0.071	4.28	8.0
5	0.090	5.39	5.5

solution and the quantity of the combined MBT was evaluated by a radiometric method. It is to be seen from Table 2 that the amount of the combined MBT increases, up to a certain point, with the increase of the order number of the fraction; that is to say, with a decrease of the molecular weight. Such behavior can be explained by the fact that the MBT adds to the polymer radicals which are formed during mechanical rupture. The rupture of the molecular chain of rubber occurs, in all likelihood, at a bond which unites allyl groups, since this bond is weakened by the effect of conjugation to approximately 45 kcal/mole. The radicals which thus arise interact with the molecules of the MBT according to the scheme:

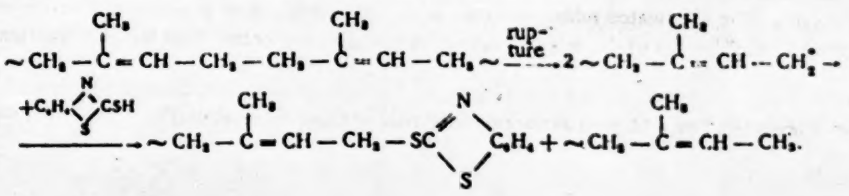

As a result the content of MBT in the low molecular fraction is considerably greater than it is in the high molecular fraction. If the MBT reacted at the double bonds there would not be observed this distribution of it among the fractions of the masticated rubber.*

The MBT which unites with the rubber during the rolling also accelerates the process of vulcanization, but to a considerably smaller degree.

In Fig. 2, there is shown the kinetics of the addition of sulfur and MBT in the process of vulcanization of SKB. In this case there is also observed the similarity between the kinetic curves for the addition of sulfur and for the addition of MBT. At the moment of the complete union of the sulfur (30 minutes) the velocity of the addition of the MBT sharply diminishes, although the concentration of the latter in the mixture is still rather high. This fact indicates that the reaction of MBT with the rubber proceeds with appreciable velocity only in the presence of sulfur, a fact which agrees with the data concerning the catalytic action of sulfur on the addition of mercaptans to olefins [7]. Actually, our experiments have shown that a subsequent addition of the sulfur into the vulcanizate during its swelling (in the stage of the depletion of the free sulfur) leads, once more, to an acceleration of the reaction of addition of MBT to the rubber (Fig. 2, 3).

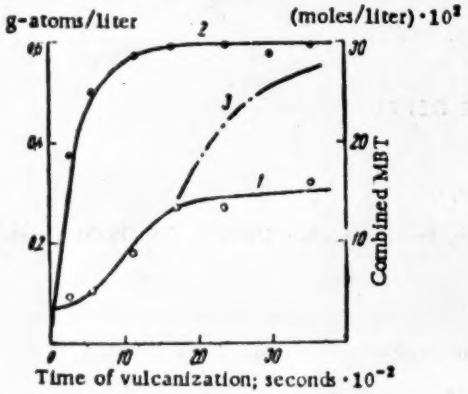

Fig. 2. The kinetics of the addition of MBT (1) and sulfur (2) during vulcanization; (3) after the introduction of 2% sulfur by diffusion from solution.

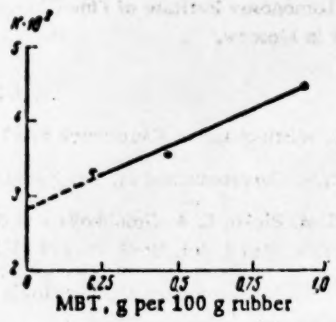

Fig. 3. The relationship between the velocity constant for the addition of sulfur and the concentration of MBT.

The kinetics of the addition of sulfur to rubber, in the presence of MBT, is satisfactorily described as a reaction of first order in the sulfur. The velocity constants calculated according to such an equation vary linearly with the concentration of the MBT (Figure 3). The energy of activation for the vulcanization of SKB under the customary ratio of sulfur to accelerator proves equal to 20.6 kcal/mole.

The ratio between the MBT consumed and the number of cross-linkages (see Table 1) is considerably less than unity and in the principal phase of the vulcanization this ratio remains constant. A calculation shows that per one combination of the accelerator there occurs approximately two instances of the formation of cross-linkages.

The experimental data which are presented here indicate the reciprocal character of the interaction of sulfur, MBT and rubber. This action clearly follows the scheme proposed earlier [8]:

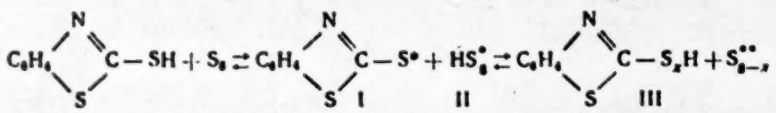

* In the presented scheme the MBT reacts in the Thiol form; the interaction in the thione form leads to exactly the same result for the distribution among the fractions.

Under the conditions of vulcanization the radical 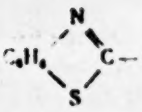 either interacts with the α methylene

groups of the molecular chains of the rubber (reducing to MBT) or adds at a point where there is a double bond. In either case there are formed polymeric radicals which are capable of interaction, either between themselves or with reactive low molecular groups. The radical $HS_n^{\bullet}$ unites with a molecule of rubber forming polymeric mercaptans; oxidation of the latter, or their interaction at double bonds, leads to the production of polysulfide bonds between the rubber chains. The recombination of the radicals I, II results in the formation of 2-benzothiazolehydropolysulfide (III), which in turn separates out a variable number of atoms of sulfur in the form of biradicals, which latter directly unite the molecular chains of the rubber at the positions of double bonds.

In the complicated sequence of the reactions of vulcanization the initial process is the interaction of the MBT and the sulfur. For this reason the speed of the combination of the sulfur and the rubber, as has already been pointed out, is found to depend linearly on the concentration of the MBT.

The M. V. Lomonosov Institute of Fine Chemical Technology in Moscow.

Received September 2, 1956

LITERATURE CITED

[1] L. Wistinghausen, Kautschuck 5, 57 (1929).

[2] E. N. Guryanova and M. Ya. Kaplunov, Proc. Acad. Sci. USSR 94, 53 (1954).

[3] G. A. Blokh, E. A. Golubkova and G. P. Miklukhin, Proc. Acad. Sci. USSR 90, 201 (1953); E. N. Guryanova, Proc. Acad. Sci. USSR 98, 229 (1954).

[4] I. Franta, Gumarenska Technologia (Prague, 1953).

[5] B. A. Dogadkin, Z. N. Tarasova and M. Ya. Kaplunov, Factory Lab. 1955 No. 4, 296.

[6] P. Flory and L. Rehner, J. Chem. Phys. 11, 512 (1943).

[7] S. O. Jones and E. E. Reid, J. Am. Chem. Soc. 60, 2452 (1938).

[8] B. Dogadkin and I. Tutorsky, Proc. Acad. Sci. USSR 108, 259 (1956).

AN APPROXIMATION METHOD FOR CALCULATING THE SURFACE TENSION OF METALS

S. N. Zadumkin

(Presented by Academician A. N. Frumkin, June 21, 1956)

A fundamental defect in the existing calculations of the surface tension of metals [1-7] is, from our point of view, to be found in the fact that the various authors have more or less arbitrarily assigned values to that quantity Z, the number of free electrons per metal atom, which enters into the different theoretical equations. Some have chosen the maximum valence of the atom as the value of Z, others have used the mean valence, still others have fixed on one free electron per atom, and so on. Such an important metallic characteristic as the quantity Z should, however, as was justly pointed out in [8], be determined, in the first instance, on the basis of experimental data.

In addition, most of these calculations of σ have given values which were supposed to be valid at the absolute zero and they have not, therefore, shown the dependence of the surface tension of the metal on the temperature. The question of this temperature dependence of σ for metals has been considered in various works [9-11].

It has seemed to us to be desirable to construct such a theory of the surface tension of metals as would show in its final equations for σ only those constants of the metals which are readily determined experimentally.

At various times and by various authors there have been proposed empirical and semi-empirical formulas for the evaluation of σ for metals; these have involved the work of removal of electrons from the metal [12, 13]; the heat of vaporization of the metal [14], and so forth. The values of σ determined from these equations are in better agreement with the experimental data than are those obtained from the theoretical formulas.

In the present work we would like to develop an approximation method for the calculation of σ from the heats of vaporization of the metals.

We take as our starting point the following variant of the polar model of the metal. Let us consider a metal in the solid state and at the temperature T. We will suppose that, on the average, the values of the coordinates of the positive ions of the metal coincide with those of the crystal lattice points, but that the mean values of the coordinates of the free electrons are so symmetrically distributed within the crystal lattice-work that there is formed an electron lattice of exactly the same structure as the positive ion lattice, displaced, however, relative to the latter. At the same time, the unit cells and the basic planes of the crystal lattice must remain neutral.

It follows that, in the polar model which we are considering, there will be a coordinate ion-electron lattice which, in the case of a face-centered cubic metallic lattice, for example, will be of the cubic type of NaCl, with the shortest distance between the cations and the "anions" equal to $a/2$, where a is the period of the metallic lattice.

In [11] we have given the following equation for the coefficient of surface tension of metals:

$$\sigma = -n_s \frac{\Delta f}{f_{kv}} [3kT \ln 2 - 2(E_0' - E_0)], \tag{1}$$

where for the proposed model of the metal f_{kv} is the coordination number of the cations relative to the "anions"; Δf is the number of missing nearest "anions" per cation on the metal surface; E_0 and E_0' are the free energies at T = 0, which a particle inside the metal would have if its mean frequencies of vibration were respectively equal to ν and $\nu/\sqrt{2}$ and its coordination numbers were f_{kv} and $f_{kv}/2$; the values of E_0 and E_0' are calculated in the following way. Since E_0 is the energy which is required for the decomposition of the metal into free ions and electrons at the temperature T = 0, it follows that introducing into the metal, first this quantity of energy, then the energy $\sum_{i=1}^{z} eV_i$, where $V_1, V_2, \ldots$ designate the first, the second, and so forth, ionization potentials of the atom, and, finally, introducing the heat of sublimation at the absolute zero of temperature, L_0, there results the starting state of the metal. From this there results:

$$|E_0| = \sum_{i=1}^{z} eV_i + L_0. \tag{2}$$

$$|E_0'| = \sum_{i=1}^{z} eV_i + L_0'. \tag{3}$$

Introducing (2) and (3) into (1) and considering, just as in [11], that the free energy is a linear function of f_{kv}, we find

$$\sigma = -n_s \frac{\Delta f}{f_{kv}} [3kT \ln 2 - L_0]. \tag{4}$$

Through equation (4) it is possible to obtain the value of the surface tension σ for the various faces of an ideal single crystal at the temperature T.

Ya. I. Frenkel has shown [15] that the crystal in the state of equilibrium possesses surface roughness because of the fluctations of the temperature. For this reason we will suppose that on the surface of the crystal only local order is retained, which corresponds to an orientation of all the basic faces of the elementary ion-electron cell. In this case the surface tension of the crystal will be expressed by

$$\sigma = -\bar{n}_s \frac{\overline{\Delta f}}{f_{kv}} [3kT \ln 2 - L_0]. \tag{5}$$

where $\bar{n}_s$ is the mean number of particles per unit of surface; $\overline{\Delta f}/f_{kv}$ is the mean value of the relative number of missing neighbors ("anions") per surface positive ion of the metal. The values of $\bar{n}_s$ and $\overline{\Delta f}/f_{kv}$ are found as follows. Let us consider some positive ion in the metal and compare the probability of its existence on a unit area of the metallic surface with the probability of its existence on a unit area of a plane parallel to this surface and lying inside the metal; we obtain

$$w''/w' = e^{-\bar{w}_i/kT}, \tag{6}$$

where w_i is the work which is required for the transfer of an ion from the interior of the metal onto the surface, a quantity which is proportional to the number of missing neighbors, Δf_i, on the surface. On the other hand, the ratio of the probabilities w^*/w' must be equal to the ratio of the number of ions $n_i^{(s)}$ on unit surface area of the metal to the number of the ions $n_0^{(s)}$ on a unit area inside the metal. It thus follows from (6) that

$$n_i^{(s)} = n_0^{(s)} e^{-w_i/kT}. \tag{7}$$

Since there are on the surface of the metal $n_i^{(s)}$ particles per cm^2 belonging to the i-th face of the cubic crystal and having an excess energy w_i it follows that

$$\sum_i \frac{n_i^{(s)}}{f_i^{(s)}} S_i = 1, \tag{8}$$

where S_i is the area of the i-th face; $f_i^{(s)}$ is the number of ions entering into the unit surface cell for that same face. From (7) it follows that

$$\bar{n}_s = n_0^{(s)} \sum_i x_i, \tag{9}$$

where $x_i = \exp\left[-\frac{\alpha \Delta f_i}{kT}\right]$ (Δ_{fi} is the number of missing neighbors for the i-th face)

The mean value of the relative number of the missing neighbors on the surface of the metal will be

$$\frac{\overline{\Delta f}}{f_{kv}} = \frac{\sum_i \frac{\Delta f_i}{f_{kv}} x_i}{\sum_i x_i}. \tag{10}$$

It is known that in a crystal of the cubic system there are six (100), twelve (110), and eight (111) faces, for which the number of missing neighbors is respectively equal to 1, 2 and 3 when these planes lie on the surface of the metal. For each of such planes $f_i^{(s)} = 2$. If (7) is taken into account and the relations $S_{(100)} = a^2$, $S_{(110)} = a^2\sqrt{2}$, $S_{(111)} = a^2\frac{\sqrt{3}}{2}$, are introduced, equation (8) can be written as

$$\frac{n_0^{(s)}}{n_{(100)}^{(s)}}\left(6x_{(100)} + 12\sqrt{2}\,x_{(100)}^2 + 8\frac{\sqrt{3}}{2}x_{(100)}^3\right) = 1, \tag{11}$$

where $x_{(100)} = \exp\left[-\frac{\alpha \Delta f_{(100)}}{kT}\right]$ ($\Delta f_{(100)}$ is the number of missing neighbors for the (100) face); $n_{(100)}^{(s)}$ is the number of particles per cm^2 of the (100) face. The calculations have been carried out for a surface which is parallel to a (100) plane within the crystal. Taking $n_0^{(s)} = n_{(100)}^{(s)}$ there follows from (11) the value of $x_{(100)}$

which satisfies the condition $0 \leq x_{(100)} \leq 1$; $x_{(100)} = 0.122$. From (9) and (10) there are obtained $\bar{n}_s = 0.924\, n^{(s)}_{(100)}$ and $\overline{\Delta l}/l_{kv} = 0.201$. Differentiating equation (5) with respect to temperature and neglecting the temperature dependence of $\overline{\Delta l}/l_{kv}$ we find the magnitude of the temperature coefficient, γ, of the surface tension of the metal:

$$\gamma \equiv \frac{d\sigma}{dT} = -\left(3k\frac{\overline{\Delta l}}{l_{kv}}\bar{n}_s \ln 2 + 2\alpha\sigma\right), \qquad (12)$$

TABLE 1

Metal	$n^{(s)}_{100}\cdot 10^{14}$	$l_0 \cdot 10^{12}$ erg/atom	Temperature °K	σ ergs·cm^{-2} calc.	σ ergs·cm^{-2} experimental	γ ergs·cm^{-2} deg^{-1} calc.	γ ergs·cm^{-2} deg^{-1} experimental
Ag	11.1	4.70[20]	1268	898	751—940 923 [18]	—0.123	—0.13 [18]
Au	110.0	5.76	1473	1100	581—1420 1120 [18]	—0.092	—0.10 [18]
Cu	14.6	5.27	1473	1380	1103—1400 1154 [18]	—0.204	—
Pb	7.62	3.50	600	470	424—536 461 [18]	—0.078	—(0.06—0.25) [18]
Al	11.5	4.15	973	832	520—914 860 [18]	—0.103	—(0.135—0.35) [18]
Pt	12.0	8.75	2273	1815	1819 [18]	—0.097	—0.1
γ-Fe	14.6	7.43	1843	1970	950—1210 1720 [21]	—0.12	—
Ca	6.61	2.71	1123	298	320	—0.048	—
β-Co	16.0	8.3	1763	2320	—	—0.142	—
β-Ni	16.2	6.97	1725	1957	1735 [18]	—0.132	—
β-Tl	8.50	3.03	573	454	436—485 [18]	—0.086	—

where α is the coefficient of linear expansion of the metal. For metals of the face-centered cubic system there are presented in Table 1 the results of calculations of the surface tension according to equation (5) and the temperature coefficient according to equation (12). In this same table there are given the experimental values of σ and γ for molten metals, the range of these experimental values from the measurements of various authors, the most probable value of σ according to the analysis of the data in [16] and the results of the most recent measurements. In all cases where this was possible, we have taken σ_{exp} from measurements in vacuum. In the case of the experimental values of the heat of sublimation, the figures shown have been recalculated by Rabinowitsch and Thilo [17] to the absolute zero of temperature; the value of Ag is from [20].

It is to be seen from Table 1 that despite the crudeness of the proposed metallic model and the approximations involved in all the calculations, the values obtained for σ and γ agree very well with the most probable experimentally determined values, especially in the case of Pb for which the data is of considerable accuracy. In the most of the other cases the deviation of σ_{cal} from σ_{exp} does not amount to more than 5% and only in Cu γ-Fe and β-Ni is it equal to approximately 10-20%.

Karbardin State Pedagogical Institute

Received November 9, 1956

LITERATURE CITED

[1] Ya. G. Dorman, Proc. Acad. Sci. USSR 41, No. 9, 386 (1943).

[2] D. V. Gogate, D. S. Kothari, Phil. Mag., 7, 20 (1935).

[3] A. G. Samoilovich, J. Exptl.-Theoret. Phys. 16, 2 (1946).

[4] A. E. Glauberman, J. Exptl.-Theoret. Phys. USSR 23, 121 (1949).

[5] L. M. Spitkovsky, J. Phys. Chem. 24, 1091 (1950).

[6] A. B. Scott, Phil. Mag., 45, No. 370, 1173 (1954).

[7] A. Kh. Breger and A. A. Zhukhovitsky, J. Phys. Chem. 20, No. 4-5, 355 (1946).

[8] V. L. Ginzburg, G. P. Motulavich, Bull. Acad. Sci. USSR, Phys. Ser. 18, No. 6 (1954).*

[9] Ya. I. Frenkel, The Kinetic Theory of Liquids (1945).

[10] A. Kh. Breger, J. Phys. Chem., 22, 920 (1948).

[11] S. N. Zadumkin, Proc. Acad. Sci. USSR, 101, No. 3, 507 (1955).

[12] S. N. Zadumkin, J. Phys. Chem. 27, 502 (1953).

[13] L. L. Kunin, Proc. Acad. Sci. USSR, 79, No. 1, 93 (1951).

[14] S. N. Zadumkin, Proc. Acad. Sci. USSR 92, No. 1, 115 (1953).

[15] Ya. I. Frenkel, The Theory of Solid and Liquid Bodies (Moscow–Leningrad, 1934).

[16] L. L. Kunin, Surface Phenomena in Metals (1955).

[17] E. Rabinowitsch, E. Thilo, Zs. f. phys. Chem., 6, 298 (1930).

[18] A. M. Korolkov, Bull. Acad. Sci. USSR, Div. Tech. Sci. 1956, No. 2, 35.

[19] W. D. Kingery, M. I. Humenik, J. Phys. Chem., 57, No. 3, 359 (1953).

[20] H. M. Schadel, C. E. Birchenall, J. Metals, 188, 1134 (1950).

[21] F. A. Halden, W. D. Kingery, J. Phys. Chem., 59, No. 6, 557 (1955).

* Original Russian pagination see C. B. Translation.

THE ENERGY OF ACTIVATION OF THE ELEMENTARY REACTION RO_2 + RH IN THE OXIDATION OF n-DECANE

D. G. Knorre, Z. K. Maizus and N. M. Emanuel

(Presented by Academician V. N. Kondratyev, July 24, 1956)

At the present time there does not exist a direct method for the study of the elementary steps involved in the process of liquid oxidation of hydrocarbons. However, in recent years some information concerning these elementary steps of the oxidation of liquid hydrocarbons has been obtained from the reaction kinetics by utilizing measurements by the method of the photochemical after-effect[2] and the rotating sector [4]. All of these results refer to the initial stages of the oxidation, when the only product present in the system is a hydroperoxide, the first oxidation product.

In the treatment of the experimental data it is assumed in every case that the formation of the hydroperoxide proceeds according to a chain reaction of the type:

$$R^{\cdot} + O_2 \rightarrow RO_2^{\cdot} \quad (1)$$

$$RO_2^{\cdot} + RH \rightarrow RO_2H + R^{\cdot} \quad (2)$$

Under sufficiently high pressures of oxygen, when the principal cause of chain rupture is the recombination of the radicals RO_2, it follows from this scheme [5] that the velocity of oxidation should be equal to:

$$w = w_i^{1/2} \frac{k_2}{k_3^{1/2}} [RH], \quad (3)$$

where w_i is the velocity of initiation, k_2 is the bimolecular velocity constant for the reaction of chain propagation, and k_3 is the velocity constant for the recombination of the radicals RO_2. The criterion for the applicability of equation (3) is the absence of a dependence on the partial pressure of oxygen in the gaseous phase for the velocity of oxidation, over the range of pressures investigated. Knowing the velocity of initiation and determining the velocity of oxidation, by equation (3) there can be calculated the ratio $k_2/k_3^{1/2}$ and the temperature dependence of this ratio, i.e., the magnitude of $E_2 - \frac{1}{2} E_3$. Since the quantity E_3, the energy of activation for the recombination of pairs of radicals, is clearly close to zero, there appears at the same time the possibility of determining the energy of activation for reaction (2).

In the present work we have attempted to apply an analogous method for evaluating E_2 in the oxidation of n-decane. The difficulties here are to be found in the fact that it is not possible to consider the peroxide as the single product of the oxidation of the n-decane, because along with it, and in comparable quantities, there are, from the very beginning of the oxidation, formed other types of compounds—alcohols, carbonyl compounds, acids and esters [6]. In preceeding work on the oxidation of n-decane it was shown, however, that all of these products result from the disintegration of hydroperoxide; that is to say, that the first step in the oxidation of this

compound, just as in the oxidation of other types of hydrocarbons, is the formation of hydroperoxides. The peculiarity of the oxidation of n-decane is the fact that, even in the earlier stages of the oxidation, the process of the disintegration of the hydroperoxide is to a significant degree superimposed on its formation according to equation (2). The breakdown of the hydroperoxide follows a monomolecular law with an energy of activation E = 24 kcal [7] and accordingly

$$w = \frac{d[\mathrm{ROOH}]}{dt} = k_3[\mathrm{RO_2}][\mathrm{RH}] - k_4[\mathrm{ROOH}]. \qquad (4)$$

where k_4 is the velocity constant for the peroxide disintegration.

Hydrocarbon oxidations are chain processes with degenerative branching of the chains. The autoacceleration of the oxidation of the n-decane shows that it is no exception to this rule. The degenerative branching is brought about, as is commonly supposed at the present time, by the breakdown of the hydroperoxide molecule into two free radicals:

$$\mathrm{ROOH} \rightarrow \mathrm{RO}\cdot + \cdot\mathrm{OH}. \qquad (5)$$

In the case of decyl hydroperoxide the energy of activation for this reaction was determined by Twigg [8] and proved to be equal to $E_5 = 31.7$ kcal. It should be kept in mind that the velocity constant for reaction (5), k_5, certainly does not correspond in magnitude to k_4, since the breakdown according to scheme (5) is not the only means of decomposition of the peroxide.

Supposing that the velocity of initation and the velocity of chain rupture are, for all practical purposes, equal and considering that rupture occurs, fundamentally, because of the recombination of the radicals RO_2, there is obtained

$$k_4[\mathrm{ROOH}] = k_2[\mathrm{RO_2}]^2, \qquad (6)$$

which makes it possible to rewrite equation (4) in the form:

$$w = k_3\sqrt{\frac{k_2}{k_4}}[\mathrm{RH}]\sqrt{[\mathrm{ROOH}]} - k_4[\mathrm{ROOH}].$$

The maximum velocity of the accumulation of the hydroperoxide is determined from the condition $dw/dt = 0$ or, which is the same thing, $dw/d[\mathrm{ROOH}] = 0$, since, in that region of the kinetic curve which is of interest here, $d[\mathrm{ROOH}]/dt > 0$. There is thus obtained

$$w_{max} = \frac{k_3^2 k_2 [\mathrm{RH}]^2}{4k_2 k_4},$$

or for the effective energy of activation of the oxidation E, determined from the temperature effect,

$$E = 2E_3 + E_2 - E_5 - E_4. \qquad (7)$$

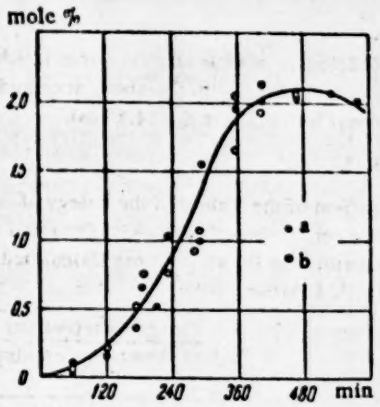

Fig. 1. The kinetic curves for the accumulation of peroxide in the 130° oxidation of n-decane by oxygen (a) and by a 1:1 mixture of oxygen and nitrogen (b).

Since the quantities E_4 and E_8 are known and E_3 the energy of activation for the recombination must be close to zero, a determination of E makes it possible to calculate E_2, the energy of activation for the elementary reaction $RO_2 + RH$ in the oxidation of n-decane.

The oxidation of n-decane was carried out in the oxidation cell which was described in our earlier work [6]. In order to convince ourselves of the correctness of the supposition that the principal cause of chain rupture is to be found in the recombination of the radicals RO_2, we obtained the kinetic curve for the accumulation of the peroxide in the course of the oxidation of the n-decane at 130° and under two different partial pressures of oxygen: 1 and 0.5 atm (the latter pressure was obtained by blowing through the n-decane a 1:1 mixture of nitrogen and oxygen). The results are given in Figure 1. It is obvious that the formation of the peroxide in a jet of oxygen proceeds with exactly the same velocity as it does in a jet of nitrogen and oxygen. There is thus confirmed the correctness of the condition (6), since it is only in the case that the chain rupture is due to the recombination of the radicals RO_2 that the velocity of oxidation is independent of the pressure of the oxygen.

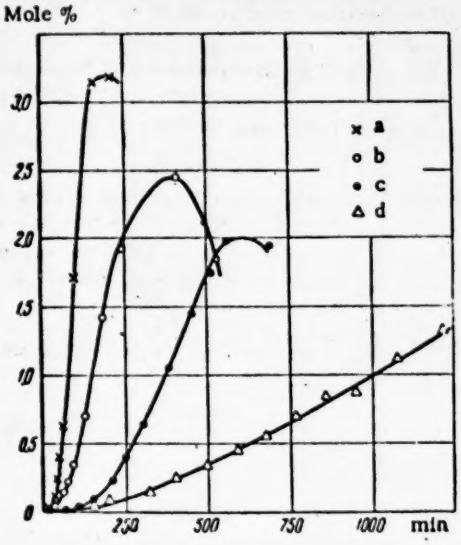

Fig. 2. The kinetic curves for the accumulation of peroxide in the oxidation of n-decane by oxygen at the temperatures: a) 150°, b) 140°, c) 130°, d) 120°

In Figure 2 there are shown the kinetic curves for the accumulation of the peroxide during the oxidation of n-decane at various temperatures. In Figure 3 there is plotted an Arrhenius curve showing the maximum velocity of the accumulation of the peroxide as a function of the temperature. From this relationship there is obtained for the over-all energy of activation a value E = = 31 kcal which, according to equation (7), gives a value of 11.5 kcal for the magnitude of E_2.

In order to decide as to the plausibility of such a result for E_2, we have evaluated the latter theoretically by the formula of Polanyi. According to this formula, for an endothermic reaction

$$E = |q| + 11.5 - 0.25|q|.$$

where q is the heat of reaction [9].

For reaction (2) the heat effect is equal to the difference in the energy of rupture of the OH bond in hydrogen peroxide and the energy of rupture of the CH bond in the original hydrocarbon.

The energy of rupture of the secondary CH bond in n-decane, which is the one which is preferentially subjected to oxidation [10], should not in any way essentially differ from that same quantity in propane. According to the data which is presented in the monograph of Kottrel, this quantity is equal to 94 kcal. The energy of the OH bond in decyl hydroperoxide should not markedly differ from the energy of this bond in hydrogen peroxide, since it is scarcely likely that the R group in the hydroperoxide exerts any considerable influence on the OH bond, from which it is separated by two simple bonds. For hydrogen peroxide $q_{H-O_2H} = q_{HO-OH} + 2q_{O-H} - q_{O=O} - q_{H-O_2}$.

The respective bond energies are to be found in the Kottrel monograph [11] (q_{HO-OH} = 48 kcal, q_{O-H} = 103 kcal, $q_{O=O}$ = 117 kcal) and in the work of Foner and Hudson [12] (q_{H-O_2} = 47 kcal) from which it follows that the OH bond energy in hydrogen peroxide must be equal to 90 kcal. With the above accepted values of the bond energies for OH and for CH, it follows from the Polanyi formula that E_2 = 14.5 kcal.

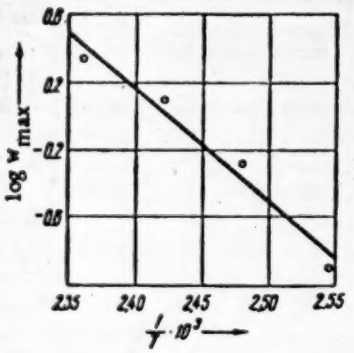

Fig. 3. The dependence on temperature of the maximum rate of accumulation of the peroxide.

TABLE 1

A Comparison of the Values of the Energy of Activation for the Reaction RO_2 + RH Obtained from Experimental Data with those Calculated by Polanyi's Equation

Hydrocarbon	Energy of activation	
	from kinetic data	according to Polanyi
Ethyl linoleate [1]	4	5
Tetralin [2]	4.3	6.5
Squalene [1]	7	7
Methyl oleate [1]	8	7
n-Decane	11.5	14.5

In view of the approximate character of the Polanyi equation and the lack of precision for the values of the bond energies the results obtained should be considered satisfactory. It should be noted that if for the CH bond energy there is accepted a value of 89 kcal [9] (instead of 94 kcal) calculation then gives k_2 = 11.5 kcal, i.e., a result agreeing well with the experimental.

It is interesting to check and to see how far, in general, the Polanyi formula is applicable to such reactions as these. In the first column of Table 1 there are presented the values of E_2 (the energy of activation for the reaction RO_2 + RH) which have been obtained by various authors from the kinetic data and Equation (3) (there is included the value, found in the present work, for n-decane). In the second column there are shown the values of E_2 calculated for these same hydrocarbons by the formula of Polanyi (the value for the CH bond energy was taken from data applying to simpler hydrocarbons of the same structure).

It is obvious from Table 1 that the energies of activation for the elementary reaction RO_2 + RH as obtained from the Polanyi equation agree very well with those which are found experimentally.

Received July 19, 1956

LITERATURE CITED

[1] J. L. Bolland and G. Gee, Trans. Faraday Soc. 42, 236 (1946).

[2] C. H. Bamford and M. J. S. Dewar, Nature 163, 215 (1949).

[3] L. Bateman and G. Gee, Trans. Faraday Soc. 47, 155 (1951).

[4] C. H. Bamford and M. J. S. Dewar, Proc. Roy. Soc. (London) 198 A, 252 (1949).

[5] L. Bateman, Quart. Revs. (London) 8, 147 (1954).

[6] D. G. Knorre, Z. K. Maizus and N. M. Emanuel, J. Phys. Chem. 29, 710 (1955).

[7] L. S. Vartanyan, Z. K. Maizus and N. M. Emanuel, J. Phys. Chem. 30, 665 (1956).

[8] G. H. Twigg, Discussions Faraday Soc. 14, 240 (1953).

[9] N. N. Semenov, Certain Problems of Chemical Kinetics and Reactivity (Acad. Sci. USSR Press 1954).

[10] J. L. Benton and M. M. Wirth, Nature 171, 269 (1953).

[11] T. Kottrel The Strength of the Chemical Bond (Foreign Lit. Press, 1956).

[12] S. N. Foner and R. L. Hudson, J. Chem. Phys. 23, 1364 (1955).

AN ELECTRON MICROSCOPIC INVESTIGATION OF THE STRUCTURE OF THE SPHEROIDAL GRAPHITE IN CAST IRON

E. A. Leontyev, V. M. Lukyanovich and B. S. Milman

(Presented by Academician M. M. Dubinin, July 30, 1956)

The introduction into cast iron of several hundredths of a percent of certain elements (in particular Mg, Ce, and Ca) leads to the crystallization of the graphite inclusions, not in the usual laminar form, but rather in the form of spheroids of varying degrees of curvature. This makes it possible to increase the yield strength of the cast iron by a factor of 2-3 and gives to the metal a certain plasticity, retaining, at the same time, a number of its technically valuable properties and the economic advantages of its method of production. The new high-yield cast iron has in many cases completely replaced steel, wrought iron and nonferrous alloys, so that the problem of its further improvement has acquired great industrial significance.

In this connection a number of works have recently been devoted to the investigation of this spheroidal graphite and several hypotheses have been advanced concerning its structure [1-5]. Because of the limited amount of experimental material this question has, however, not been finally settled. The authors of these works in which the electron microscope was used [2, 4, 5] have limited themsleves to the investigation of the customary metallographic sections, but since the surfaces of the graphite inclusions of the latter were, of necessity, strongly deformed in the processes of preparation, such works cannot possibly give trustworthy information for the understanding of the structure of the graphite.

The work [6] is an exception since here valuable information concerning this structure was obtained through cathodic corrosion of the polished sections.

We have carried out an electron microscopic investigation of the undeformed surfaces of the graphite inclusions, using the method of replicas, and we have also investigated their internal structures by chemically cleaving them and photographing the products of their disintegration. The spheroidal graphite which was studied was separated out from a cast iron containing Mg by means of electrolytic dissolution (Figure 1). A 20% solution of HCl served as the electrolyte; the current strength was 5 amp. The separated graphite was washed with an alkaline solution and with water and was then dried.

The problem of obtaining replicas from the surfaces of the separated spheroidal particles of about 100 μ diameter was a difficult one. After a series of attempts we fixed on the following technique. On the surface of a small glass plate there was laid down a thin layer of 0.1% collodion solution and after 1-2 minutes the powdered graphite was sifted onto it. The excess was then shaken off so that the collodion film remained covered with a graphite layer which was one grain in depth. The conditions were so chosen (by observation in a stereomicroscope) that $^1/_3$–$^1/_4$ of each globule, by height, was wetted by the solution. After 24 hours, when the film had completed its solidification, molten sulfur was poured over the glass strip. Since the sulfur readily wet the graphite but did not wet the film, the layer of sulfur with the globules adhering to it was easily detached from the plate after its solidification. On the plate there remained the collodion film which retained the imprint of the graphite grains. By means of thermal vaporization in vacuum there was deposited on it a final quartz replica [7] which was reinforced by the application of a layer of gelatine of 0.1-0.2 mm thickness. The underlying collodion layer was then dissolved in acetone; the quartz replica which had separated with the gelatine layer was washed and was placed on the surface of water with the gelatine downward. After dissolution of the gelatine the quartz replica

was washed with water and caught on a meshed object-holder. To the replica there was immediately applied a drop of alcohol and then one of ether following which the excess of liquid was soaked up with a piece of filter paper. The strengthening of the quartz replica with gelatine and the replacement of water by a liquid of lower surface tension during the drying of this replica are indispensible if its rupture is to be avoided.

Photographing was carried out on the UEM-100 electron microscope with a magnification factor of 8200.

A study of the stereophotographs of the quartz replicas (Figure 2) indicated that the graphite surface had a coarse relief; it was of uneven form, covered with circular protuberances of from one to several microns magnitude.

For the studies of internal structure, the graphite was first pulverized in an agate mortar and the products of granulation were then examined in the electron microscope. There was thereby observed the picture which is typical for ordinary graphite; thin semi-transparent sheets which are formed as the result of the separation of the crystals along their cleavage surfaces. These results were in agreement with those obtained by x-ray analyses, according to which the spheriodal graphite contains well defined crystals.

Especial interest attached to an attempt to determine the magnitude of these crystals, for which purpose it was necessary to separate them, individually if possible, out of the spheroidal grain. The mechanical pulverization described above did not solve this problem because accompanying it was an unavoidable and uncontrolled deformation of the crystals. We accordingly carried out an energetic oxidation of the graphite in solution, as a result of which atoms of oxygen penetrated into the interplanar spaces of the graphite lattice and, chemically uniting with the atoms of carbon, formed the oxides [8]. On subsequent warming to 180-200° there occurred an explosive separation of carbon monoxide and carbon dioxide which led to the splitting of the crystals along the c axis into blocks containing a small number of basic planes. When viewed in the electron microscope, the cleavage products from ordinary graphite resemble leaves of crumpled paper.

The oxidation of the graphite was carried out in the following way. The graphite (0.1 g) in a quartz vessel was covered with a mixture of concentrated acids: 3 ml of H_2SO_4 and 1 ml of HNO_3. After 15-20 minutes of agitation there was added 1 g of finely pulverized and carefully dried $KClO_3$, and the mixture was allowed to stand for $2\frac{1}{2}$-3 hours. The graphite was then washed with water until a negative reaction for the Cl' ion resulted and it was then dried over P_2O_5 in a dessicator. On heating to 180-200° there occurred the rupture of the graphite with the formation of a product which was externally similar to carbon black and which, in the optical microscope, proved to consist of separate worm-like particles of several microns diameter.

This preparation was placed on the grid of the object-holder and was there studied in the electron microscope. One typical photograph is shown in Figure 3. There is to be seen here a part of one of the worm-like particles which is obviously a crystal of graphite which did not fully develop: at places there are to be noted dark fields (indicated by arrows) which can only be relatively thick blocks of the basic planes of the graphite lattice which did not cleave. A higher degree of cleavage of the graphite crystal is shown in Figure 4. According to the data of the literature the disintegration of the basic planes themselves, as a rule, does not occur here so that the diameters of those formations which are observed in the photograph (several microns in magnitude) must correspond in width to the initial crystals of the graphite (measured in the directions of the a and the b axes). In this way the forms which are to be seen in the photograph must be analogous to those which would be observed in the tearing of a weakly glued pile of paper sheets under an applied force in the direction perpendicular to their planes. The apparent fibrousness of the structure which is seen in Figure 4 is due, most likely, to the formation of creases on the basic planes of the crystal during the cleavage. During photography in the transmitted beam of electrons the presence of such creases would give the impression of a fibrous structure, just as do the folds on a crumpled sheet of cigarette paper.

It is significant that the elongated formations in Figures 3 and 4 correspond in their cross-sectional diameters (several microns) to the circular protuberances which are observed in the stereophotographs (see Figure 2). It can be supposed that these protuberances are crystals of graphite which are growing out of the surface of a spheroid and that their cross-sectional dimensions correspond to those of the crystals in the directions of the a and the b axes. This supposition agrees with the concept of the radial growth of the crystals of graphite in the spheroids and with the data on the dimensions of these crystals which are to be found in the paper [6].

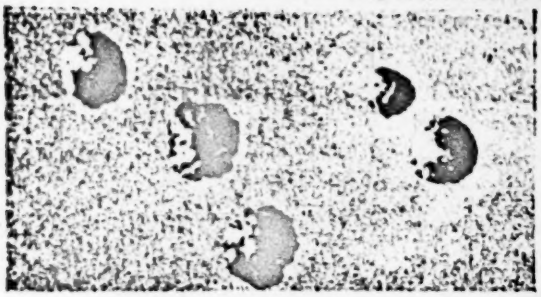

Fig. 1. Spheroidal inclusions of graphite, separated from cast iron by electrolytic dissolution. Optical microscope 110x.

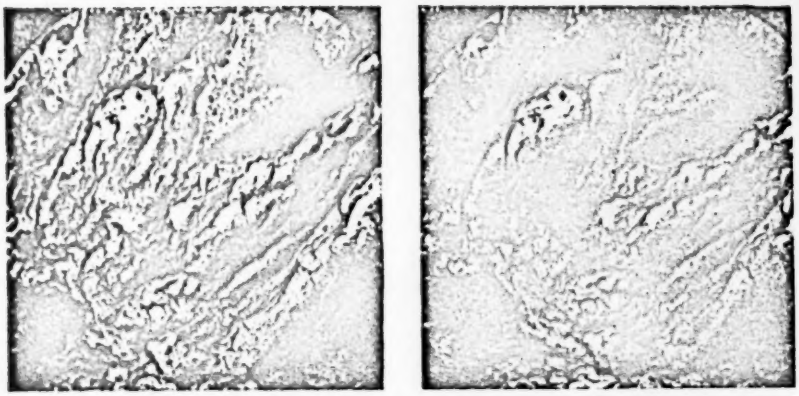

Fig. 2. Stereoscopic photograph of the quartz replica of the surface of spheroidal graphite 8200 x.

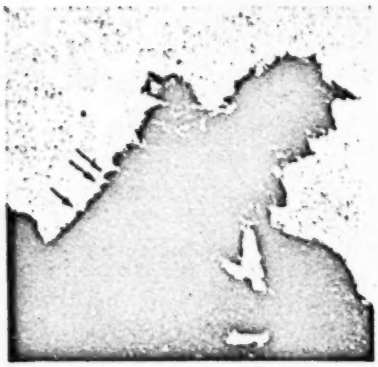

Fig. 3. The product of chemical cleavage of spheroidal graphite 8200 x.

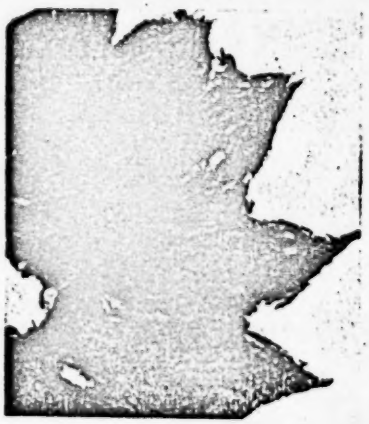

Fig. 4. The product of chemical cleavage of spheroidal graphite. The degree of cleavage is higher than in Figure 3. (8200 x).

It is not possible to draw final conclusions concerning the structures of the spheroidal graphite using only those measurements which are made on the electron microscope; it is essential to apply here other methods of investigation as well. It seems to us, however, that the data presented above opens new possibilities for the solution of this problem. By the application of graphite oxidizers which differ in their intensities it would be possible to realize the sequential cleavage of the inclusions and, observing these processes with the aid of the optical and the electron microscopes, there would be obtained a deeper insight into these structures.

This method could also be employed for the investigation of the structures of other semi-crystalline graphite bodies.

The Institute of Physical Chemistry of the Academy of Sciences of the USSR
The Central Scientific Research Institute for Technology and Machine Construction

Received July 10, 1956

LITERATURE CITED

[1] K. P. Bunin, Yu. N. Taran and A. V. Chernovol, Cast Iron with Spheroidal Graphite (Kiev, 1955).

[2] K. L. Vashchenko, N. A. Golovan and R. P. Todorov, Foundry Production 1956, No. 3, 19.

[3] P. L. Stepin, Article in the Collection: Metal Working and Modern Methods of Thermal Treatment of Cast Iron (1955), page 108.

[4] H. Thyssen, T. Coheur and L. Habraken, Rev. universelle mines, 1950, No. 3, 63.

[5] A. De-Sy, J. Vidt and G. Vandermersche, Fonderie belge 1953, No. 1, 14.

[6] H. Tsuchikura, T. Kusakawa and T. Okumoto, J. Electron Microscopy (Japan) 4, 26 (1955).

[7] Electron Microscopy, A. A. Lebedev, ed. (Moscow, 1954).

[8] U. Hoffmann, Kolloid Z. 61, 297 (1932).

[9] V. M. Lukyanovich and L. V. Radushkevich, Article in the Collection: Methods of Investigating the Structures of Highly Dispersed and Porous Bodies (Acad. Sci. USSR Press, 1952); G. L. Ruess and W. R. Ruston, Fuel 25, 156 (1946).

THE ADSORPTION OF VAPORS ON THE SURFACE OF GOLD

A. I. Sarakhov

(Presented by Academician M. M. Dubinin, July 23, 1956)

In connection with the very interesting results which were obtained during the investigation of the adsorption of vapors on mercury [1, 2] an attempt was made to study the adsorption of water vapor on the surface of gold. The working material was a gold sheet of 99.99% purity which had been rolled to a thickness of 7.8μ on a steel roller. Separate leaflets of this foil were fastened with a gold wire so as to form a small booklet. Any grease which might have gotten onto the surface during the rolling was removed by extraction with benzene in a Soxhlet apparatus. Following this the sample was treated with hydrochloric and with nitric acids in order to eliminate any possible contamination from the steel of the rollers.

For the determination of the adsorption isotherms use was made of the adsorption balance of Bering and Serpinsky [3], the sensitivity of which was raised for the present investigation to $5.2 \cdot 10^{-6}$ g per 1 g load. The need for this latter change arose from the fact that the foil which was employed here had a geometrical surface of only 143 cm^2 for a weight of 1.09 g. This increase of the sensitivity was brought about by a better balancing of the beam and resulted in a narrowing of the range of weighings to 1 mg.

The manometric part of the apparatus was also subjected to an alteration since it was necessary to freeze out the vapors of mercury during the investigation of the water vapor adsorption. For this reason the mercury monometer was replaced at low pressures from 10^{-5} to 0.1 mm of Hg) by a Pirani gauge and at higher pressures (from 0.01 to 30 mm of Hg and upward) it was replaced by a membrane manometer. The Pirani gauge was made from a platinum wire of 30 μ diameter and 10 cm length which was stretched in a glass tube of 4 mm internal diameter. This tube was surrounded by a water jacket through which there was passed a glass coil with circulating water from a thermostat of the type TS-15. The temperature of the wire was held constant (100°) by adjusting the current supplied to it by a Wheatstone bridge, one arm of which was formed by the wire itself. That bridge current which was necessary to maintain constancy of temperature and, accordingly, constancy of the wire resistance, was a function of the pressure and was measured with the aid of a PN-4 potentiometer. The membrane manometer had a membrane diameter of 30 mm and was made from glass; the deformation was measured with a mechanical system involving a mirror and an automatic collimating tube. Both of these manometers were inserted in the air thermostat of the balance.

The very first experiments with this adsorbent showed that the electrostatic charge which accumulated on the metallic screen of the balance and on the gold foil, which was hung from the quartz suspension, could not be removed to an adequate degree by the external electrostatic shield that had been used in previous work (a grounded aluminum foil with which the case of the balance was enclosed on the outside had earlier served as a screen). The introduction of a radioactive preparation into the balance case not only did not decrease the electrostatic interference but also gave rise to still more electrification, as was seen from the formation of separate flashes of electrical discharge within the case. In this connection the interior surface of the balance case and all of the details of the balance itself which were in the neighborhood of the adsorbent were covered with a layer of gold, condensed in vacuum and grounded. It was only after this was done that the balance gave steady, reproducible readings.

For the removal of those substances which the gold had adsorbed from the air or had taken up in the process of its preparation, the sample was subjected to a heating at a temperature of 420-450° on the balance and in vacuum. In the course of 4-5 days there was observed a loss of mass; then in the following 2-3 days the mass remained unchanged.

Figure 1 shows the adsorption isotherm for water vapor at 18° as it was determined by us. During the adsorption experiments under relative pressures from 0 to 0.8 P/P_s there was observed an extremely rapid, almost instantaneous, initial process (Curve 1) followed by a slow (20-30 hours) increase of the mass adsorbent up to the establishment of an equilibrium (curve 2). They are shown in the graph the results of three series of independent measurements. For the experiments of desorption at relative pressures of 0.8 and less the desorption points lay on curve 2. As is to be seen from the graph, curve 2 did not pass through the initial point, i.e., an extended (up to 10 days) pumping out of the gold at 18° did not remove the material adsorbed by it. Subsequent adsorption and desorption points fell continually on curve 2. It is thus possible to conclude that the rapid initial adsorption of the water vapor on the gold surface was accompanied by a chemical adsorption. Naturally, curve 1 cannot be considered as the curve of reversible physical adsorption because, despite the rapid performance of the measurements during the successive introductions of the water vapor, in addition to the reversible physical adsorption, partial chemical adsorption also occurred. The kinetic curve for this process is presented in Figure 2. Unfortunately, the energy of activation could not be calculated from this curve because the smallness of the adsorbent surface led to measurements which were of insufficient accuracy for such purposes.

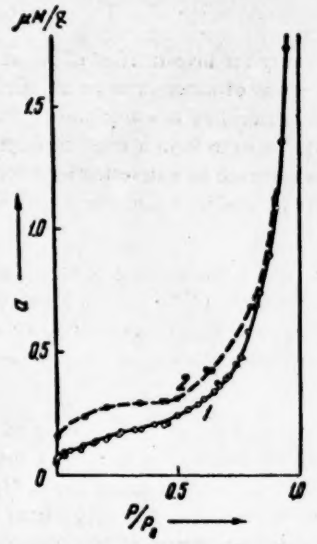

Fig. 1. The 18° sorption isotherms for water vapor on gold:
1) adsorption, 2) desorption.

By extended heating (30-40 hours) of the gold in vacuum and at a temperature of 420-450° there was brought about the complete removal of the adsorbed substances. A subsequent investigation, following the removal of this adsorbed material, fully reproduced the described sequence of events.

In order to be certain the observed irreversibility was not due to the adsorption by the gold of mercury vapor, vacuum grease or any other contaminant which by accident had entered into the apparatus, a control experiment was run with nitrogen. After the complete removal of the adsorbed material by heating, dry nitrogen at a pressure of 4 mm of Hg was admitted into the balance. In the course of 15 days no increase was observed in the mass of the gold.

The nitrogen was then replaced with oxygen (at a pressure of 4 mm of Hg); in 24 hours the mass of the gold underwent an insignificant increase (not more than 0.01 μM/g). Without heating, the oxygen was then pumped off, the weight of the sample undergoing no change, and into the balance water vapor was admitted (up to a pressure of 4 mm of Hg). The resulting points at first fell between the curves 1 and 2, then, in the course of 2 hours they moved on to curve 2 and, during the next 24 hours, there was no further observable alteration of the mass. The points of adsorption and desorption after this continually fell on curve 2. It was thus possible to draw the conclusion that the vapors of water were chemically adsorbed by gold, in all likelihood, with the formation of a surface oxide or hydroxide. A preliminary chemical adsorption of oxygen accelerated this process.

For quantitative calculations we were interested in the true surface area of the investigated sample. For this reason the attempt was made to measure the adsorption isotherm for nitrogen at the temperature of its boiling-point. However, the small magnitude of the adsorption was overshadowed by the effects of the convection currents within the balance; it was impossible to completely eliminate these. For the determination of the specific surface area there was, therefore, developed the adsorption isotherm of benzene (Figure 3). This isotherm

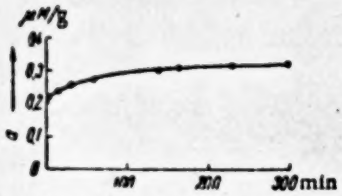

Fig. 2. The kinetics of the adsorption of water vapor on gold at 18°. Relative pressure ~0.4 P/P_s.

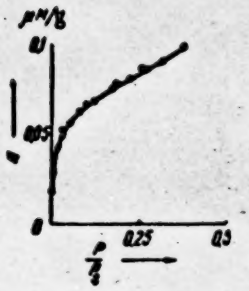

Fig. 3. The adsorption of benzene vapor on gold at 18°.

is well described by the BET equation in the interval 0.02-0.35 P/P_s. Applying this equation and accepting 45 $Å^2$ as the value of the area which is occupied by the benzene molecule in the densely packed monomolecular adsorption layer (a mean value from the data of A. V. Kiselev [4] on the adsorption of benzene on carbon) we obtained $s = 180$ cm^2 as the specific area of the gold. Thus, the coefficient of roughness amounted to approximately 1.4. This was in agreement with the data of Bouers [5] who found for aluminum a value of 1.3 for this quantity.

The convexity of the initial isotherm (Curve 1) indicated that it was here a matter of an adsorption of the electrostatic type under the action of image forces. The whole surface of the adsorbent was active in this process.

After desorption at 18° there remained on the adsorbent about 0.155 μM/g of irreversibly bound water. If it was assumed that this quantity of water covered the gold surface with a monomolecular film, then, making use of the calculated specific surface area, there was obtained the result that each water molecule on the surface of the gold occupied an area of 17 $Å^2$. This result considerably deviated from the accepted 14.8 $Å^2$ and from the value 13.8 $Å^2$ which is given by Harkins and Jura [6]; it agreed, however, very well with the area occupied by each atom of gold in the surface (16.55 $Å^2$). Accordingly, within the limits of experimental error, to each surface atom of gold there corresponded one molecule of firmly bound water and the area occupied by the water molecule on this surface was determined, not merely by the size of the molecule itself, but also by the crystal parameters.

At the present time we are carrying out work for the confirmation of these data and for increasing the accuracy of the investigation, the present method being insufficiently precise. This may be seen from the fact that the whole effect of the adsorption of water vapor at $P/P_s = 0.5$ on our sample, namely $5.7 \cdot 10^{-6}$ g, was determined, even in the best of cases, with an accuracy of only 5%.

In conclusion I would like to express my deep appreciation to Academicians M. M. Dubinin and V. M. Lukyanovitch for their continuing interest and valuable advice and to N. N. Moskvitin for his help in carrying out certain extended measurements.

The Institute of Physical Chemistry of the Academy of Sciences of the USSR

Received July 10, 1956

LITERATURE CITED

[1] B. P. Bering and K. A. Iolleva, Bull Acad. Sci. USSR, Div. Chem. Sci. 1955, No. 1, 9.

[2] B. P. Bering and K. A. Iolleva, Bull Acad. Sci. USSR, Div. Chem. Sci. 1955, No. 2, 216.

[3] B. P. Bering, V. V. Serpinsky, Proc. Acad. Sci. USSR, 94, No. 3, 497 (1954).

[4] A. P. Kamaukhov, A. V. Kiselev and E. V. Khrapova, Proc. Acad. Sci. USSR 92, No. 2, 361 (1953).

[5] R. Bouers, Phyl. Mag., 44, 467 (1953.

[6] S. Brunauer, The Adsorption of Gases and Vapors (Foreign Lit. Press, 1948) p. 724.

THE PROBLEM OF THE POLYMORPHISM OF DI-CALCIUM SILICATE

N. A. Toropov, B. V. Volkonsky, and V. I. Sadkov

(Presented by Academician P. A. Rebinder, July 21, 1956)

Di-calcium silicate is one of the chief minerals of the Portland cement clinker. It is for this reason that the study of the polymorphic transformations of this compound has always attracted the attention of many investigators.

The polymorphic transformations of di-calcium silicate have been investigated by various methods: the petrographic method, in which the differences in modification are established through the optical constants, the method of x-ray analysis, the dynamic method based on the heating and cooling curves, and finally, the static method of instantaneous cooling or quenching.

At one time there were associated with di-calcium silicate the three modifications: α, β and γ. Further investigations, however, pointed to the existence of additional α' and β' modifications of the compound.

Bredig [1] considered that along with an α-modification of C_2S, which is isomorphous with α-K_2SO_4, there also exists an α'-$2CaO{\cdot}SiO_2$, isomorphic with the rhombic form of β-K_2SO_4 and stable in the interval between the limit of stability of the α form and 850°. F. I. Vasenin [2], by the method of heating and cooling curves, has established the existence of a form of C_2S, which he considered as β'-C_2S. Later Tromel and Muller [3] also noted the existence of an α'-C_2S. Saalfeld [4] confirmed the existence of an α'-C_2S.

Interesting data are presented by Metzger [5]. He considers it to be the generally accepted opinion that the C_2S in the Portland cement clinker exists exclusively either in the form of α-C_2S or β-C_2S. A similar point of view has been supported by Nurse [6] in his report to the International Symposium on the Chemistry of Cement in London in 1952. He admitted, however, the possibility of an additional α' modification. The method of models, which was proposed by Goldschmidt [7], involved the use of the low melting system NaF-BeF_2 as a model for the system CaO-SiO_2. This work was continued by Thilo [8]. The results which the latter obtained agreed to a considerable extent with those of the indirect investigation of C_2S, which were mentioned earlier; so, for example, in Na_2BeF_4 – the model for C_2S – there appears as the modification stable at the highest temperatures, a form with a hexagonal lattice which, just as α-C_2S, has a structure of the same type as does Na_2SO_4.

We have used the method of the high-temperature x-ray analysis for the study of the polymorphism of di-calcium silicate. With this method we have succeeded in following the processes of polymorphic transformation in this compound; we have established the temperature limits of these transformations, and analyzing the α' and the β' modifications, we have obtained their x-ray characteristics. As a starting material there was chosen, according to an earlier established classification, the γ modification of the compound.

The γ modification of C_2S, during heating to 760°, maintains a crystal lattice which is characterized by three strong diffraction maxima for which the values of the interplanar spacing are equal to: $d/n = 3.00$ A; 2.73 A; 1.90 A and the respective intensities to $I/I_1 = 100$, 53, and 41. At a temperature of 760° the lattice of the γ modification begins to change and in the interval from 760° to 900° there is recorded the β modification of di-calcium silicate, the lattice of which, as is known, has two characteristic strong diffraction maxima: 2.77 and 2.73 A, with the corresponding intensities $I/I_1 = 100$ and 92.

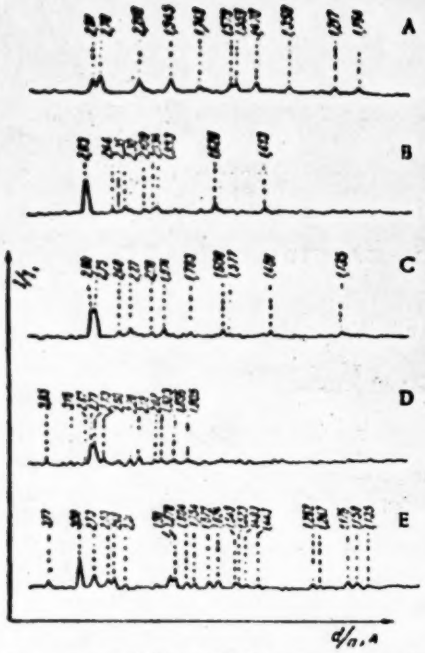

Fig. 1. X-ray diffraction diagrams for the five polymorphic forms of di-calcium silicate. A) α modification; B) α' modification; C) β'-modification; D) β modification; E) γ modification.

Then, at a temperature of 900° the β modification of the compound goes over into a modification which we have designated as the β'. This modification exists up to a temperature of 1230° and has the following x-ray characteristics for the most pronounced diffraction maxima: d/n = 2.80 A; 2.75 A; 2.27 A; 1.97 A; 1.608 A; 1.401 A; with the corresponding intensities I/I_1 = 100, 74, 22, 22, 28 and 28.

On reaching a temperature of 1230° there is again observed a transformation of the crystal lattice of di-calcium silicate and in the next temperature interval there is recorded a special structure which we considered as the α' modification of the compound.

TABLE 1

β' modification		α' modification	
d/n, A	I/I_1	d/n, A	I/I_1
2.80	100	2.83	100
2.75	74	2.44	9
2.40	11	2.36	4
2.27	22	2.30	18
2.08	6	2.109	4
1.974	22	2.034	4
1.783	6	1.993	4
1.608	28	1.626	23
1.577	6	1.413	14
1.401	28		
1.195	11		

This α' modification of di-calcium silicate has, as the x-ray characteristics of the principal diffraction maxima, the following values: d/n = 2.83 A; 2.30 A and 1.62 A, with the corresponding intensities I/I_1 = 100, 18 and 23.

On elevating the temperature beyong 1420° the lattice of the α' modification of the compound goes over into the well-known high-temperature α form.

On cooling, these same polymorphic changes are observed in the reverse order.

The temperature limit for the transfer from the β' into the β modification is displaced in the direction of decreasing temperatures to 650°, while the temperature for the transformation from the β modification into the γ is displaced to 450°.

Through the direct registration of these x-ray diagrams at high temperatures, the method of analysis which was employed here has made it possible to establish the existence of an α' and a β' modification of di-calcium silicate and, at the same time, to obtain the x-ray characteristics of these forms (Figure 1). In Table 1 there are presented numerical values for the diffraction maxima, the intensities, and the corresponding interplanar spacings in the crystal lattices of the α' and the β' modifications of di-calcium silicate.

The All-Union Scientific Research Institute "Giprotsement"

Received June 28, 1956

LITERATURE CITED

[1] M. A. Bredig, J. Am. Chem. Soc. 63, No. 9 (1941); J. Phys. Chem., 46, 801 (1942); Am. Mineral. 28, 594 (1943); J. Phys. Chem. 49, 537 (1945); J. Am. Ceram. Soc. 33, No. 6 (1950).

[2] F. L. Vasenin, J. Appl. Chem. 21, 10 (1948).

[3] G. Tromel, H. Muller, Zement-Kalk-Gips 5, No. 8 (1952).

[4] H. Saalfeld, Ber. 30, 185 (1953).

[5] A. Metzger, Zement-Kalk-Gips 6, 269 (1953).

[6] R. W. Nurse, Proc. 3rd International Symp. on the chem. of Cement (London, 1952), p. 56.

[7] V. M. Goldschmidt, Skrifter Norske Videnskaps-Akad. Oslo, 1 Mat-Naturwiss Kl. (1927) No. 8, 7.

[8] E. Thilo, H. A. Lehmann, Z. anorg. Chem. 258, Nos. 3-5, 332 (1949).

THE ENERGY OF ADSORPTION OF HYDROCARBONS ON GRAPHITE

N. N. Avgul and A. V. Kiselev

(Presented by Academician M. M. Dubinin June 29, 1956)

Theoretical calculations of the energy of the adsorption bond can be checked experimentally by comparing them with the calorimetrically measured heats of adsorption. They have great practical significance for the understanding and the solution of those problems which arise in chromatographic adsorption separations, especially in the case of mixtures of the hydrocarbons. The simplest situation is that of the adsorption of hydrocarbons on the surface of an atomic lattice, such as graphite.

Calorimetric measurements of the differential heats of adsorption of the hydrocarbons on graphitic carbons have been carried out in several works; 1-butene and n-butane have been investigated in Beebe's laboratory [1] and n-pentane, n-hexane [2], n-heptane and benzene [3] in our own. We have accordingly, also undertaken theoretical calculations of the energy of the adsorption bond for these and some other hydrocarbons. We have attempted to explain the influence of the following factors on the energy of adsorption: 1) the lengthening of the carbon chain in the n-alkanes, 2) the branching of the chain in the iso-alkanes, 3) the closing of the chain in the naphthene ring, 4) the double bond, and 5) the aromatic ring. The calculations were carried out for the following hydrocarbons: n-butane – 1-butene; n-pentane – neopentane – cyclopentane – 1-pentene; n-hexane – 1-hexene – benzene; n-heptane.

1. The method of calculation of the energy of the adsorption bond. In determining the energy of adsorption of complex molecules we have followed the method of calculation which was used in [2] for the n-alkanes on the basal plane of graphite. In these calculations the molecule of the hydrocarbon was broken down into sections and there was found the energy of interaction of each of these sections with all of the atoms in the lattice in the various relative positions and under equilibrium distances of separation, r_0. The summation over the sections, in the case where these are equivalent, (for example, with the CH_2 groups in the n-alkanes and in cyclopentane), was simplified by the additive properties of polarizability and magnetic susceptibility of the hydrocarbons. The interaction of any one section with the entire lattice was calculated through the summation over the first hundred nearest lattice atoms, as in [4], followed by an integration over the remaining volume of the crystal [2]:

$$\Phi = -C\left[\sum\left(\frac{1}{r^6} - \frac{r_0^6}{2r^{12}}\right) + \frac{\pi\nu}{6(r')^3}\right] = -Cf(r, r_0). \qquad (1)$$

The constant of attraction was calculated for dispersive interaction according to the quantum mechanical formula of Kirkwood:

$$C = -6mc^2 \frac{\alpha_1 \alpha}{\alpha_1/\chi_1 + \alpha/\chi}, \qquad (2)$$

where m is the mass of the electron, c is the velocity of light, α_1 χ_1, and α, χ, are the polarizibility and the magnetic susceptibility of the interacting centers.* The quantity r in Equation (1) represents the distance between the interacting particles; the quantity r_0 was presumed to be equal to the sum of the half interplanar spacing in the crystal of graphite, 1.7 A, and the van der Waals' radius of the molecular section (2.0 A, for example, in the case of the plane oriented molecules of the n-alkanes and 1.85 A in that of benzene [5]). Integration was carried out from r' = 8.5 A on, ν being the number of atoms of carbon per cm^3 of the graphite: the second member represented only 4% of the entire magnitude of $f(r, r_0)$. The calculations presented in [2] have shown that a change of r by 0.05 A (a conceivable error in the magnitude of r_0) would alter Φ by approximately 5%. The molecules of the hydrocarbons, under the usual conditions of temperature, form mobile layers on the surface of the graphite and, accordingly, the values of the quantity Φ which were adopted in these calculations were averaged for the various positions of the molecular sections relative to the atoms of the lattice.

The properties of the molecular sections of the molecules of the adsorbate influence the magnitudes of r_0 and C. For adsorption on the basal plane of the graphite lattice ($\alpha_1 = 0.937 \times 10^{-24}$ cm^3 and $\chi_1 = 10.54 \times 10^{-30}$ cm^3 [4]).

$$C = -6.58 \cdot 10^{-17} \frac{\alpha}{\alpha_1 \chi - 0.888 \cdot 10^5} \frac{\text{kcal} \cdot \text{cm}}{\text{mole}}, \qquad (3)$$

where α and χ are the polarizability and the magnetic susceptibility of the hydrocarbon or its section. For the case of the complex hydrocarbons the energy of interaction was determined by summing over the sections:

$$\Phi = \sum \Phi_i = \sum_i C_i f(r, r_{0i}). \qquad (4)$$

2. The energy of adsorption of the n-alkanes and the influence of the lengthening of the chain. This problem was solved in the form of a linear equation showing the dependence of Φ on the number of the carbon atoms, n, in the molecule [2]:

$$-\Phi = [2C_{CH_3} + (n-2)C_{CH_2}] f(r, r_0 = 3.7\text{A}) =$$
$$= [2(C_{CH_3} - C_{CH_2}) + nC_{CH_2}] f(r, r_0 = 3.7\text{Å}) = 0.9 + 1.85n \text{ kcal / mole} \qquad (5)$$

3. The energy of adsorption of an isoalkane. Here a basic factor is the separation of some of the molecular sections from the surface of the adsorbent. We carried out the calculations for the symmetrical molecule of neopentane. For three of the CH_3 groups r_0 = 3.7 A, just as in the n-alkanes;** for the quaternary carbon atom, and specifically for the fourth CH_3 group, r_0 is larger. For each r_0 there was determined a value of $f(r, r_0)$. Starting from the additivity of α and χ we decomposed the molecule of neopentane into sections and for each of these determined the magnitude of the constans C_i and Φ_i. In view of the increase of r_0, the energy for some of these sections was distinctly less than in the n-alkanes, which makes it possible to carry out a chromatographic separation on charcoal.

4. The energy of adsorption of cyclopentane. This is a plane molecule which orients itself parallel to the surface of the adsorbent; the five CH_2 groups are equivalent and r_0 for them is uniform and equal to 3.7 A. The energy of adsorption of cyclopentane is less than that of n-pentane but considerably greater than that of neopentane.

* The calculation of C by London's equation, using α and the ionization potential, leads to poorer results because of the crude assumptions which are involved in the equation's derivation.

** It is possible that the magnitude of r_0 is here somewhat different than it is for the n-alkanes.

5. The energy of adsorption of the α-monoolefins. In this case, with $r_0 = 3.7$ A for the saturated part of the molecule and $r_0 = 3.6$ A at the double bond, the calculations gave a lower value than for the corresponding n-alkanes. The dependence on n is given by the equation:

$$-\Phi = 0.1 + 1.85\,n \text{ kcal/mole} \qquad (6)$$

6. The energy of adsorption of benzene. Here $r_0 = 3.55$ A; the smaller mean values of α and χ lead, however, to an energy of adsorption of benzene on graphite which is less than that for the n-alkane which also contains six carbon atoms per molecule. Thus, graphitic bodies are unsuitable for the separation of the aromatic and the unsaturated hydrocarbons. Use should be made of the ability of these hydrocarbons to form π-complexes with protonic acids; i.e., there should be employed such acidic adsorbents as silica gel and aluminosilica gel which, in actuality, give good separations of these hydrocarbons [6].

7. Possible errors and necessary refinements. The constant of repulsion was determined through a condition of minimizing the potential of interaction with a single atom of the adsorbent. Taking the interaction of the entire lattice into account increases this value somewhat and decreases Φ. Further, there has been taken into account only the dipole-dipole term in the attractive potential of the nonpolar van der Waals' forces; the quadripole-dipole and the quadripole-quadripole members, $-D/r^8$ and $-\epsilon/r^{10}$, were not included. The second of these, for $r_0 > 3.5$-3.7 A, can be neglected. An estimate of the quadripole-dipole term for the interaction of two CH_4 molecules at $r = r_0$ showed that it amounts to 20% of the dipole-dipole term [7]. Taking the interaction with the lattice into account considerably decreases the contribution which is made by this term to the over-all adsorption.* Here there is need for a more exact calculation.

In the calculations which are presented we have accepted the mean values of the polarizability and the magnetic susceptibility since the effect of the additivity of the nonpolar van der Waals' forces considerably exceeds that of anisotropy [8]. If for benzene, which shows strong anisotropy in its properties, there were taken the values of α and χ in a direction perpendicular to the plane of the ring ($6.35 \cdot 10^{-24}$ cm^3 and $189 \cdot 10^{-30}$ cm^3), there was obtained $C = 3.42 \cdot 10^{-45}$ kcal $\cdot$ cm^6/mole, which is near to the result obtained using the mean value of α and χ, the changes in these latter mutually compensating one another. This question needs further study.

Further, the energy of adsorption on the prismatic plane should be calculated. The distribution of the carbon atoms on this plane is considerably less dense. We have carried out a preliminary calculation of $f(r,r_0)$ for the case of adsorption on the prismatic plane with $r_0 = 3.7$ A, whereby summation was extended over those 65 nearest carbon atoms which are found at distances up to 9 A, and the farther lying atoms were taken into account by integration. The magnitude of $f(r,r_0)$ amounted to $1.6 \cdot 10^{45}$ cm^{-6} which was 40% less than the corresponding quantity for the basal plane; if, however, account was taken of the anisotropy of α_i and χ_i for graphite, the quantity C for the prismatic plane proved to be considerably greater than that for the basal plane, which, in turn, led to a value for Φ which was close to that for the basal plane.

8. A comparison of the calculated values of the energy of the adsorption reaction with heats of adsorption. A number of difficulties arise in an attempted comparison of the energies of molecular interaction with thermochemical quantities. The energy of interaction is itself insufficient for a calculation of the point of equilibrium; a statistical-molecular treatment is also needed. It is, accordingly, impossible to directly compare the molecular potential, and in particular the adsorption potential with the free energy of the process [9]. A comparison with the total energy; i.e., with the heat of adsorption, is possible, but only under two assumptions. In the first place, the calculation of adsorption interaction refers to elementary acts; the heat of adsorption, even the differential heat, is, on the other hand, a macroscopic quantity. Experiments have shown, however, that, over a considerable interval of the covering of the surface of the graphitic carbon, the differential heat of adsorption is essentially constant and that the adsorption isotherm is well described by the Langmuir equation [2]. This gives an indication

* For adsorption on graphite the magnitude of this term is considerably less than that of the repulsion term and does not compensate the latter, as was assumed in [8].

TABLE 1

A Comparison of the Calculated Energies of Adsorption, $-\Phi$, of various hydrocarbons on the basal plane of graphite and the differential heats of adsorption, Q_d, on graphitic carbon.

Hydrocarbon	r_0, A	$f(r, r_0)\cdot 10^{-12}$ cm^{-6}	$\alpha\cdot 10^{24}$ cm^3	$\chi\cdot 10^{24}$ cm^3	$C\cdot 10^{58}$, kcal$\cdot$ cm^6 /mole	$-\Phi$, kcal/ mole	Q_d kcal/mole
n-Butane	3.7	2.86	8.12	85.2	2.9	8.3	8.6
1-Butene	3.7; 3.6	2.98	7.8	68.0	2.51	7.5	8.2
n-Pentane	3.7	2.86	9.95	104.1	3.54	10.1	10.0*
Neopentane							
$3CH_3$	3.7	2.86	6.78	71.0	2.41	6.9	
C	4.2	1.75	0.961	12.3	0.379	0.66	8.0 —
CH_3	5.7	0.59	2.26	23.8	0.809	0.48	
Cyclopentane	3.7	2.86	9.10	94.7	3.24	9.3	—
1-Pentene	3.7; 3.6	2.94	9.75	86.8	3.10	9.3	—
n-Hexane	3.7	2.86	11.78	123.0	4.19	12.0	11.9
1-Hexene	3.7; 3.6	2.92	11.55	106.0	3.84	11.2	—
Benzene	3.55	3.20	10.32	92.0	3.37	10.8	10.0
n-Heptane	3.7	2.86	13.61	141.9	4.84	13.8	13.4*

* The heats of adsorption of the vapors of n-petane and n-heptane were measured, as in [2], by G. L. Berezin, I. A. Lygina and the authors of the present paper.

of the uniformity of the carbon surface and permits the assumption as to the equivalence of the elementary acts over the region of small coverage. In the second place, it is necessary to assume that the energy of the adsorption bond does not depend on the temperature; in the case of the adsorption of the hydrocarbons on graphite this is approximately justified. Further investigations are also needed here.

In Table 1 there are compiled results of the calculations of the energy of the adsorptive bond and the values of the differential heat of adsorption on graphitic carbons.

It is to be seen from Table 1 that the theoretical calculations not only give a correct qualitative description of the passage from one hydrocarbon to another but also are in good quantitative agreement with the measured differential heats of adsorption. Thus the energies of adsorption of the hydrocarbons on graphite are satisfactorily described by the theoretical calculations.

LITERATURE CITED

[1] R. A. Beebe, M. H. Polley, W. R. Smith and C. B. Wendell, J. Am. Chem. Soc. 69, 2294 (1947).

[2] N. N. Avgul, G. I. Berezin, A. V. Kiselev and I. A. Lygina, J. Phys. Chem. 30, 2106 (1956).

[3] N. N. Avgul, G. I. Berezin, A. V. Kiselev and I. A. Lygina, Bull. Acad. Sci. USSR, Div. Chem. Sci. 1956, 1304.

[4] R. Barrer, Proc. Roy. Soc. (London) A 161, 476 (1937).

[5] L. Pauling, The Nature of the Chemical Bond (Moscow-Leningrad, 1947).

[6] A. V. Kiselev, Proc. Acad. Sci. USSR 106, 1046 (1956).

[7] H. Margenau, Rev. Mod. Phys. 11, 1 (1939).

[8] J. De-Boer, Adv. in Coll. Sci. 3, 1 (1950).

[9] A. V. Kiselev, Sci. Records Moscow State Univ., Chem. 86, 147 (1946).

The Institute of Physical Chemistry of the
Academy of Sciences of the USSR

Received June 19, 1956

A DYNAMIC METHOD FOR STUDYING THE STRUCTURES AND THE SPECIFIC SURFACES OF ADSORBENTS

V. T. Bykov and O. E. Presnyakova

(Presented by Academician M. M. Dubinin, August 25, 1956)

The initial process in the case of monomolecular adsorption by coarsely porous and by nonporous adsorbents is largely determined by the magnitude and the nature of the adsorbent surface. On the porous structure of the adsorbent depends the completion of the sorption process by polymolecular adsorption and capillary condensation or capillary stratification [1- 3]. Under dynamic conditions the adsorption by porous bodies can be separated into the two periods "before breakthrough" and "after breakthrough" [4]. The "before breakthrough" period is characterized by a steady rate of sorption in the course of the basic process of monomolecular adsorption. A diminishing velocity of adsorption characterizes the "after breakthrough" period. Here, the determining factor is internal diffusion which depends, to a large degree, on the structure of the adsorbent; thus, by investigating the dynamics of sorption it is possible to obtain some conception as to the structure of the adsorbent.

TABLE 1

The Magnitude of the Adsorption, a, expressed in milli-molecular moles/g, obtained under static and dynamic conditions of measurement.

Sample	Using phenol		Using benzyl alcohol		Using thymol	
	static	dynamic	static	dynamic	static	dynamic
KSM	2.040	2.070	1.770	1.790	1.300	1.170
KSK	1.653	1.500	1.450	1.420	0.945	0.890
173-b	0.690	0.710	0.560	0.571	0.245	0.246
172-b	0.264	0.262	0.264	0.277	0.188	0.117
171-b	0.066	0.052	0.066	0.050	0.033	0.026
55	0.412	0.421	0.354	0.338	0.166	0.135

For studying the structure of adsorbents on this basis we have followed the method of probes which has been proposed by M. M. Dubinin [5, 6], so modifying it that the experiments of molecular probing were carried out under dynamic conditions at those velocities of flow of the solution which assured the establishment of adsorption equilibrium. Whereas, in the study of adsorption from solution by static methods, decisions concerning the process of adsorption must be reached from the initial and the final data alone, without there being any possibility of observing those very interesting features which are connected with the kinetics of adsorption, the passage to dynamic conditions of experimentation permits judgements as to the velocity of the sorption process and the structure of the adsorbent to be reached on the basis of the shapes of the resulting discharge curves.

Various high molecular compounds: phenol, benzyl alcohol and thymol (5-methyl-2-isopropylphenol were selected as molecular probes. Carbon tetrachloride, an inert and weakly adsorbed substance, served as the solvent.

Technique of Investigation. The substance which was to undergo adsorption was passed in carbon tetrachloride solution through a layer of the sorbent in a chromatographic column. In our experiments the flow of solution did not exceed 10-15 ml/hour. The layer of sorbent had a fixed height of 7.5 cm. Thus, as far as possible, constancy of experimental conditions was assured. For the development of the discharge curves, samples of the solution

which had passed through this layer of sorbent were collected at every 0.5 ml and their content of adsorbed material was measured. The content of adsorbed material in the discharged solution was determined by interferometry.

The results are represented graphically, with the volume of the test solution passed through the sorption layer plotted on the axis of abscissas and the concentration of the discharged solution, as read from a calibration curve, plotted on the axis of ordinates.

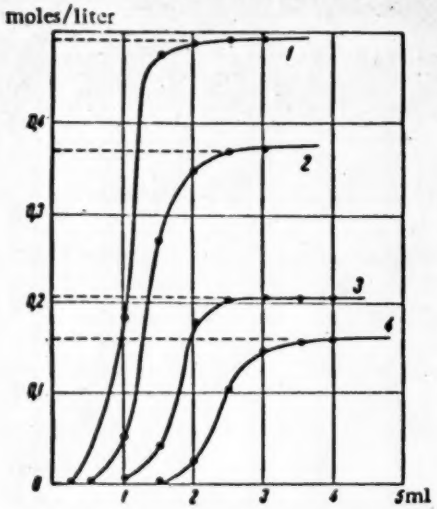

Fig. 1. Discharge curves for solutions of various concentrations of thymol in CCl_4 on sample No. 55.
1) 0.49 millimoles/liter 2) 0.359 millimoles/liter 3) 0.208 millimoles/liter 4) 0.161 millimoles/liter

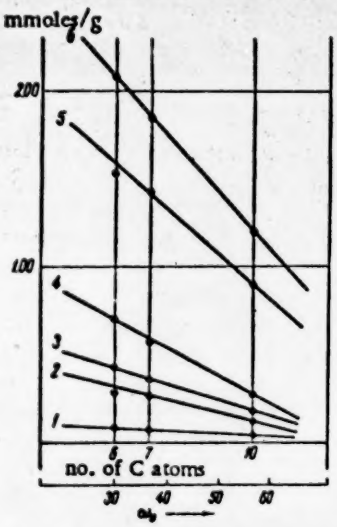

Fig. 2. The relationship between the amount of adsorption and the size of the molecule which is being adsorbed. Sample: 1) 171-b 2) 172-b 3) 55 4) 173-b 5) KSK 6) KSM

It was, first of all, necessary to be assured of the establishment of adsorption equilibrium in these dynamic experiments. A comparison of the amount of adsorption, determined under dynamic and under static conditions, is presented in Table 1; it shows that adsorption equilibrium was attained in our dynamic experiments carried out under fixed conditions.

It was further necessary to determine the influence of the concentration of the solution of the molecular probe on the form of the discharge curves obtained under steady conditions. We developed discharge curves for solutions of thymol in carbon tetrachloride, using adsorbent 55, (sulfunit), and changing the concentration of the thymol from 0.161 to 0.495 millimoles/liter, i.e., threefold. The areas bounded by the discharge curves and the coordinate axes are, practically, superposed, as is to be seen from Figure 1. It is thus possible to suppose that monomolecular coverage of the adsorbent surface has taken place during adsorption from solution and that the magnitude of the adsorption and the specific surface of the adsorbent can be determined from the corresponding area.

The influence of the form and the dimensions of the molecule of the substance undergoing adsorption, i.e., the molecular probe, is brought out by dynamic experiments on the individual adsorbents. For adsorption on highly dispersed bodies a decrease in the available surface area of the adsorbent accompanies an increase in the dimensions of the molecules of the adsorbate. A decreasing linear relationship was established between the magnitude of the adsorption, the area occupied by the molecule of the adsorbate and the number of carbon atoms in this molecule (Figure 2). The area occupied by the molecular probe was determined by us on a standard silica gel, KSK.

The discharge curves for the standard silica gels KSK and KSM, when developed dynamically under steady conditions with solutions of any one of the alcohols, showed marked differences. The area which is bounded by the discharge curve and the coordinate axes, concentration and volume of solution, is proportional to the specific surface area and differs markedly for these standard adsorbents KSK and KSM, as is shown in Figure 3. According to the forms of their discharge curves, the various natural adsorbents occupy a certain intermediate position.

The porous structure of certain natural adsorbents of varying Far Eastern origin was investigated under dynamic conditions by the method of molecular probes (32 samples, using three molecular probes). Under dynamic conditions of experimentation the method of molecular probes can give a quantitative characterization of the porous structure of an adsorbent. The value of the adsorption limit, a_{∞}, can be split into two factors: a_1, the magnitude of the adsorption before "breakthrough" and a_2, the magnitude of adsorption from "breakthrough" to complete saturation.

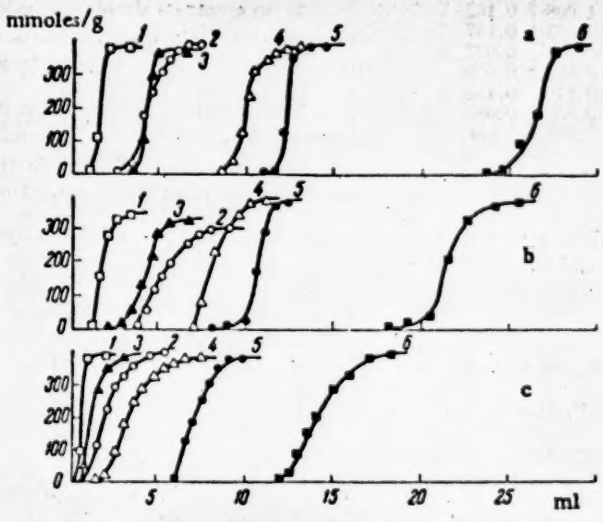

Fig. 3. Discharge curves using phenol (a), benzyl alcohol (b) and thymol (c) in CCl_4 solutions with standard silica gels. See Figure 2.

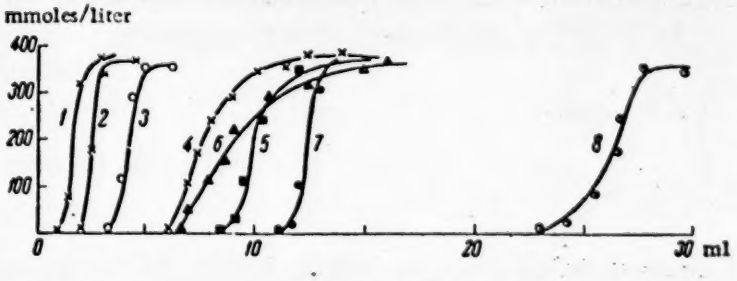

Fig. 4. Discharge curves using phenol in CCl_4 solution on diatomites (1,2), decomposed fresh tuffs (3-5), and gubrin (6). For comparison the discharge curves for KSK and KSM have been plotted also. Samples:
1) 345 2) 327 3) 55 4) 172-b 5) 173-b 6) 304 7) KSK 8) KSM

For coarsely porous adsorbents the quantity a_1 will, for the most part, determine the adsorption capacity, the magnitude of a_2 being small. For finely porous adsorbents at a sufficiently high value of a_1 the magnitude of a_2 can also be large. The values of a_1 and a_2 for a number of natural sorbents and standard silica gels are given in Table 2.

TABLE 2

A Comparison of the Amount of Material Adsorbed on Various Adsorbents (millimoles/g) up to Breakthrough (a_1) and from Breakthrough to Saturation (a_2)

Adsorbent	Using phenol		Using thymol	
	a_1	a_2	a_1	a_2
KSM	1.770	0.304	1.008	0.162
KSK	1.420	0.080	0.743	0.147
171	0.042	0.022	0.004	0.022
172	0.262	0.261	0.095	0.069
173	0.624	0.088	0.112	0.134
55	0.351	0.070	0.052	0.083
223	0.274	0.095	0.044	0.058

The natural sorbents can be classified according to the forms of their discharge curves: the diatomites have, for example, discharge curves which would relate them to the coarse porous sorbents, gubrin acts as a finely porous sorbent, and so forth (Figure 4).

It is clear from the experimental data that the application under dynamic conditions of the method of molecular probes makes it possible:

1) to relate the kinetics of the adsorbtion process to the porous structure of the sorbent;

2) to employ a simple dynamic technique with the determination of the concentrations in the discharge fluids either by interferometry of by refractometry;

3) to obtain an idea as to the structural type of an investigated adsorbent and to determine its specific area, with small expenditure of time, in dynamic experiments extending from two to four hours; and

4) to obtain a quantitative characterization of the porous structure of an adsorbent by additively compounding the adsorption before and after "breakthrough."

LITERATURE CITED

[1] M. M. Dubinin, The Physicochemical Basis of Sorption Practice (Moscow, 1935).

[2] G. V. Tsitsishvili, D. N. Barnabashvili, Proc. Acad. Sci. USSR 101, 711 (1955).

[3] N. N. Avgul, O. M. Dzhigit, A. V. Kiselev, J. Phys. Chem. 29, 316 (1955).

[4] P. G. Romankov, E. F. Nemet, Outlines of the Papers Delivered at the Scientific-technological Conference at the Lensoviet Technological Institute in Leningrad (Leningrad, 1955), p. 99.

[5] M. M. Dubinin, Bull. Acad. Sci. USSR 1950, No. 3.

[6] M. M. Dubinin Reports Delivered at the 13th International Conference on Chemistry (Acad. Sci. USSR Press, 1953).

The Far Eastern Branch of the Academy of the USSR, Vladivostok

Received August 25, 1956

THE THERMOELECTRICAL PROPERTIES OF THE SILICIDES OF CHROMIUM

L. N. Guseva and B. I. Ovechkin

(Presented by Academician I. P. Bardin, August 6, 1956)

The investigation of the electrical and the thermoelectrical characteristics of the alloys of chromium with silicon is of interest in connection with the search for materials which would possess the properties of semiconductors.

Chromium forms a series of chemical compounds with silicon. The compositions of the compounds $CrSi_2$, CrSi and Cr_3Si have been established and their crystal structures have been studied [1]. There are data pointing to the existence of silicides of the compositions Cr_2Si [2] and Cr_5Si_2 [2, 3]. A study of the phase diagram, which we have carried out by x-ray analysis and by analyses of microstructures, has failed to disclose these latter two compounds and has shown the existence of a single intermediate phase, of the composition Cr_5Si_3, between the compounds CrSi and Cr_3Si.

There is a lack of information concerning the thermoelectrical properties of the alloys of chromium and the data on their electrical properties is, also, very limited. Data on the specific resistance of the alloys of chromium with silicon is presented in [3]. These authors employed silicon which contained up to 1.3% of metallic contaminants and their data cannot, therefore, characterize the electrical properties of the individual silicides.

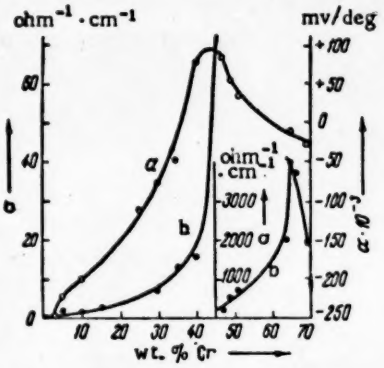

Fig. 1. The thermoelectric power, α (a) and the specific conductivity, σ (b) of the quenched alloys of chromium and silicon.

We have studied the electrical and the thermoelectrical properties of the separate silicides and of the heterophase alloys which are rich in silicon.

The alloys, with barium chloride as a flux, were fused in quartz crucibles in a high frequency furnace. Electrolytically refined chromium and silicon of 99.8% purity served as the starting materials. Homogenizing annealing was carried out for four days in vacuum and at 1100°, and was followed by a water quenching. The phase compositions of the silicides of chromium were established by x-ray and by microstructural analyses. Their properties were determined by the compensation method using a potentiometer of the type PPTV-1. The thermoelectric power was measured against copper.

After its smelting, the alloy of the composition Cr_5Si_3 proved to be porous; it was, accordingly, pulverized, pressed and sintered, after which its properties were studied.

The results of the measurements are presented in Figure 1. The conductivity of the alloys in the heterophase region from 0 to 40 weight per cent Cr shows an insignificant increase with increasing content of chromium and for the compound $CrSi_2$ amounts to about 150 ohms^{-1}·cm^{-1}. With the appearance in the alloys of the silicide CrSi (at concentrations of chromium exceeding 48 weight per cent) the electrical conductivity sharply increases, attaining, at 65 weight per cent Cr a maximum value of 4000 ohms^{-1}·cm^{-1}.

The thermoelectric power of the alloys also changes with their composition. At small contents of chromium the thermoelectric power falls to zero, changes in its sign, and, increasing in proportion to the increase in the chromium concentration, reaches a maximum positive value at a composition near to that of the compound $CrSi_2$. In the region of compositions bounded by the silicides $CrSi_2$-CrSi the thermoelectric power falls to $-12 \cdot 10^{-3}$ mv/degree.

The thermoelectric power and the electrical conductivity of the silicide $CrSi_2$ do not depend on its previous thermal working.

Data on the electrical conductivity and the thermoelectric power of the individual silicides are given in Table 1.

It is to be seen from this table that, in terms of thermoelectric power and electrical conductivity, only the compound $CrSi_2$ can be classed as a substance of the semiconducting type; for this we therefore carried out an investigation of the relationship between the conductivity and the thermoelectric power over the interval of temperature from 20 to 600° (see Figures 2,3,4).

TABLE 1

Compound	$CrSi_2$	CrSi	Cr_5Si_3	Cr_3Si
Composition, Wt.% Cr	47.5	65.0	75.4	84.0
σ, $ohms^{-1}$, cm^{-1}	150	4000	1500	22 000
$\alpha \cdot 10^{-3}$, $\mu v/deg$	+90	−12	−2	—

From the curve showing the change of σ with temperature (Figure 2, b) it is obvious that up to 400° there is a gradual fall in the conductivity of the $CrSi_2$. With further increase in the temperature, however, there is observed a rise in the conductivity, and the semiconducting nature of this compound is thus confirmed.

In Figure 3 there is presented a semilogarithmic plot of the conductivity vs. the reciprocal temperature, from which it follows that the conductivity at the low and the conductivity at the high temperatures are of different character. Up to 400° the electrical conductivity is principally determined by the carriers of the additives; for still higher temperatures it is fixed by the carriers of the basic substances. Over the region of intrinsic conduction the increase of the electrical conductivity with temperature follows an exponential law and is covered in the graph by a straight line. The width of the energy gap for this silicide can be determined from the magnitude of the tangent of the angle of inclination of this straight line to the axis of abscissas. It amounts to 1.3 ev

$$\Delta E_{CrSi_2} \approx 2.2 \cdot 10^{-12} \text{ erg} \approx 113 \text{ ev}.$$

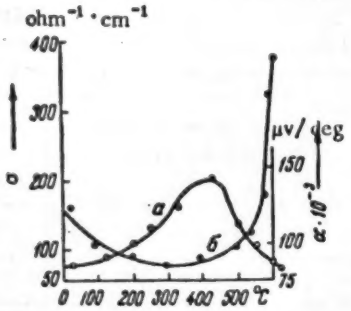

Fig. 2. The relationship between the thermoelectric power, α, (a) and the specific conductivity, σ, (b) for the compound $CrSi_2$.

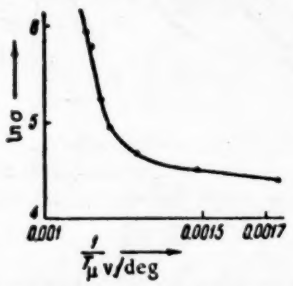

Fig. 3. The $\ln \sigma$ vs $1/T_{abs}$ relation for the compound $CrSi_2$.

The temperature dependence of α is also shown in Figure 3. In the region of additive conduction the thermoelectric power increases with temperature from $90 \cdot 10^{-3}$ to $140 \cdot 10^{-3}$ millivolts/degree. On entrance into the region of intrinsic conductivity its value falls to $80 \cdot 10^{-3}$ millivolts/degree at 610°. This change of the thermoelectric power with temperature follows the law which has been deduced for electron and hole semiconduction[4].

Through the electrical and the thermoelectrical properties of the silicides of chromium it is thus shown that the compounds Cr_3Si, Cr_5Si_3 and CrSi are conductors of the metallic type; the compound $CrSi_2$ is a semiconductor having an energy of activation of approximately 1.3 ev.

LITERATURE CITED

[1] B Boren, Ark. Kemi. Miner. Geol. 11A (10), 1 (1933).

[2] N. N. Kurnakov, Bull. Sect. Phys. Chem. Anal. 16, 4, 77 (1948).

[3] R. Kiffer, F. Benesovsky and H. Schroth, Z. Metall. 44, (10), 437 (1953).

[4] A. F. Ioffe, Semiconductors in Modern Physcis (Acad. Sci. USSR Press 1954), p. 201.

The A. A. Baikov Institute of Metallurgy of the Academy of Sciences of the USSR

Received July 31, 1956

A RADIOMETRIC STUDY OF THE CHROMATOGRAPHY OF DI- AND TRIVALENT IONS OVER THE INTERVAL OF CONCENTRATIONS FROM 10^{-1} TO 10^{-9} N

S. Yu. Elovich and V. N. Prusakov

(Presented by Academician A. N. Frumkin April 24, 1956)

The development of theoretical work in the field of chromatography has led to the conclusion that the chromatographic processes depend on factors of physicochemical equilibrium as well as on transfer phenomena. Attempts at solving the chromatographic problem in its general mathematical form have led to extremely complicted equations, the exact solutions of which cannot always be obtained [1].

In this work we have set ourselves the task of evaluating the role of transfer phenomena in the chromatography of di-and trivalent ions over the interval of concentrations from 10^{-1} to 10^{-9} N.

It is possible to embrace so wide a range of concentrations by using the radioactive isotopes Ce^{144} and Sr^{89}, without carriers. The technique which we have employed was characterized by the fact that the movement of the ions through the column was followed radiometrically with the aid of a method of coincidences. In view of the strong adsorption of the β radiation from Sr^{89} (E~1.5 Mev) by the walls of a glass column, we constructed a column with walls of x-ray film of 0.1 mm thickness.

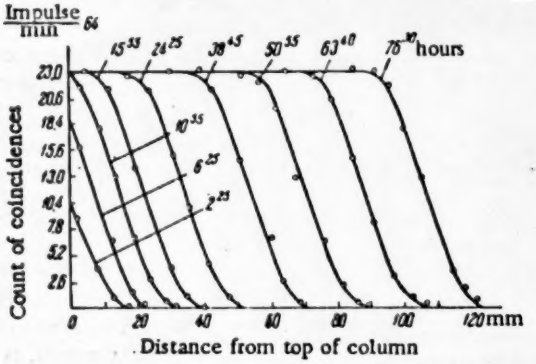

Fig. 1. The dynamics of the sorption of Ce out of a 0.01 N $CeCl_3$ solution. Volume velocity of flow, 0.5 ml/cm^2 · min.

As an adsorbent we employed the cation exchanger KU-2 with a capacity of 1.9 mg-equiv/ml. This substance has the one functional group, HSO_3.

We first investigated the dynamics of adsorption of the ions of Sr^{89} and Ce^{144} on a column containing 15 g of the pulverized (40 mesh) cation exchanger Ku-2 in the H form. The general course of the dynamics of the sorption on this adsorbent is shown in Figure 1. It is clear that after the period of the establishment of the front of the Ce^{+3} ions, a regime of parallel transfer is maintained. It is possible to prove that for both the divalent Sr^{+2} and the trivalent Ce^{+3} ions there is valid the well-known equation of Shilov:

$$\theta = aL - \tau, \tag{1}$$

where θ is the time of the filtration of the solution, L is the length of the employed layer of the adsorbent and τ is the time for the establishment of the front. The velocity of the movement of this front is subject to the Shilov equation:

$$W = u \frac{C_0}{q_{Me} + \alpha C_0}. \tag{2}$$

Here u is the linear flow velocity of the solution; C_0 is the concentration of the metallic ions in solution; q_{Me} is the adsorbed quantity of cations on 1 ml of exchanger in the exhausted layer and α is the empty volume in the layer of adsorbent. Thus, knowing the constants for ionic exchange of the ions Sr^{+2} and Ce^{+3}, we can calculate the rate of movement of the ion front. The constants for the exchange of $Ce^{+3} - H^+$ and $Sr^{+2}-H^+$, as determined by us, are respectively equal to 2.94 and 1.72.

Making use of the Nikolskoy equation of ion exchange:

$$q_{Me} = k_3^z \frac{f_{Me} C_{Me}}{f_H C_H^z} q_H^z \tag{3}$$

(where f is the activity coefficient; C_{Me}, C_H are, respectively, the concentrations of the metallic and the hydrogen ions; q_H is the quantity of the adsorbed hydrogen ion and Z is the ionic charge), we can calculate the velocity of the movement of the ion front under equilibrium conditions.

The results of a comparison of the calculated and the experimental values are presented in Table 1.

TABLE 1

The Movement of the Fronts of Ce^{+3} and Sr^{+2} During Adsorption

Ion	Concentration of the Me ions, g-equiv/liter	conc. H^+ ions g-equiv/l	Velocity of filtration, u_0, ml/cm^2·min	Velocity of movement of the front, W, cm/hour	
				calculated	experimental
Sr^{2+}	0.005	10^{-3}	0.5	0.080	0.072
Sr^{2+}	0.01	10^{-3}	0.5	0.16	0.149
Sr^{2+}	0.1	10^{-3}	0.5	1.58	1.46
Sr^{2+}	0.01	10^{-3}	1.22	0.38	0.35
Sr^{2+}	0.01	10^{-3}	3.0	0.95	0.86
Sr^{2+}	0.01	10^{-3}	6.0	1.90	1.72
Sr^{2+}	0.1	0.3	0.5	2.20	1.99
Ce^{3+}	0.01	10^{-3}	0.5	0.16	0.14
Ce^{3+}	0.1	1.2	0.5	2.75	2.40

The data of Table 1 show that it is possible to calculate the velocity of the ion movement along the column under changes of concentration ranging from 0.005 to 0.1 N for the metallic ions and from 10^{-3} to 1.2 N for the hydrogen ion. The process proceeds under conditions which approximate those of equilibrium.

A comparison of the form of the fronts (Figure 2) shows that a compression of the front is brought about by the passage from low to high concentrations. At a concentration of 0.3 N this compression ceases and the front becomes stable. Thus, from this most sensitive criterion of the dispersion of the front, it is possible to conclude that it is permissible to neglect the phenomena of transfer under the customary conditions of chromatography, with volume velocities which are equal to 0.5-1.0 ml/cm^2·min and under ion concentrations which are greater than 0.1-0.3 N. The role of ultra-small concentrations of ions was cleared up by the study of displacement chromatography.

The balance equation in terms of the displaced ions can be written for an infinitely thin section of the column as:

$$u_0 \frac{\partial C_{Me}}{\partial x} = -\frac{\partial q_{Me}}{\partial l} - \alpha \frac{\partial C_{Me}}{\partial t}. \tag{4}$$

Here t is the time and and x is the distance measured along the column.

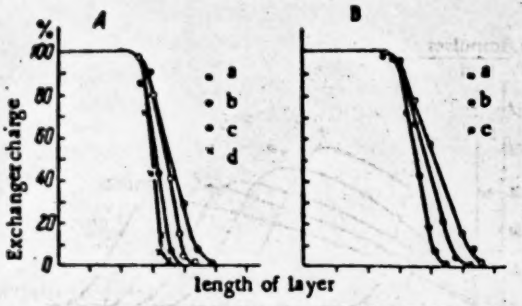

Fig. 2. The influence of the concentration of the filtered solution on the diffusion of the sorption fronts of the Sr and Ce ions. Volume velocity of flow, 0.5 ml/cm^2·min. A) $SrCl_2$: a) 0.005N, b) 0.01 N, c) 0.1 N, d) 0.3-0.4 N ; B) $CeCl_3$: a) 0.01 N, b) 0.1 N, c) 0.3-0.5 N.

In writing down this equation it was assumed that the solution moves uniformly through the pores of the charge and that the volume of the cation exchanger remains unchanged during the process. Also, no account was taken of longitudinal diffusion. The justification for this last was tested with the aid of Ce^{144}. A column on which there was adsorbed a micro-zone of cerium was filled up with 1.4 N HCl and was allowed to stand for several days. The distribution of the active zone was scarcely changed thereby. It is clear that the migration of ions along the column could be neglected in our experiments.

During the displacement of metallic ions from the column by hydrogen ions of varying concentration, $q_{Me} = f(C_{Me}, C_H)$ and the change in adsorption, $\partial q_{Me}/\partial C_{Me}$, depends on C_{Me} as well as on C_H. In general C_{Me} and C_H depend on time, and on other parameters as well.

$$\frac{\partial q_{Me}(C_{Me}C_H)}{\partial t} = \frac{\partial q_{Me}}{\partial C_{Me}}\frac{\partial C_{Me}}{\partial t} + \frac{\partial q_{Me}}{\partial C_H}\frac{\partial C_H}{\partial t}. \qquad (5)$$

Introducing the sumbolism $\partial q_{Me}/\partial C_{Me} = q'_{Me}(C_{Me})$ and $\partial q_{Me}/\partial C_H = q'_{Me}(C_H)$ and substituting into the balance equation, we have:

$$u_0\frac{\partial C_{Me}}{\partial x} = q'_{Me}(C_{Me})\frac{\partial C_{Me}}{\partial t} + q'_{Me}(C_H)\frac{\partial C_H}{\partial t} + \alpha\frac{\partial C_{Me}}{\partial t}. \qquad (6)$$

A similar equation is also valid for the phenomenon of liquid molecular chromatography with an exchange mechanism of the molecular adsorption. In the special case where $C_{Me} + C_H = \text{constant}$, integration of this equation leads to the formula:

$$\left(\frac{x}{t}\right)_{C_{Me}} = \frac{u_0}{q'_{Me}(C_{Me}) - q'_{Me}(C_H) + \alpha}. \qquad (7)$$

Thus the velocity of movement of the cross-sectional zone must be determined by the difference of the two derivatives.

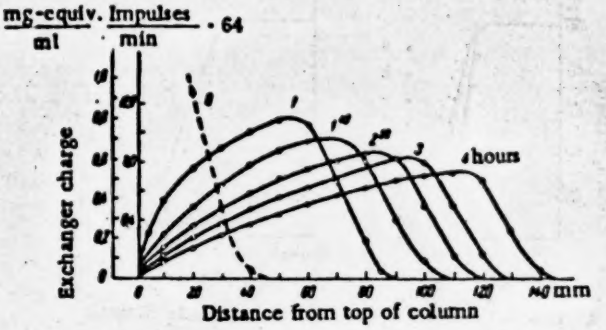

Fig. 3. The dynamics of desorption of Ce (by 1.4 N HCl solution). Volume velocity of flow 1 ml/cm² · min.

In the case of equivalent ionic exchange and constant adsorption capacity, it is possible to write:

$$C_0 = C_{Me} + C_H; \quad S = q_{Me} + q_H, \tag{8}$$

where C_0 is the concentration of the displacer and S is the capacity of the ion exchanger. Equation (6) then goes over into the following:

$$\left(\frac{x}{t}\right)_{C_{Me}} = \frac{u_0}{\partial q_{Me}/\partial C_{Me} + \alpha}. \tag{9}$$

Introducing here the value of the derivative taken from the isotherms for the two and three valent ions [Equation (3)], we obtain:

for the Sr^{+2} ion:

$$\left(\frac{x}{t}\right)_{C_{Me}} = \frac{u_0}{\frac{q_{Me}^2}{C_{Me}^2}\frac{C_0^2 - C_{Me}^2}{k_1^2(S^2 - q_{Me}^2)} + \alpha}; \tag{10}$$

for Ce^{+3} ion:

$$\left(\frac{x}{t}\right)_{C_{Me}} = \frac{u_0}{\frac{q_{Me}(C_0^3 - 3C_0C_{Me}^2 + 2C_{Me}^3)}{C_{Me}[3k_1^3C_{Me}(S - q_{Me})^2 + (C_0 - C_{Me})^3]} + \alpha}; \tag{11}$$

$k_1 = k_0 f_{Me}^{1/Z}/f_H$.

Thus, in equilibrium displacement chromatography the velocity of the movement of the front depends on a series of parameters.

Under constancy of the concentration of the displacer, C_0, and of the relationship between the activity coefficients, the isotherm for ultra-small concentrations of Ce^{144} and of Sr^{89} can be written as $q_{Me} = k_2 C_{Me}$. In these conditions equations (10) and (11) go over into $(x/t)C_{Me} = \frac{u_0}{k_2} + \alpha$ and all of the points on the wave must move with a steady velocity, as has been pointed out earlier, [2].

In Figure 3 there is shown a typical picture of the dynamics of the displacement of cerium ions by hydrochloric acid. In Figure 4 there are plotted the experimental points from one of our runs. The points lie nicely on the calculated curve.

Thus, even for displacement chromatography under conditions such that macro-quantities are adsorbed at velocities of liquid movement ranging from 0.5 to 1 ml/cm^2·min, it is possible to make use of the equation of equilibrium chromatography.

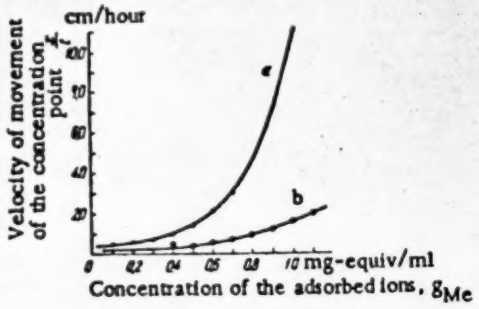

Fig. 4. The concordance between the experimental points and the theoretical curve for the displacement of the ions of Ce and Sr by HCl solutions. a) $C_0 = 1.2$ g-equiv/liter $u_0 = 0.5$ ml/cm^2·min; b) $C_0 = 0.3$ g-equiv/liter $u_0 = 0.5$ ml/cm^2·min.

In the adsorption of ultra-small quantities of Ce^{144} and of Sr^{89} we employed a narrow, highly radioactive, ring in the upper part of the column. The charge of the adsorbent was approximately 10^{-6} of its capacity. After adsorption the column was washed out with hydrochloric acid of another concentration. Here the constancy of the velocity of the movement of the cross-sectional zone was not observed. Equation (9) clearly is not valid. It follows that with ultra-small concentrations under our conditions, it is necessary to take the phenomenon of ionic diffusion into account even at small volume velocities of movement of the liquid current. The velocity of the diffusion process becomes material then for the over-all process.

LITERATURE CITED

[1] DeVault, J. Am. Chem. Soc. 65, 532 (1943); S. Goldstein, Proc. Roy. Soc. 219, 151, 171 (1953); N. N. Tumitsky and E. P. Chemeva, J. Phys. Chem. 24, 1350 (1950); A. A. Zhukhovitsky, Ya. L. Zabezhinsky and A. P. Tikhonov, J. Phys. Chem. 19, 253 (1945); S. E. Bresler, Proc. Acad. Sci. USSR 90, No. 2, 205 (1953); O. M. Todes, J. Appl. Chem. 18, 591 (1945).

[2] E. Wicke, Angew. Chem. 1947, 15.

The Institute of Physical Chemistry
of the Academy of Sciences of the USSR

Received March 3, 1956

THE USE OF INFRARED ABSORPTION SPECTRA IN STUDYING THE SENSITIZATION OF THE PHOTOOXIDATION OF ORGANIC COMPOUNDS BY ANTHRAQUINONE DERIVATIVES

A. V. Karyakin and A. V. Shablya

(Presented by Academician A. N. Terenin, July 14, 1956)

Many investigations [1] have been concerned with the study of the sensitized oxidation of organic compounds and the number of such works has continually increased in recent years. To the sensitized oxidation of those organic compounds which we have studied there has already been devoted the following work. The photochemical oxidation of benzaldehyde under the action of ultraviolet light has been studied by many investigators and the fact was established that this is a chain reaction with a quantum yield of 10,000 [2]. This reaction has been sensitized to visible light with the aid of benzophenone, acetophenone and other substances [3]. It was shown at the same time that rhodamine 6G and auromine did not induce this chain reaction. The photooxidation of tetralin could, however, be brought about by using derivatives of anthraquinone as sensitizers [4]. It should be noted that the sensitized oxidation of ethyl alcohol can be induced by derivatives of anthraquinone [5].

In recent years there have appeared the numerous papers of Schenk on the photosensitized oxidation of various organic substances, including isopropylbenzene, using fluorescent dyes (eosin, chlorophyll methylene blue, and others) in the presence of oxygen [6].

In all of the above mentioned reactions of photooxidation of organic substances a manometric method was applied for following the consumption of oxygen.

Experiments on the use of anthraquinone and its derivatives for sentsitizing the photooxidation of benzaldehyde and tetralin in visible light were carried out in our laboratory [1]. Here the products of reaction of sensitized photooxidation of the benzaldehyde and tetralin were determined through infrared absorption, just as in the case of the direct photooxidation of organic substances [7].

It was the aim of the present work to investigate the use of anthraquinone and its α-and β-oxo and amino derivatives for sensitizing to visible light the photooxidation by molecular oxygen of benzaldehyde, tetralin and isopropylbenzene (cumol). These substances were selected by us because of the fact that there is a marked difference in the action of oxygen on their excited molecules. In the vaporous form and in the absorbed state, the fluorescence of anthraquinone and its β derivatives is strongly quenched by oxygen, whereas the fluorescence of the α derivatives is scarcely suppressed at all [8]. Utilizing the various derivatives of anthraquinone as photosensitizers for the oxidation of organic compounds, it is thus possible to correlate the initial stages of the sensitization of the oxidation reaction with the quenching of fluorescence.

The sensitized oxidation of these organic compounds was carried out in the apparatus described earlier [7] and was followed through the absorption bands at 6800 and 4220 cm^{-1} (OH) in the near infrared region of the spectrum, using an automatic infrared spectrometer with a quartz prism. High-pressure quartz mercury lamps of the types SVDSh-250-Z and SVDSh-500, in combination with various glass filters for the separation of those parts of the spectrum which were absorbed only by the sensitizer, were employed as the source of light. A water filter (a 50 mm layer of water) served for the absorption of the infrared radiation of the mercury lamp.

The concentration of the sensitizers – the derivatives of anthraquinone in the organic substances – ranged from 10^{-4} to 10^{-5} moles/liter.

A solution of benzaldehyde in CCl_4 (10%), containing either anthraquinone or β-aminoanthraquinone, showed the following changes in the infrared absorption spectrum after illumination at $\lambda > 400$ mμ (quartz mercury lamp SVDSh-500 with filter ZhS-12) for five hours under continuous aeration with oxygen (at a velocity of 0.2 liters per minute). At 4220 cm^{-1} there appeared an absorption band which corresponded to the band found at approximately this same frequency in the spectrum of benzoic acid in CCl_4. At the same time there was noted a decrease in the intensity of the absorption bands at 4525 and 4435 cm^{-1} which are associated with the vibrations C-H_{al}. Using α-aminoanthraquinone, or a simple solution of benzaldehyde, no change in the infrared tion spectrum was noted as the result of illumination at these same wavelengths under simultaneous aeration with oxygen. Hence, in the cases of anthraquinone and β-aminoanthraquinone there is a direct relationship between the possibility of sensitizing the photooxidation of benzaldehyde and the extinction of fluorescence. Similar conclusions could be drawn from a comparison of the quenching of the fluorescence of anthraquinone and six of its derivatives by oxygen and their sensitization of the oxidation of tetralin. In the case of tetralin it was possible to utilize larger quantities of the anthraquinone derivatives for sensitization since the natural absorption of tetralin begins only at $\lambda > 320$ mμ. Because of the low rate of the sensitized reaction of the oxidation of tetralin and in order to exclude secondary dark reactions, we employed here a more powerful source of ultraviolet light; namely, a quartz mercury lamp of the type SVDSh-500 in combination with a BS-7 filter which transmitted wave lengths $\lambda > 320$ mμ, the experiments extending over eight hours. The existence of sensitized oxidation of the tetralin was established by the appearance of the band of the first OH (2ν) overtone in the near infrared absorption spectrum at 6800 cm^{-1} (Figure 1, II). The photooxidation of tetralin was sensitized by anthraquinone, β-oxy-and β-aminoanthraquinone, anthranol and α-chloroanthraquinone. With α-oxy, α-aminoanthraquinone and 1,4 dioxyanthraquinone no oxidation was detected.

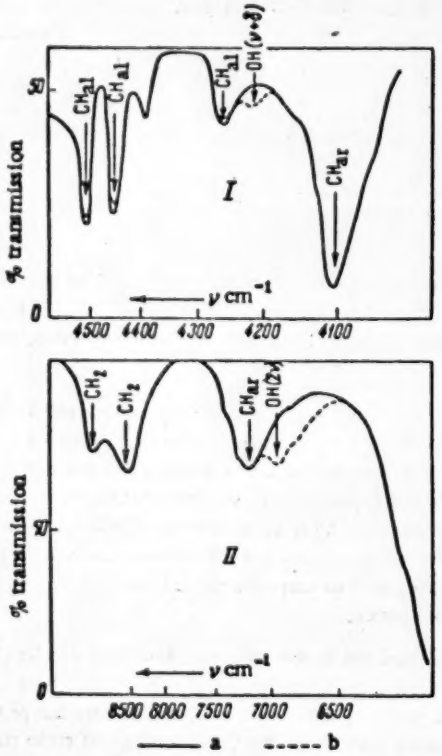

Fig. 1. I) benzaldehyde, II) tetralin; a, before and b, after oxidation.*

From the absorption spectra it was established that anthraquinone is approximately twice as effective as its derivatives in sensitizing the photoreaction of oxidation, the sensitizing action of these derivatives being approximately the same.

The experimental data point to a close interdependence between the sensitizing action of anthraquinone and its derivatives, the strong quenching of the fluorescence of these compounds by molecular oxygen and the phenomenon of retarded fluorescence, i.e., the existence of a triplet level.

The same conclusion could be drawn from the sensitization of the oxidation of isopropylbenzene by anthraquinone, α- and β- aminoanthraquinone, for which the sensitizing reaction proceeded much more slowly than in the case of tetralin, all other conditions being the same.

The quenching of the fluorescence of the derivatives of anthraquinone was earlier explained [8] in terms of a transition of the excited molecules, resulting from their collisions with O_2 and leading into a metastable triplet state, which for β-aminoanthraquinone was situated ~0.2 ev lower than the singlet level. Fluorescent quenching does not occur when the distance between these levels is definitely greater than 0.2 ev as it is, for example, in α-aminoanthraquinone (0.8 ev). In the triplet state the molecule, as a result of the existence of two unpaired electrons, is capable of uniting with an unsaturated oxygen molecule which functions as a biradical, there being formed

*Subscripts: al = aliphatic; ar = aromatic.

an unstable oxide complex [10]. The quenching of fluorescence is, therefore, an indication of the union of oxygen with an optically excited molecule which has a close lying triplet level.

From the data of the literature [2, 3, 5, 6] and on the basis of a comparison of the associated phenomena of sensitization and fluorescence it is possible to draw the following conclusions concerning the mechanism of sensitizing the oxidation reaction.

On adsorption of a quantum of light, the sensitizer passes into an excited condition and then, under the action of the paramagnetic O_2 molecule, into a metastable (triplet) state

$$S \xrightarrow{h\nu} S^{\cdot} \xrightarrow{O_2} {}^{\cdot}\tilde{S}^{\cdot} \qquad (1)$$

(the symbol ~ designates an excess of vibrational energy). The biradical, i.e., the molecule in the triplet condition, can combine with oxygen forming an unstable complex with the properties of a biradical.

$$\cdot S \cdot + O_2 \rightarrow \cdot SO_2 \cdot. \qquad (2)$$

It is the biradical $\cdot SO_2 \cdot$ which, with its enhanced chemical activity, is responsible for the sensitization of the photooxidation of the organic compounds. Thus, the following become the possible initial stages of the chain reaction of oxidation:

a) the biradical $\cdot SO_2 \cdot$ gives its electronic energy of excitation to the molecule which is undergoing oxidation, carrying the latter into the state of a biradical, this transfer of energy having a high probability since a similar process takes place during sensitized fluorescence [1, 11].

b) the biradical $\cdot SO_2 \cdot$ dehydrates the molecule undergoing oxidation, forming a corresponding radical. Such dehydration of organic compounds must proceed with a smaller likelihood than does the transfer of energy, this process demanding a large quantity of energy for the rupture of the C-H bond.

The sensitized oxidation of benzaldehyde occurs chiefly by means of a transfer of the energy of excitation, the benzaldehyde molecule being carried over into the form of a biradical.*

$$\cdot SO_2 \cdot + C_6H_5-C\begin{matrix}O\\H\end{matrix} \rightarrow C_6H_5C\begin{matrix}O\cdot\\H\end{matrix} + S + O_2 \qquad (3)$$

Further development of the chain reaction is brought about by the benzaldehyde biradical, as was shown in [1, 7]. The dehydration of the molecule of benzaldehyde by $\cdot SO_2 \cdot$ is possible, but less likely

$$\cdot SO_2 \cdot + C_6H_5-C\begin{matrix}O\\H\end{matrix} \rightarrow C_6H_5C\begin{matrix}O\\\cdot\end{matrix} + \cdot SO_2H \qquad (4)$$

* This conclusion agrees with the results of a supplementary investigation of the possibility of sensitizing the oxidation of benzaldehyde with the 2 and 3 amino derivaties of acridine, one of which has a triplet level corresponding to $\lambda > 500$ mμ and undergoes quenching of fluorescence. Despite these facts, neither substance sensitizes the reaction of photooxidation of benzaldehyde; acridine and its β derivatives do sensitize it, however, although in them the triplet level lies in the blue region of the spectrum at $\lambda < 500$ mμ.

A metastable (triplet) state is not known for tetralin or for isopropylbenzene but, in analogy with benzene and its derivatives, it can be supposed that these triplet levels would lie considerably higher, in the ultra-violet region of the spectrum. It is consequently to be supposed that the transfer of the energy of excitation is unlikely and that the biradical $\cdot SO_2\cdot$ brings about the dehydration of the hydrocarbon with the formation of a corresponding biradical which initiates the chain reaction.

The mechanism of sensitized oxidation of tetralin and, by analogy, that of isopropylbenzene, can be represented in the form of the equation:

$$\cdot SO_2\cdot + >CH_2 \rightarrow \cdot SO_2H + \cdot >CH$$

$$\cdot >CH + O_2 \rightarrow >C(H)-O-O\cdot$$

$$>C(H)-O-O\cdot \; + >CH_2 \rightarrow >C(H)-O-O-H \; + \cdot >CH \text{, etc.} \qquad (5)$$

The regeneration of the sensitizer can proceed according to the following scheme:

$$\cdot SO_2H \rightarrow .S + HO_2\cdot \qquad (6)$$

$$2HO_2\cdot \rightarrow H_2O_2 + O_2 \qquad (7)$$

The present work was carried out under the direction of Academician A. N. Terenin to whom the authors express their deep appreciation.

LITERATURE CITED

[1] A. N. Terenin, The Photochemistry of Dyes (Acad. Sci. USSR Press, 1948); Problems of Chemical Kinetics, Catalysis and Reactivity (Acad. Sci. USSR Press 1955), . 85.

[2] H. Suida, Ber. 46, 3530 (1913); H. L. I. Bäckström, J. Am Chem. Soc. 49, 1460 (1927); W. P. Jorissen, P. A. A. van der Beek, Rec. trav. chim., 46, 42 (1927); 47, 286 (1928); 49, 138, 140 (1930); H. L. I. Bäckström and H. A. Beatty, J. Phys. Chem. 35, 2530 (1931); H. L. I. Bäckström, Z. Physik. Chem. 25, 99 (1934).

[3] H. L. I. Backstrom, Medelanden fran K. Vetenskapsakademiens Nobelinstitut 6, H. 2, No. 6, 1 (1927); The Swedberg memorial volume (Uppsala, 1944), p. 45; Almquist och Wiksells Boktryckeri.

[4] C. H. Bamford, M. I. S. Dewar., J. Soc. Dyers Colourists, 65, 674 (1949); Proc. Roy. Soc. (A) 198, 252 (1949).

[5] I. L. Bolland and H. R. Cooper, Proc. Roy. Soc. 225, 405 (1954).

[6] G. O. Schenck, Naturwiss. 35, 28 (1948); Z. Elektrochem. 55, 505 (1951); Angew. Chem. 64, 12 (1952); O. G. Schenck, Naturwiss 43, 71 (1956).

[7] A. V. Karyakin, V. A. Nikitin and K. I. Ivanov, J. Phys. Chem. 27, 1856 (1953); A. V. Karyakin and V. A. Nikitin, Bull. Acad. Sci. USSR, Phys. Ser. 17, No. 5, 636 (1953); J. Phys. Chem. 27, 1867 (1953).

[8] A. V. Karyakin and A. N. Terenin, Bull. Acad. Sci. USSR, Phys. Ser. 13 (1949); A. V. Karyakin J. Phys. Chem. 23, 1332, 1345, 1949.

[9] A. V. Karyakin, Ya. I. Kalenichenko J. Phys. Chem. 26, 103 (1952);

[10] A. N. Terenin, A. V. Karyakin and Ya. I. Kalenichenko, Proc. Acad. Sci. USSR 67, 305 (1949); A. N. Terenin and A. V. Karyakin, J. Exptl.-Theoret. Phys. 21, 107 (1951); A. V. Karyakin and A. N. Terenin Proc. Acad. Sci. USSR 97, 479 (1954).

[11] A. N. Terenin and A. V. Karyakin, Bull. Acad. Sci. USSR, Phys. Ser. 15, 550 (1951); Proc. Acad. Sci. USSR 96, 269 (1954).

Received July 2, 1956

CONCERNING THE NEGATIVE DIFFERENCE EFFECT ON MAGNESIUM

D. V. Kokoulina and B. N. Kabanov

(Presented by Academician A. N. Frumkin July 11, 1956)

In the anodic dissolution of magnesium in aqueous salt solutions there is a characteristic increase in the rate of evolution of hydrogen with increasing anodic current density which is known in the theory of corrosion as the negative difference effect. The negative difference effect is observed only for the active, easily oxidized, metals such as Mg and Al [1-4]. For magnesium there has been described a negative effect for salt solutions and a positive effect in solutions of HCl [5].

There are two hypotheses which explain this negative difference effect. The first of these correlates the increased evolution of hydrogen solely with an increased corrosion of the anode resulting from the destruction by anodic polarization of the oxidized layer which protects the metal [1, 3, 4, 6-8]. The second hypothesis ties up the evolution of hydrogen exclusively with the fact that the metal in the anodic process enters solution, in part, in a lower valence form, (Mg, for example, as the univalent ion), and that the water then oxidizes it to the normal valence with the liberation of hydrogen. It is supposed here that the spontaneous dissolution of the anode at polarization, to all intents and purposes, does not occur [9, 10]. The various experimental observations on the magnesium anode – the evolution of hydrogen after breaking the circuit [9], the direct proportionality between the rate of evolution of hydrogen and the density of the anodic current [7, 8], the uniform velocity of the hydrogen evolution during the passage of direct and of interrupted currents of low frequency (60 cycles per second) [9], the reduction of oxidizing agents at the magnesium anode – all can be explained from either point of view. It can be doubted that the reduction of a solution of an oxidizer actually occurs during the introduction into it of an anolyte when there is no direct contact of the anode with a solution of an oxidizing agent which is definitely more stable in solution than is the Mg^+ ion, since the magnitude of this effect lies at the limit of the sensitivity of the measurements. It is thus so that the factual material available at the present time cannot serve as a convincing demonstration of the correctness of the one or the other of these proposed hypotheses. It was in this connection that the present work was undertaken.

In anodic polarization at current densities larger than that which is associated with spontaneous dissolution, but smaller than that corresponding to the passivity of magnesium in the given solution, the steady potential of the magnesium anode does not depend on the current density. This potential is subject, however, to a change with time which is analogous to that which is observed with the aluminum electrode [1]. The change in potential with respect to time which results from the alteration of the current density is indicated in Figure 1. The steady values of the potential at the two current densities are almost identical; however, immediately after a change in the current density the potential of the electrode proves to be different from this steady value. These changes undoubtedly indicate an alteration in the surface condition of the electrode; immediately after decreasing the current or breaking the circuit, the surface of the magnesium is, for several seconds, in a more active form than it is in its steady state under these same conditions. The question as to whether this change in the surface condition essentially influences the over-all rate of hydrogen evolution is one which remains open.

We have measured the potential of the magnesium electrode and the velocity of hydrogen evolution in $MgSO_4$ solutions during the passage of anodic currents in the form of rectangular pulses for which the duration of the current flow and the current interruption were equal. In Figure 2 it is seen that the electrode potential was subjected to pronounced variations, the amplitude of which depended on the impulse frequency in such a way

that the mean value around which these variations of the potential occurred was approximately 0.15 volts more negative than the stable potential for polarization by a direct current of the same strength.

The anode undergoes activation during the passage of the current pulse and, over the interval of interruption of the current, passivation occurs. At high frequencies of the current pulses the surface will not succeed in completely passifying during the time of current interruption nor will it succed in completely activating during the time of current passage; in general, the spontaneous dissolution under these conditions should not be equal to that which is observed during the passage of a direct current.* If the spontaneous dissolution of the anode is the cause of interrupted difference effect it should follow that the velocity of evolution under an the negative current would differ from the velocity of evolution under a direct current of the same strength. If, on the other hand, the cause of the hydrogen evolution is the chemical reaction of the oxidation of the Mg^+ ion by water, then the velocity of evolution would be determined exclusively by the amount of Mg^+ which is formed in a unit time, which amount is proportional to the density of the current which is transmitted and is independent of the existence of current interruptions and of changes in the surface condition.

As is to be seen from Figure 3, the velocity of hydrogen evolution in $MgSO_4$ solutions proved to be the same for both the direct and the interrupted currents, being independent of the latter's frequency and the concentration of the solution and depending only on the density of the transmitted current. Under a direct current the entire curve corresponded to an almost steady potential of ~ − 1.75 v (n.c.e.)** whereas under interrupted currents of various frequencies it corresponded to an alternating potential, the mean value of which fell in the interval from -1.9 to -2.0 v (n.c.e.). The velocity in both cases proved, however, to be the same, i.e., the velocity of hydrogen evolution at the anode did not depend on the potential.

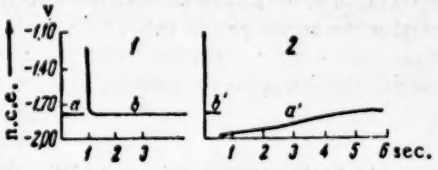

Fig. 1. The change in the potential of the magnesium anode under changing current density:
1) for the increase from 7 to 67 ma/cm².
2) for the decrease from 67 to 7 ma/cm².
The segments a and a' represent the potentials at a current density of 7 ma/cm²; the segments b and b' the potentials at 67 ma/cm².
1 N $MgSO_4$ solution.

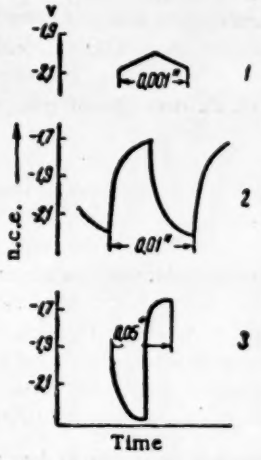

Fig. 2. The change in potential during the process of polarizing Mg by an interrupted current:
1) 1000 impulses/sec 2) 100 impulses/sec 3) 20 impulse sec 1 N $MgSO_4$ solution. Density of current pulse, 51.3 ma/cm²

We also discovered the evolution of hydrogen on magnesium when the measured anodic potential was from 0.4 to 0.6 volts more negative than the equilibrium hydrogen potential (2 N $MgSO_4$ solution, with the addition of 0.5 M K_2CrO_4, under an anodic current density of 20-30 ma/cm²). Under these conditions the resistance of the electrode, measured with alternating current, amounted to about 1 ohm/cm² and this could not have given a

* In comparing the velocities it is necessary to compare the amount of hydrogen liberated by the steady current over a definite period with the amount liberated by the interrupted current over a period twice this long. The velocity of spontaneous dissolution would be the same for the steady and the interrupted currents only if it is true that the evolution of hydrogen is retarded just as much in the first instant of passage of a current pulse as it is accelerated in the first instant after the interruption of the current so that these processes mutually compensated one another; however, a balance such as this, which would be maintained over wide intervals of anodic current density and frequency of current pulses, is very unlikely.

** N.c.e. = normal calomel electrode.

significant distortion of the observed electrode potential. This result agreed with the supposition as to the entrance into solution of univalent magnesium; however, taking into account the great lack of uniformity of the surface, it was impossible to consider the hydrogen evolution at potentials more positive than equilibrium as fully proven.

These two experimental facts: the constancy of the velocity of the hydrogen evolution regardless of current interruptions and the electrode potential, cannot be explained in terms of the electrochemical processes of spontaneous anodic dissolution, but, on the other hand, served as confirmation for the supposition that the elementary electrochemical act during the anodic dissolution of magnesium is a single electron transfer with the formation of the Mg^+ ion.

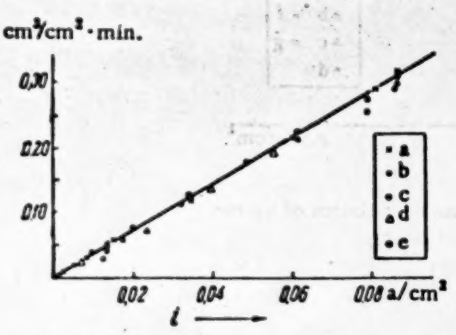

Fig. 3. The dependence of the evolution of hydrogen from $MgSO_4$ solutions on the anodic current density. Polarization under a steady current: a) 1 N solution, b) 0.1 N solution. Polarization under an interrupted current: c) 1 N solution, d) 0.1 N solution (1000 impulses/sec), e) 1 N solution (6 impulses/sec).

We have measured the velocity of hydrogen evolution during anodic polarization of magnesium in a series of solutions. The results of these measurements are presented in Figure 4. In solutions of NH_4Cl and HCl, with increasing current density there is first observed a diminution in the rate of hydrogen evolution (positive difference effect); under further increases of current density a minimum velocity is reaced and there then occurs a reversal from positive to negative difference effect, with a velocity of hydrogen evolution close to that which is observed in neutral solutions.

On the basis of our experimental data we consider that the evolution of hydrogen at the magnesium anode is determined by two factors: 1) the reaction of chemical oxidation of the Mg^+ ion by water, the rate of this reaction, V_1, being proportional to the velocity of the dissolution of the magnesium and independent of the potential of the electrode, the concentration and the composition of the solution, and, 2) the reaction of spontaneous dissolution of the anode, the velocity of which, V_2, depends on the electrode potential, the condition of its surface and the composition of the solution. The over-all rate of hydrogen evolution, if changes in the surface state are neglected, is expressed by the equation:

$$V = V_1 + V_2 = \frac{6.95i\,(2-n_i)}{n_i} + V_0 \exp\left(\frac{-\alpha_1 \Delta\varphi F}{RT}\right), \qquad (1)$$

where V_0 is the velocity of hydrogen evolution without current, α_1 is a coefficient which characterizes the cathodic process of hydrogen evolution on Mg under the given surface conditions, $\Delta\varphi$ is the displacement of the potential from the stationary value during anodic polarization, i is the density of the anodic current, in amps/cm², n_i is the effective valence of the dissolving magnesium; 6.95 is a proportionality factor used for expressing the rate of hydrogen evolution in cm³/cm²·min.

Equation (1) approximately describes the quantitative relationships which are observed during the evolution of hydrogen on the magnesium anode. With an increase of anodic current density the first term increases and the second diminishes.* On a (V, i) curve there must accordingly be observed a minimum, the presence of which indicates a change in the sign of the difference effect from positive to negative. In neutral solutions, under all of the investigated current densities, there is found only an increase in the rate of hydrogen evolution, the velocity of spontaneous dissolution being low and the minimum occurring at some tenths of a milliampere

* Increases, provided that $\Delta\varphi$ increases. For an invariant surface condition $\Delta\varphi$ should increase according to the equation $i = \frac{V_2}{6.95} \exp\left(\frac{\beta \Delta\varphi F}{RT}\right)$. In actuality, and because of the activation of the surface, beginning at a certain current density, $\Delta\varphi$ no longer increases; consequently the second term remains unchanged, or even increases, since activation leads to a decrease of the hydrogen overvoltage.

per cm^2; in acid solutions both effects are observed.

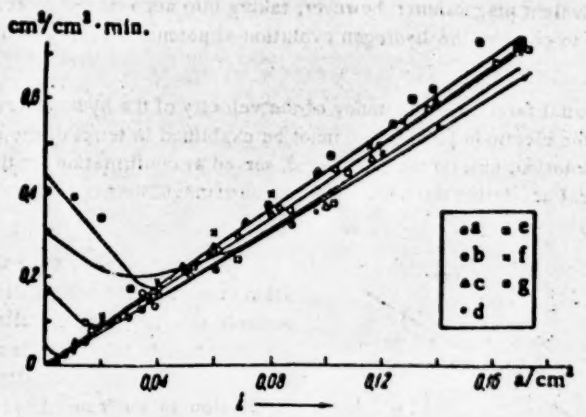

Fig. 4. The dependence of the rate of evolution of hydrogen at the Mg anode on the current density: a) 1 N $MgSO_4$, b) 4.6 N $MgCl_2$ c) 5 N $CaCl_2$, d) 1 N NH_4Cl e) 0.5 N NH_4Cl , f) 0.039 N HCl, g) 0.117 N HCl.

The evolution of hydrogen under current densities which are much greater than the current density of spontaneous dissolution is conditioned in each solution principally by one fact: the reaction of oxidation by water of the Mg^+ ion (or the radical MgOH) which is formed through anodic polarization of the magnesium. Under certain definite conditions, however, an increase in the evolution of hydrogen is, in part, brought about by anodic activation of the metal, if this is possible in the given solution. The inversion of the difference effect occurs because of the superposition of the reactions of spontaneous dissolution of the Mg and oxidation of the Mg^+ ion.

We wish to express our thanks to Academician A. N. Frumkin for his valuable advice.

Note added during correction of proofs. During the printing of our work there appeared the article of Greenblatt [11] on the mechanism of anodic dissolution of Mg in NaCl solution. Her results agree with our conclusions.

LITERATURE CITED

[1] N. D. Tomashov and V. N. Modestova, Investigations on the Corrosion of Metals, Trans. Inst. Phys. Chem. (Acad. Sci. USSR, 1955) V, 4, 75.

[2] M. A. Streicher, Trans. Electrochem. Soc. 93, 285 (1948).

[3] M. F. Straumanis and Y. N. Wang, J. Electrochem. Soc. 102, 304 (1955).

[4] V. O. Krenig and V. N. Uspenskaya, Transactions of the 1st Conference on the Corrosion of Metals (Moscow-Leningrad, 1935) p. 482.

[5] B. Roald and W. Beck, J. Electrochem. Soc. 98, 277 (1951).

[6] E. V. Barelko, Dissertation (Moscow, 1950).

[7] G. L. Ilchenko, Dissertation (Moscow, 1955).

[8] N. D. Tomashov, V. S. Komissarova and M. A. Timonova (Transactions of the Inst. of Phys. Chem., Acad. Sci. USSR: vol. V, Investigations of the Corrosion of Metals) 4, 172, 1955.

[9] R. L. Petty, A. W. Davidson, J. Kleinberg, J. Am. Chem. Soc. 76, 3622 (1954).

[10] B. D. Laughlin, J. Kleinberg, A. W. Davidson, J. Am. Chem. Soc. 78, 559 (1956); E. Raljola, A. W. Davidson, J. Am. Chem. Soc. 78, 556 (1956);

[11] J. H. Greenblatt, J. Electrochem. Soc. 103, 539 (1956).

The Institute of Physical Chemistry
of the Academy of Sciences of the USSR

Received July 11, 1956

THE CONDENSATION OF AEROSOL PARTICLES BY ELECTROSTATIC ATTRACTION ON A CYLINDER AROUND WHICH THEY ARE STREAMING

G. L. Natanson

(Presented by Academician A. N. Frumkin July 12, 1956)

The condensation of aerosol particles on a cylinder under the action of electrical forces plays a role in the operation of high tension lines [1] and in the filtration of aerosols by certain fibrous materials [2]. This problem has been investigated in one particular case by Cochet [1] (see below). The condensation of aerosols out of a stream onto a spherical impediment under the action of electrostatic attraction has been considered by Cochet [3], L. M. Levin [4] and Kraemer and Johnstone [5].

If there is designated by ψ a current function for flow around an infinite cylinder standing perpendicular to the stream, by F(r) the force attracting the particle to the cylinder, and by B the particle mobility, and if there is neglected the force of gravity, the particle's inertia and its Brownian movement, then, in polar coordinates, the components of the particle velocity will be

$$v_r = \frac{dr}{dt} = \frac{1}{r}\frac{\partial \psi}{\partial \theta} - BF(r), \quad v_\theta = \frac{r d\theta}{dt} = -\frac{\partial \psi}{\partial r}. \tag{1}$$

From this there is obtained the differential equation for the trajectory of the particle

$$\frac{\partial \psi}{\partial r} dr + \frac{\partial \psi}{\partial \theta} d\theta = d\psi = BrF(r)\, d\theta, \tag{2}$$

the integral of which we will represent in the form:

$$\psi = f(\theta, C) \tag{3}$$

(C is the constant of integration).

When $\theta \to \pi$, the trajectory of the particle will follow the flow line which is characterized by the value $\psi = f(\theta = \pi, C)$. The coefficient of capture, ϵ, of the particles by the cylinder is equal to

$$\varepsilon = \frac{\psi_{\lim}}{v_0 a} = \frac{f(\theta = \pi, C\lim)}{v_0 a}, \tag{4}$$

where C_{lim} is the value of C for the limiting trajectory, the particles of which will be just captured by the cylinder, v_0 is the velocity of the unperturbed current, and a is the cylinder radius.

We will set $r_0 = a + R$, R being the radius of the particle. A particle which is moving along the limiting trajectory must, at the point of capture, ($r = r_0$, $\theta = \theta_0$), have $v_r \leq 0$. For $v_r < 0$ the limiting trajectory intersects, and for $v_r = 0$ grazes the surface, $r = r_0$. If for $r = r_0$ the condition $v_r < 0$ is fulfilled for any value of θ from 0 to π, then the limiting trajectory passes through the point with the coordinates $r = r_0$ and $\theta = \theta_0 = 0$. Setting these values into (3) and taking into account the fact that for $\theta = 0$ and $r = r_0$, $\psi = 0$, we obtain an expression for the determination of C_{lim}

$$f(\theta = 0,\ C_{lim}) = 0 \tag{5}$$

which is valid when $v_r \leq 0$ with $r = r_0$ and $\theta = 0$, i.e., when

$$\frac{Br_0F(r_0)}{(\partial\psi/\partial\theta)_{r=r_0,\ \theta=0}} \geqslant 1. \tag{6}$$

If for $r = r_0$ the condition $v_r \leq 0$ is fulfilled only in the event that $\theta \geqslant \theta_0$, then the limiting trajectory passes through the point with the coordinates $r = r_0$ and $\theta = \theta_0$, where the value of θ_0 is determined by the equation $v_r = 0$ with $r = r_0$ and $\theta = \theta_0$. Setting these values of the coordinates into (3) there is obtained an expression for the determination of C_{lim}:

$$\psi(r_0, \theta_0) = f(\theta_0, C_{lim}). \tag{7}$$

which is valid when $v_r \geqslant 0$ with $r = r_0$ and $\theta = 0$ and in which θ_0 is determined, according to (1), by the expression

$$\left(\frac{\partial\psi}{\partial\theta}\right)_{r=r_0,\ \theta=\theta_0} = Br_0F(r_0). \tag{8}$$

The value of the coefficient of capture, ϵ, is calculated from the result found for C_{lim} with the aid of (4). The formulas thus obtained are applicable for any type of central forces between the cylinder and the particles.

We will now consider certain concrete problems.

1. Charged cylinder and charged particles. If there is designated by ρ the volume density of the cylinder charge and by e the charge of the particle, then, when inductive forces are neglected, $F(r) = 2\pi\rho ea^2/r = \alpha/r$. The integration of (2) gives in this case:

$$\psi = f(\theta, C) = B\alpha\theta + C. \tag{9}$$

Under those relationships of the problem parameters for which condition (6) is fulfilled the value of C_{lim} is, according to (5) and (9), equal to $C_{lim} = 0$ and the value of ϵ, according to (4) is:

$$\varepsilon = \frac{B\alpha\pi}{v_0 a} = \frac{\pi a\rho e}{3\sigma_0\eta R}. \tag{10}$$

Here B is determined by Stoke's resistance law and η is the viscosity of the medium. The result obtained for ϵ does not depend on the nature of the function ψ.

On the other hand, the nature of condition (6) and the expression for ϵ when (6) is not valid, depend on the character of the flow. When (6) is no longer valid then according to (4), (9) and (7) $\epsilon = [B\alpha(\pi - \theta_0) + \psi(r_0, \theta_0)]/v_0 a$. For a potential flow ($\psi = v_0(r - a^3/r)\sin\theta$) the magnitude of θ_0 is, according to (8), determined by the expression $B\alpha = v_0(r_0 - a^3/r_0)\cos\theta_0$ and condition (6) takes the form $B\alpha \geq v_0(r_0 - a^3/r_0)$.

In Figure 1 there are given trajectories of particles for a potential flow, these having been calculated from Equation (9).

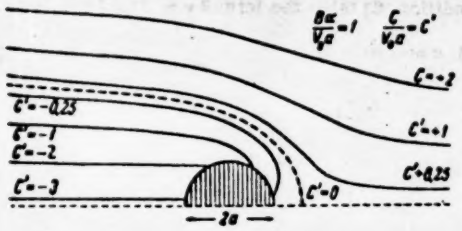

Fig. 1.

2. Charged cylinder and uncharged particles. If the action of the polarized particle on the field of the cylinder is neglected, then $F(r) = 4\pi^2\rho^2 a^4 \frac{D_1 - 1}{D_1 - 2}\left(\frac{R}{r}\right)^3 = \frac{\beta}{r^3}$, where D_1 is the dielectric constant of the particle. Equation (2) takes on the form

$$d\psi = \frac{B\beta}{r^3}\, d\theta. \qquad (11)$$

For $r/a \gg 1$ ($\epsilon \gg 1$) the cylinder does not act on the current, $\psi = v_0 r\sin\theta$, and (11) passes over into $\psi^2 d\psi = B\beta v_0^2 \sin^2\theta\, d\theta$, from which $\psi = f(\theta, C) = \left[\frac{3}{2} B\beta v_0^2\left(\theta - \frac{1}{2}\sin 2\theta\right) + C\right]^{1/3}$. Condition (6) acquires the form $B\beta > v_0 r_0^3$. When this is valid the value of ϵ is, according to (5) and (4), equal to

$$\epsilon = \left(\frac{3B\beta\pi}{2v_0 a^3}\right)^{1/3} = \left(\frac{D_1 - 1}{D_1 + 2}\,\frac{\pi^3\rho^2 a R^3}{v_0\eta}\right)^{1/3}. \qquad (12)$$

If condition (6) is not fulfilled, the value of ϵ can be determined from (4) and (7), inserting into the latter the result $\cos\theta_0 = B\beta/v_0 r_0^3$, obtained from (8). The solution for $r/a \gg 1$ coincides with that obtained by Cochet [1] for the capture of falling droplets by a charged cylinder, if in place of v_0 there is inserted the Stoke's velocity of sedimentation of the droplets.

For $(r - a)/a = \kappa \ll 1$ ($\epsilon \ll 1$); $r \sim a$ and equation (11) takes on the form $a^2 d\psi = B\beta\, d\theta$. Integration gives $\psi = f(\theta, C) = B\beta\theta/a^2 + C$. When condition (6) is fulfilled the value of C_{lim} is, according to (5), equal to $C_{lim} = 0$. The coefficient of capture is equal to

$$\epsilon = \frac{B\beta\pi}{v_0 a^3} = \frac{D_1 - 1}{D_1 + 2}\,\frac{2\pi^3\rho^2 a R^3}{3v_0\eta}. \qquad (13)$$

This expression does not depend on the character of the function ψ. On the other hand, the expression for condition (6), and for ϵ when condition (6) is not fulfilled, depend on the character of the flow. For potential flow, ($\psi = 2v_0 a\kappa\sin\theta$), condition (6) takes on the form $B\beta \geq 2v_0 a^3\kappa_0^3$, where $\kappa_0 = (r_0 - a)/a = R/a$ and for viscous flow, ($\psi = 2wa\kappa^2\sin\theta$, where $2w = v_0/(2{,}00 - \ln \mathrm{Re})$ and $\mathrm{Re} = 2v_0 a/\nu$) $B\beta \geq 2wa^3\kappa_0^2$. When (6) is not valid, according to (4) and (7) $\epsilon = \left[\frac{B\beta}{a^2}(\pi - \theta_0) + \psi(r_0, \theta_0)\right]/v_0 a$, where for potential flow $\cos\theta_0 = B\beta/2v_0 a^3\kappa_0$, and viscous flow $\theta_0 = B\beta/2wa^3\kappa_0^2$.

3. Uncharged cylinder and charged particles. For $\kappa \ll 1$ and $r - a \gg R$ ($\epsilon \ll 1$) the interaction of the particle and the cylinder is equivalent to the interaction of a point charge and a plane. In this case $F(r) = \frac{D_2 - 1}{D_2 + 1} \frac{e^2}{4a^2\kappa^2} = \frac{\gamma}{\kappa^2}$ where D_2 is the dielectric constant of the cylinder. Equation (2) takes the form

$$d\psi = \frac{B\gamma a}{\kappa^3} d\theta. \tag{14}$$

For potential flow, after elimination of κ, equation (14) passes over into $\psi^3 d\psi = 4B\gamma v_0^2 a^3 \sin^2\theta \, d\theta$, which gives $\psi = f(\theta, C) = \left[6B\gamma v_0^2 a^3 \kappa \left(\theta - \frac{1}{2}\sin 2\theta\right) + C\right]^{1/4}$. Condition (6) takes the form $B\gamma \geq 2v_0\kappa_0^3$. When this latter is fulfilled the value of ϵ is, according to (4) and (5), equal to

$$\epsilon = \left(\frac{6B\gamma\pi}{v_0}\right)^{1/6} = \left(\frac{D_2 - 1}{D_2 + 1} \frac{e^2}{4v_0 a^2 \eta R}\right)^{1/6}. \tag{15}$$

When (6) is not valid the expression for ϵ is obtained from (4) and (7) by the substitution in the latter of the value $\theta_0 = B\gamma/2v_0\kappa_0^3$, resulting from (8).

For viscous flow, after the elimination of κ equation (14) becomes $\psi \, d\psi = 2B\gamma w a^2 \sin\theta \, d\theta$, from which $\psi = f(\theta, C) = (-4B\gamma w a^2 \cos\theta + C)^{1/2}$. Condition (6) has the form $B\gamma \geq 2w\kappa_0^4$. When this condition is fulfilled, according to (5), $C_{\text{lim}} = 4B\gamma w a^2$, which with the aid of (4) gives

$$\epsilon = \left(\frac{8B\gamma w}{v_0^2}\right)^{1/6} = \left(\frac{D_2 - 1}{D_2 + 1} \frac{e^2 w}{3\pi v_0 a^2 \eta R}\right)^{1/6}. \tag{16}$$

When (6) is not valid, taking into account the fact that according to (8) $\cos\theta_0 = B\gamma/2w\kappa_0^4$ we obtain from (7). $C_{\text{lim}} = 4w^2 a^2 \kappa_0^4 + B^2\gamma^2 a^2 \kappa_0^{-4}$. Substituting into (4) there is obtained

$$\epsilon = 2\frac{w}{v_0}\kappa_0^2 + \frac{B\gamma}{v_0\kappa_0^2} = 2\frac{w}{v_0}\left(\frac{R}{a}\right)^2 + \frac{D_2 - 1}{D_2 + 1} \frac{e^2}{24\pi v_0 \eta R^2}. \tag{17}$$

The first member of this expression corresponds to capture due to simple contact.

4. van der Waal's interaction between the cylinder and the particles. This effect can play a role in the process of filtration of aerosols by fibrous materials [6]. According to [6] the force of van der Waal's interaction between the particles and the surface ($\kappa \ll 1$, $\epsilon \ll 1$) is equal to $F = 2\pi^2 ARh^2/3(h^2 - R^2)^2$ where A is the constant of interaction (of the order $10^{-14} - 10^{-13}$ ergs), and h is the distance from the center of the particle to the surface. This expression, however, contains an error which has been introduced in the differentiation which leads from equation (5) to equation (6) of [6] and the corrected expression is $F = 2\pi^2 AR^2/3(h^2 - R^2)^2$. In the approximation $a \gg r - a \gg R$, $F(r) = 2\pi^2 AR^2/3a^4\kappa^4 = k/\kappa^4$. Equation (2) takes the form

$$d\psi = \frac{Bka}{\kappa^4} d\theta. \tag{18}$$

For potential flow, elimination of κ gives $\psi^4 d\psi = 16Bkv_0^4 a^3 \sin^4\theta \, d\theta$ from which $\psi = f(\theta, C) = \left[10Bkv_0^4 a^3 \left(3\theta - 2\sin 2\theta + \frac{1}{4}\sin 4\theta\right) + C\right]^{1/5}$ condition (6) leads to $Bk \geq 2v_0\kappa_0^5$.

When the latter condition is valid ϵ is, according to (4) and (5) equal to

$$\epsilon = \left(\frac{30Bk\pi}{v_0}\right)^{1/6} = \left(\frac{10\pi^2 AR^2}{3v_0 a^4 \eta}\right)^{1/6}. \tag{19}$$

When (6) is not valid the expression for ϵ is obtained from (4) and (7) by the substitution $\cos\theta_0 = Bk/2v_0\kappa_0^{\frac{2}{3}}$.

For viscous flow elimination of κ from (18) gives $\phi^2 d\phi = 4Bkw^2a^3\sin^2\theta\, d\theta$. By integration we obtain $\phi = f(\theta, C) = \left[6Bkw^2a^3\left(\theta - \frac{1}{2}\sin 2\theta\right) + C\right]^{1/3}$. Condition (6) gives $Bk \geq 2w\kappa_0^{\frac{2}{3}}$. When this condition is fulfilled ϵ is, according to (4) and (5), equal to

$$\epsilon = \left(\frac{6Bkw^2\pi}{v_0^2}\right)^{1/6} = \left(\frac{2\pi^2w^2AR^2}{3v_0^2\alpha^2\eta}\right)^{1/6}. \qquad (20)$$

When (6) is not valid the expression for ϵ is obtained from (4) and (7) by a substitution of the value $\cos\theta_0 = Bk/2w\kappa_0^{\frac{2}{3}}$, which results from (8).

LITERATURE CITED

[1] R. Cochet, Rev. gener. d'Electr., 62, 113 (1953).

[2] A. Rossano, and L. Silverman, Heating and Ventilating, 51, No. 5, 102 (1954); T. Gillespie, J. Coll. Sci. 10, 299 (1955).

[3] R. Cochet, Ann. de Geophys., 8, 33 (1952).

[4] L. M. Levin, DAN (Proc. Acad. Sci. USSR) 94, 467 (1954).

[5] H. Kraemer and H. Johnstone, Ind. Eng. Chem., 47, 2426 (1955).

[6] N. N. Tunitsky and I. P. Petryanov ZhFKh (J. Phys. Chem.) 17, 408 (1943).

The L. Ya. Karpov Physicochemical Institute

Received June 20, 1956

THE MEASUREMENT OF THE VAPOR PRESSURES OF THE SOLID SOLUTIONS Au – Ag and Au – Cu

An. N. Nesmeyanov, L. A. Smakhtin and V. I. Lebedev

(Presented by Academician V. N. Kondratyev July 31, 1956)

In the present work there were measured the partial pressures of the vapors of gold, copper and silver above the solutions which these elements form with one another. These measurements were carried out by the Knudsen effusion method, use being made of the apparatus which is sketched in Figure 1. This latter was a modification of the apparatus which has been developed in our laboratory by Yu. A. Priselkov.

The effusion chamber was constructed entirely from molybdenum, which does not react with any of the experimental metals. The area of the effusion aperture did not exceed $1 \cdot 10^{-3}$ cm^2, thus assuring an equilibrium pressure of the vapors within the chamber. The heating of this chamber was carried out with an inductor which was fed from a high-frequency generator. The temperatures were measured with a Pt/Pt-Rh thermocouple which had been calibrated, in the apparatus, at the melting points of silver and of gold. The temperature was held constant to within ± 1°.

Gold, silver and copper containing the radioactive isotopes Au_{198}, Ag_{110} and Cu_{65} were employed here.

After washing out the condensate from the receiver and precipitating the element in question, with its carrier, (in the form of a sulfide in the case of gold, a bromide in the case of silver and with 8-oxyquinoline in the case of copper) the quantity of the vaporized metal was determined from the activity of the precipitate. The activity was measured on an apparatus of the type "B", using the counting tubes AMM-4, for the silver, and AS-1 and AS-2 for the gold and the copper, comparison being made with the activities of standards. These standards were prepared by dissolving weighed quantities of the active metal and then precipitating the reactive metal out of aliquot portions of the solutions, using the above described procedures.

In order to more exactly determine the quantites of the vaporized metals in the cases of gold and copper, disintegration curves were plotted for each sample and for each standard.

The pressure of the saturated vapor, or the partial pressure of a metal above its alloy, was calculated from the formula:

$$P = \frac{17.14 \cdot m}{t \cdot s \cdot K} \sqrt{\frac{M}{T}},$$

where P is the pressure of the vapor, expressed in mm of Hg; m is the quantity of vaporized metal, in grams; t is the time of vaporization, in seconds; s is the area of the effusion aperture, in cm^2; T is the absolute temperature; M is the molecular weight of the metal and K is the dimensionless coefficient of Clausing which takes into account the resistance of the effusion aperture to the molecular beam of the vaporizing metal.

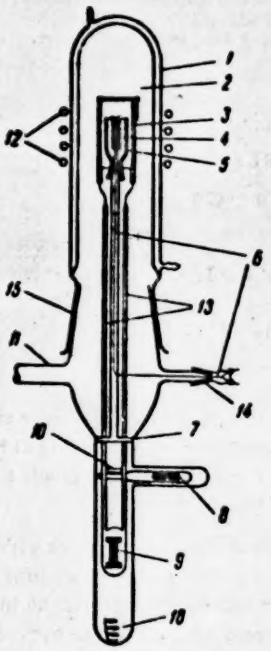

Fig. 1. Apparatus for measuring the vapor pressures of metals.
1) Water jacket 2) Receiver 3) Quartz cup for fixing the beginning and the end of an exposure 4) Effusion chamber 5) Quartz mantle for screening, 6) Thermocouple 7) Position of attachment of quartz tube to the apparatus 8) Armature of adjustor, 9) Armature of elevating mechanism for the quartz cup, 3, 10) Mechanism for fixing the position of the quartz cup, 3 11) Line to vacuum system 12) Inductor for heating 13) Glass column for elevating mechanism 14) Ground joint for introduction of thermocouple 15) Ground joint joining receiver to apparatus, 16) Bumper.

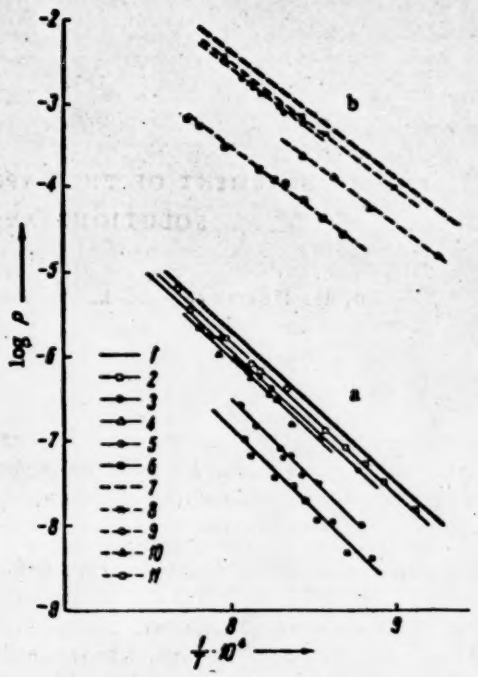

Fig. 2. The partial pressures of gold (a) and of silver (b) in the Au-Ag system:
1) pure gold, 2-6) systems with varying content of gold (at.%), 2) 81.3, 3) 68, 4) 60, 5) 29 6) 15; 7) pure silver, 8-11) systems with varying content of silver (at.%), 8) 79.5, 9) 71, 10) 44, 11) 18.7.

From the experimental data there were developed the following equations for the saturated vapor pressure curves of gold, silver and copper:

For gold in the interval of temperature from 800-1000°:

$$\log P_{\text{mm}} = -18016/T + 8.683.$$

For silver in the interval of temperature from 760 to 960°:

$$\log P_{\text{mm}} = -14058/T + 8.855.$$

For copper in the interval of temperature from 900 to 1070°:

$$\log P_{\text{mm}} = -17320/T + 9.320.$$

Making use of the experimental data on the saturated vapor pressures and the values of the quantities $\left(\frac{F_0 - H_0^0}{T}\right)_{solid}$ and $\left(\frac{F_0 - H_0^0}{T}\right)_{gas}$ [2], we have calculated the latent heats of sublimation of gold, silver and copper at the absolute zero, ΔH_0^0, and also the latent heats of sublimation of these metals, ΔH_T, at the midpoints of the temperature intervals over which the measurements of vapor pressures had been carried out.

TABLE 1

	Au.	Ag	Cu
ΔH_t kcal/mole	82.4	64.4	79.3
ΔH_0 kcal/mole	86.8	67.7	80.9

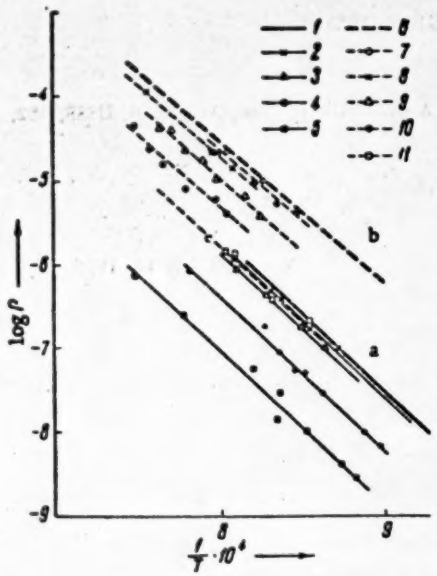

Fig. 3. The partial pressures of gold (a) and copper (b) in the Au-Cu system: 1) pure gold, 2-5) systems with varying content of gold (at. %): 2) 94, 3) 74.7, 4) 34.7, 5) 10.13: 6) pure copper, 7-11) systems with varying content of copper (at. %): 7) 83.8, 8) 70.4 , 9) 50, 10) 29.6, 11) 10.34

The data obtained for the partial pressures of gold, silver and copper above the gold-silver and the gold-copper alloys are presented in Figures 2 and 3 where log p, 1/T relations have been plotted.

The attempt was made to simultaneously determine the partial pressures of the silver and the gold above gold-silver alloys. For this purpose there were prepared alloys which contained the radioactve isotopes of both silver and gold. The partial pressures of the vapors of gold and silver above these alloys are shown in Figure 2 (alloys with 28.9 and 81.3 at. % of gold and with 71.1 and 18.7 at. % of silver).

From the resulting values of the partial vapor pressures and the pressures of the saturated vapors, there were calculated the activities of gold, silver and copper in the gold-copper and the gold-silver alloys.

In Figure 4 there is shown the relation existing between the activities of gold and copper and their concentrations in gold-copper alloys (a) and between the activity of gold and of silver and the concentrations of gold-silver alloys (B) using the data obtained from the present work and from the work of other authors. It is to

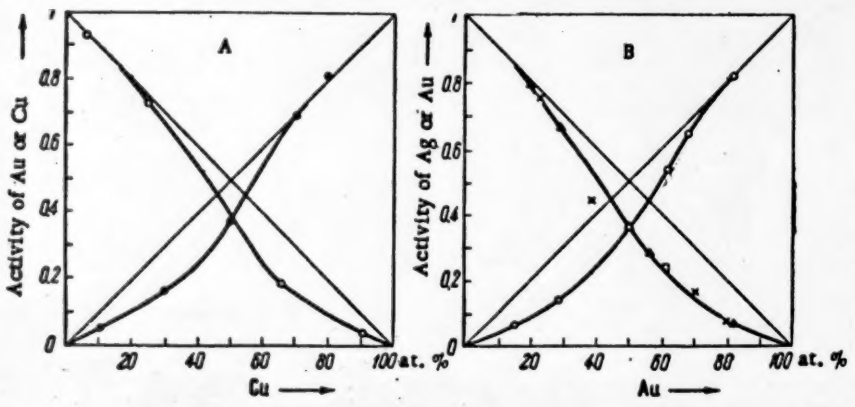

Fig. 4. The activites of gold and copper in the Au-Cu system (A) and of gold and silver in the Au-Ag system (B): 1) gold, 2) copper, 3-6) silver (3) original data, 4) data from [1], 5) data from [3], 6) data from [4].

be seen that the activity of silver in the investigated gold-silver alloys agrees very well with the activity values which are found in the work of others [1, 3, 4]. From the various diagrams which are presented, it is clear that negative deviations from Raoult's law are to be found in the gold-silver and the gold-copper systems.

LITERATURE CITED

[1] C. L. McCabe, H. M. Schadel, C. E. Birchinall, J. Metals 5 (1953).

[2] K. K. Kelly, Bur. Mines Bull., No. 383 (1935).

[3] A. A. Zhukhovitsky, S. N. Kryukov, M. E. Yanitskaya, A. G. Golitsyn, Proc. Acad. Sci. USSR, 102, No. 1, 1955.

[4] V. V. Komev, Proc. Acad. Sci. USSR 107, No. 5, 1956.

The M. V. Lomonosov State University in Moscow

Received July 19, 1956

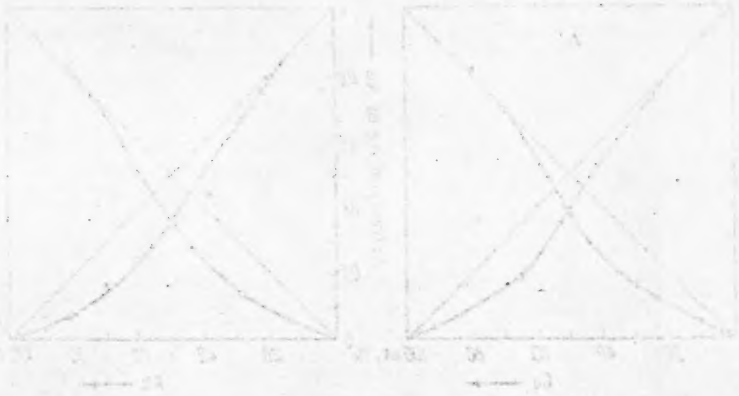

THE REACTIONS OF FREE RADICALS IN SOLUTION: THE THERMAL DECOMPOSITION OF THE TRIAZENES IN VARIOUS MEDIA

L. M. Romanov, B. A. Dolgoplosk and B. L. Erusalimsky

(Presented by Academician L. N. Nazarov May 25, 1956)

Recently much attention has been given to the study of the kinetics of the decomposition of the various compounds which can serve as sources of free radicals. This is especially true in regard to the organic peroxides and hydroperoxides [1-4]. As was shown by Kh. S. Bagdasaryan and R. L. Milyutinskaya [5], and also by others [1, 2], benzoyl peroxide at comparatively high temperatures decomposes according to a chain mechanism.

In the present work there was studied the kinetics of the decomposition of a number of triazines in various systems. The velocity of decomposition was determined from the rate of the evolution of gas in the course of reaction.

In the case of ethylphenyltriazene (EPT) and propylphenyltriazene it was shown that with an increase of the concentration of the triazene in solution, the velocity constant for the reaction of decomposition also increased (Table 1). This fact indicates that, under the given conditions, a chain decomposition takes place.

At concentrations of 15-20 mole % and under a temperature of 120° the quantity of radicals in the system is very great and the chain decomposition of the triazenes proceeds to such an extent that the kinetic curves no longer follow a monomolecular law (Figure 1).

In the decomposition of ethylphenyltriazene in styrene the increase of the velocity constant of the reaction with increase of concentration goes much further than it does in isopropylbenzene, a fact which is connected with the large increase in the concentration of free radicals resulting from the development of a chain reaction of polymerization.

Along with the increase of the velocity constants for the decomposition of the triazenes, which accompanies an increase of their concentrations in solution, there is observed a decrease in the yield of those products RH, which are formed according to the reaction:

$$R\cdot + LH \rightarrow RH + L\cdot,$$

LH representing a molecule of the solvent.

It is most likely that this decrease in the yield of the products resulting from the breaking of hydrogen out of the molecule of the solvent is related to the development of the chain process of decomposition with the associated consumption of the radicals in the reaction with triazene.

The chain character of the decomposition of the triazenes at elevated compositions is confirmed by the fact that the velocity constant for breakdown diminishes on the introduction of sulfur into the system (Figure 2 and Table 3). Sulfur is, as has been shown by M. P. Tikhomolova and others [6], a good acceptor of free radicals.

TABLE 1

The Velocity Constants, $K_1 \cdot 10^{-4}$ sec^{-1}, for the Reaction of Decomposition of Ethylphenyltriazene in Various Media at 100°

Solvent	Concentration, (C), mole%			
	1.3	4	13	25
Isopropylbenzene	1.2	1.6	2.2	2.7
Styrene	2.4	6.1	—	—

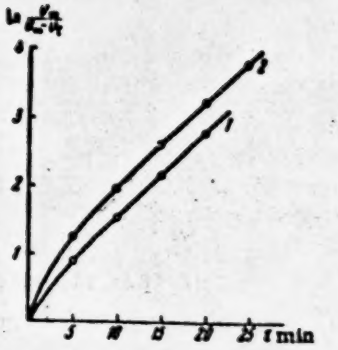

Fig. 1. The kinetics of the decomposition of propylphenyltriazene at 120°: 1) C = 15 mole %, 2) C = 20 mole %.

Sulfur is unable, however, to completely suppress the development of the chain process, as is to be particularly noted at the higher temperatures. Thus, at 120° and a concentration of triazene of 25 mole %, $K_1 = 15 \cdot 10^{-4}$ sec^{-1} in the presence of sulfur (at a concentration of 1.3 mole %, $K_1 = 3.5 \cdot 10^{-4}$ sec^{-1}). Under these same conditions the decomposition without sulfur runs almost to completion in 7-10 minutes, which excludes the possibility of obtaining exact kinetic data.

TABLE 2

The Relation Between the Yield of the Products RH and the Initial Concentrations of the Triazenes at 120°.

Ethylphenyltriazene				
Concentration, mole %	1.3	25		
Yield of RH_1, % Theoretical	37	22		
Propylphenyltriazene				
Concentration, mole %	1.3	15	20	25
Yield of RH_1, % Theoretical	24	22	20	15

TABLE 3

The Velocity Constants for the Decomposition of Ethylphenyltriazene in the Presence of Sulfur in Isopropylbenze at 100°, S/EPT (wt. %) = 2.

Concentration, mole %	1.3	4	13	25
$K \cdot 10^{-4}$ sec^{-1}	1.2	1.2	1.4	1.7

In the case of isopropylphenyltriazene the presence of sulfur brings about an unexpected effect: namely, a strong acceleration of the process of decomposition. The kinetic curve; computed according to the monomolecular equation, shows a break at a point corresponding to 70% decomposition. Below this point $K_1 = 20.8 \cdot 10^{-4}$ sec^{-1}; above it $K_1 = 10 \cdot 10^{-4}$ sec^{-1}. In the absence of sulfur $K_1 = 9.0 \cdot 10^{-4}$ sec^{-1}. It is perhaps possible to explain the acceleration of the decomposition in the presence of sulfur by the fact that in this case those sulfide radicals which are formed are sufficiently active for the development of the chain decomposition of the triazenes. As has been shown by Kooyman [7], RS· radicals in which R is an alkyl substituent with an iso structure [$(CH_3)_2$. CH, $(CH_3)_3C$] have greater activity in the reaction of breaking off of hydrogen than do those with a normal structure.

It is known that α, α-diphenyl-β-picrylhdrazyl has recently been employed for the capture of free radicals and the exclusion of chain decompositions in various compounds, in particular, peroxides and azo substances. This procedure proves to be inapplicable to the case of the triazenes because the α,α-diphenyl-β-picrylhydrazyl strongly accelerates their decomposition.

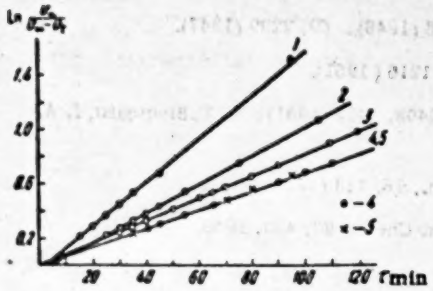

Fig. 2. The kinetics of the decomposition of ethylphenyltriazene at 100°:
1) C = 25 mole% (without S), 2) C = 25 mole %, 3) C = 12.5 mole %, 4) C = 1.3 mole %, 5) C = 4 mole %.

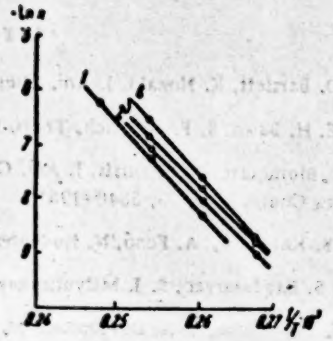

Fig. 3. The temperature dependence of the velocity constants for the reactions of decomposition of the triazenes:
1) methyl- 2) ethyl-, 3) benzyl-
4) hexyl-phenyltriazene

It follows from the data presented in the Tables 2 and 3 that the chain decomposition is essentially absent at a concentration of 1.3 mole %. The kinetic data obtained at this concentration was used for determing the energies of activation for the decomposition reactions of methyl-, ethyl-, benzyl-, and hexyl-phenyltriazene. For methyl- and ethyl-phenyltriazene the measurements were repeated in the presence of sulfur. In these two cases the velocity constants for the decompositions at various temperatures are exactly the same as they were without the sulfur. The values of the velocity constants and the energies of activation are presented in Figure 3 and in Table 4.

TABLE 4

The Velocity Constants and the Energies of Activation for the Reactions of Thermal Decomposition of the Triazenes.*

Triazene	E, kcal/mole	$K \cdot 10^4$ sec^{-1} temperature, °C			
		100	110	120	130
Methylphenyltriazene	31 ± 2	—	2.4	6.6	18.8
Ethylphenyltriazene	29 ± 2	1.2	3.1	8.5	—
Benzylphenyltriazene	28 ± 2	1.5	4.1	10.5	—
Hexylphenyltriazene	31 ± 2	1.6	4.9	13.8	—

* The data which was published earlier, [8], proved to be in error because the starting materials were not sufficiently pure.

EXPERIMENTAL

All of the triazenes were synthesized by the action of bromomagnesium derivatives on phenylazide [9, 10]. The decomposition of the triazenes was carried out in an atmosphere of nitrogen, using the earlier described technique [11].

LITERATURE CITED

[1] P. D. Bartlett, K. Nozaki, J. Am. Chem. Soc., 68, 1686 (1946); 69, 2299 (1947).

[2] C. E. H. Bawn, S. F. Mellish, Trans. Farad. Soc., 47, 1216 (1951).

[3] A.T. Blomquist, A. F. Ferris, J. Am. Chem. Soc., 73, 3408, 3412 (1951); A. T. Blomquist, J. A. Berstein, J. Am. Chem. Soc., 73, 5546 (1951).

[4] M. S. Kharasch, A. Fono, N. Nudenberg, J. Org. Chem., 16, 113 (1951).*

[5] Kh. S. Bagdasaryan, R. I. Milyutinskaya ZhFKh (J. Phys. Chem.) 27, 420, 1953.

[6] E. L Tinyakova, B. A. Dolgoplosk, M. P. Tikhomolova ZhOKh (J. Gen. Chem.) 25, 1387, 1955.*

[7] P. Bruin, A. F. Bickel, E. C. Kooyman, Rec., 71, 1115 (1952).

[8] B. A. Dolgoplosk, P. G. Ugryumov, V. A. Krol, DAN (Proc. Acad. Sci. USSR) 96, 757, 1954.

[9] O. K. Dimroth, Ber., 38, 670, 2328 (1905).

[10] O. K. Dimroth, Ber., 40, 2390 (1907).

[11] B. A. Dolgoplosk, B. L. Erusalimsky, V. A. Krol, L. M. Romanov, ZhOKh (J. Gen. Chem.) 24, 1775, 1954.*

The Institute for High-Molecular Compounds of the Academy of Sciences, of the USSR

Received February 20, 1956

* Original Russian pagination see C. B. Translation.

THE CHARACTERISTIC FREQUENCIES OF THE OLEFINS

L. M. Sverdlov

(Presented by Academician G. S. Landsberg November 4, 1956)

The question of the characteristic frequencies of the olefins has been most thoroughly studied in the work of Goubeau [2] in which for each class of olefins there are given groups of characteristic frequencies which have been established through comparisons of the observed spectra. It is obvious, however, that in order to confirm the choice of the one or the other group of frequencies as characteristic and to relate these frequencies to definite vibrations, there is needed a theoretical analysis, carried out according to the method of M. A. Elyashevich B. I. Stepanov [6] and L. S. Mayants [7].

In order to analyze the regularities of the vibrational spectra of the complex olefins of the six possible types: $RHC = CH_2$, $R_1R_2C = CH_2$, cis- and trans- $R_1CH = CHR_2$, $R_1R_2C = CHR_3$, $R_1R_2C = CR_3R_4$, we have undertaken a complete theoretical calculation of the frequencies of the normal vibrations of the simplest alkyl substituted ethylenes: propylene, isobutylene [8], cis- and trans- butene-2 [9], trimethylethylene and tetramethylethylene [9], since the spectrum of each of these molecules possesses its own peculiarities. As the calculations show, each of the considered molecules has vibrations which are, in the extended sense, characteristic, according to their form [7], for the group of coordinates corresponding to the structural element $\begin{matrix} X \\ Y \end{matrix}\!\!>\!C=C\!<\!\!\begin{matrix} Z \\ U \end{matrix}$. Since, this structural group enters into compounds of the type:

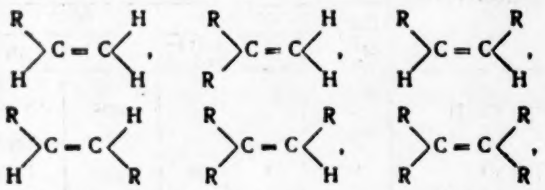

the molecules of each of the indicated homologous series should possess the same characteristic frequencies as do the molecules of propylene, isobutylene, cis-and trans-butene-2, trimethylethylene and tetramethylethylene. Thus, the groups of characteristic frequencies which have been established by us are the frequencies of the characteristic stable vibrations for a series of compounds containing a saturated chemical group. This conclusion is well supported by a large amount of the experimental material on the infrared and combination spectra for the indicated homologous series (we have collected data on more than 90 olefins).

In Tables 1-6 there are presented the groups of characteristic frequencies which have been established by us for these six homologous series and the approximate intensities of these lines, taken from the data of the literature [1-4], together with an indication of their referents and the data of other authors. In each table there are given the structural elements with which the whole group of characteristic frequencies is connected.

TABLE 1

The Characteristic Frequencies of the Monoalkyl Substituted Ethylenes, $RHC=CH_2$

Coordinate	$H_2C \diagdown H \diagup C-C \diagup H \diagdown H$						
	Our data	Intensity**		Source			
		combination	infrared	(*)	(*)	(*)	(*)
$\varphi^{-}_{CH_2}(C-H)$	3087	m	m	3080	3079	3081	3082
$\varphi^{+}_{CH_2}(C-H)$	~2990	w	m	3001	2998	2979	3001
$\varphi_{-CH_2}(C-H)$	~3010	s				3000	
$Q(C=C)$	1642	s	m	1642	1642	1642	1642
$\alpha_{-CH_2}(HCH)$	1416	m	m	1416	1415	1416	1416
$\beta(C=CH)$	1297	m	w	1292*	1298*	1297	1292*
$\beta^{-}(C=CH_2)$	1170	w	w			1166	
$\chi^{CCH}_{CH_2}$	991	w	s	990*	992*	996	991*
ρ_{CH_2}	912	w	s	912*	911*	910	910*
ρ_{CCH}	632	w	m		631*	630	
$\gamma(C=C-C)$	432	w	w		435*		630

* Not definitely assigned.

** s = strong, m = medium, w = weak.

TABLE 2

The Characteristic Frequencies of the Unsymmetric Dialkyl Substituted Ethylenes $R_1R_2C=CH_2$

Coordinate	$H_2C \diagdown H_2C \diagup C-CH_2$				
	Our data	Intensity		Source	
		combination	infrared	(*)	(*)
$\varphi^{-}_{CH_2}(C-H)$	3081	w	m	3078	3086
$\varphi^{+}_{CH_2}(C-H)$	2985	s		2987	2985
$Q(C=C)$	1653	s	m	1653	1653
$\alpha_{-CH_2}(HCH)$	1412	m	m	1414	1412
$Q^{-}(C-C)$	1290	w	m	888	
$\beta(C=CH_2)$	1000	w		1383	1282
ρ_{CH_2}	888	w	s	1002	887
$Q^{+}(C-C)$	804	s		804	
$\chi^{CCC}_{CH_2}$	703	w	w	703	700
$\gamma(C=CC)$	434	w		434*	
$\gamma(CCC)+\rho_{CCC}$	390	w		394*	
				261*	

* Not definitely assigned

It follows from these tables that many frequencies either have been incorrectly assigned by other authors or have not, in general, been assigned to definite vibrations. In addition, Goubeau selected, as characteristic in a number of cases those frequencies which are obviously related to the hydrocarbon radical R and which cannot, therefore, be considered as characteristic frequencies for the olefins, since they are observed in the spectra of all saturated hydrocarbons with long carbon chains.

TABLE 3

The Characteristic Frequencies of the Trans-Alkenes RCH = CHR

Coordinate	H_2C / H > C — C < H / CH_3				
	Our data	Intensity		Source	
		combination	infrared	(*)	(*)
φ(C—H)	~ 3010	w		3001	3007
Q(C=C)	1675	s		1671	1676
β(C=CH)	1306	s		1303	1308
Q^+(C—C)	870	m		802	
ρ_{CCH}	745	w		742	742
γ(C=C—C)	495	w		488	
φ(C—H)	~ 3020		m		3021
β(C=CH)	1306		w	1376	1302
Q^-(C—C)	1070		w	1023*	
χ^{CCH}_{CCH}	966		s	809*	964
γ(C=C—C)	263			210	
ρ_{CCH}	233				

* Not definitely assigned

TABLE 4

The Characteristic Frequencies of the Cis-Alkenes RCH = CHR

Coordinate	H_2C / H > C — C < CH_3 / H				
	Our data	Intensity		Source	
		combination	infrared	(*)	(*)
φ(C—H)	~ 3020		m	3013	3020
φ(C—H)	~ 3010	m			2985
Q(C=C)	1660	s	m	1656	1660
β(C=CH)	1410	s	m	1376	1406
β(C=CH)	1267	s		1263	1259
Q^-(C—C)	972	m		970	
ρ_{CCH}	895	m		640	970(?)
Q^+(C—C)	875			892	
ρ_{CCH}	700	w	s	702	700
γ(C=C—C)	590	w		581	
χ^{CCH}_{CCH}	402	w		413	
γ(C=C—C)	304	w		297	

We have further considered the influence on the spectra of chain branching. In this case when branching of the chain occurs at a position far from the double bond, the specificity of the vibrations which are noted in the tables cannot be disturbed, the structural groups with which these vibrations are connected being fully retained. However, if branching takes place at a carbon atom which is adjacent to the double bond (e. g. R—CH—CH = CH_2) then this must be reflected in the specificity of certain vibrations because in this situation there no

TABLE 5

The Characteristic Frequencies of the Trialkyl Substituted Ethylenes $R_1R_2C=CHR_3$

Coordinate	H_3C H_3C $C-C$ H CH_3				
	Our data	Intensity		Source	
		comb.	infra-red	(*)	(*)
φ (C—H)	3024	w	m	3023	3024
Q (C=C)	1676	s	m	1673	1676
β (C=CH)	1350	w	w	1350	1350
Q^-(C—C)	1212	w	m	1003	
Q (C—C)	950	w	m	808	
ρ_{CCH}	803	w	s	958	803
Q^+(C—C)	760	m	w	745	
γ (C=C—C)	520	w		526*	
ρ_{CCC}	440	w		470*	
γ (CCC)	390	w		385*	
γ (C=C—C)	295	w		301*	
χ^{CCH}_{CCC}	254	w		251*	
				1382*	
				1304*	
				1112*	

* Not definitely assigned

TABLE 6

The Characteristic Frequencies of the Tetraalkyl Substituted Ethylenes $R_1R_2C=CR_3R_4$

Coordinate	H_3C H_3C $C-C$ CH_3 CH_3				Coordinate	H^*C H^*C $C-C$ CH^* CH^*			
	Our data	Intensity		Gou-beau [2]		Our data	Intensity		Gou-beau [2]
		comb.	infra-red				comb.	infra-red	
Q (C=C)	1680	s		1672	Q^- (C—C)	1151		s	821*
Q^- (C—C)	1269	w		1024	Q^+ (C—C)	893		s	745*
Q^+ (C—C)	690	s		690	γ (CCC)	405			319*
γ (C=C—C)	505	m		503	$\rho_{C=C}$	273			
ρ_{CCC}	411	w		547	$\gamma(C=C-C) + \chi^{CCC}_{CCC}$	190			
γ(C—C—C)	319	w		409					

* Not definitely assigned.

longer exists that smallest group of coordinates for which these vibrations are characteristic. Both of these propositions are completely confirmed. So, for example, in the spectrum of the molecule of 4-methyl-4-ethylhexene [1] (with the first type of branching) all of the characteristic frequencies noted in Table 1 will be observed: 437, 627, 913, 995, 1180 (double), 1296, 1416, 1641, 3006 and 3078 cm^{-1}. On the other hand, in the case of the molecule of 3,6-dimethylheptene-1 (with the second type of branching) the specificity of the vibrations $\gamma(C=C-C)$ and ρCCH (which are those most strongly interacting with the coordinates of the group $-CH_2-CH=$) is destroyed while that of the remaining vibrations: 914, 994, 1176, 1294, 1419, 1641, 2997 and 3082 cm^{-1} is maintained. Similar examples can be produced for the olefins of the five remaining types.

LITERATURE CITED

[1] P. A. Bazhylin, Kh. E. Sterin, Izv. An SSSR, ser. fiz. (Bull. Acad. Sci. USSR, phys. ser.) 11, 456, 1947; S. V. Markova, P. A. Bazhulin, M. M. Sushchinsky, Optika i spektroskopiya (Optics and Spectroscopy) 1, 41, 1956.

[2] J. Goubeau, Die Raman-spectren von Olefinin. Beih. No. 56 zu der Zs. Angew. Chem. 1948.

[3] N. Sheppard, G. B. Sutherland, Proc. Roy. Soc., A196, 195 (1949); S. Sheppard, D. Simpson, Quart. Rev., 6, 1 (1952).

[4] H. McMurry, V. Thomton, Anal. Chem., 24, 318 (1952).

[5] P. F. Gruzdev ZhFKh (J. Phys. Chem.) 28, 507, 1954.

[6] M. V. Volkenshtein, M. A. Elyashevich, B. I. Stepanov, Kolebaniya molekul (Molecular Vibrations) Gostekhizdat (State Tech. Press) 1949.

[7] L. S. Mayants Tr. FIAN, 5, 65 (1950).

[8] L. M. Sverdlov, O. N. Vinokhodova DAN (Proc. Acad. Sci. USSR) 100, 34, 1955; DAN (Proc. Acad. Sci. USSR) 106, 73, 1956.

[9] L. M. Sverdlov, Optika i spektroskopiya (Optics and Spectroscopy) 1, 163, 1956.

The V. M. Molotov Highway Institute in Saratov

Received September 19, 1956

CONCERNING THE RELATION BETWEEN THE ENERGY OF ACTIVATION AND THE HEAT OF REACTION

N. D. Sokolov

(Presented by Academician V. N. Kondratyev August 16, 1956)

It was long ago empirically established [1] that for many reactions, both in the gaseous and in the liquid phase, there exists a simple relation between the energy of activation, E, and the heat of reaction, Q, which for the exothermic direction can be written in the following form:

$$E = a - bQ, \qquad (1)$$

a and b being constants, with $0 < b < 1$. Such a linear relationship between Q and E has, furthermore, been observed and discussed by many authors [2-6]. A sufficiently clear-cut basis for Relation (1) is not, however, to be found in the literature. The most detailed theoretical analysis of it has been made by Evans and Polanyi [7] but their derivation cannot be considered as entirely acceptable. In order to deduce Equation (1) these authors have postulated that the heat of reaction and the energy of activation depend linearly on a certain parameter χ. In a given series of reactions this parameter, according to their point of view, must reflect the characteristics of the molecular interaction and its dependence on the structural properties of the reactants. It is very doubtful, however, that it would be possible, in the general case, to find such a parameter as would satisfy this condition and at the same time would be capable of showing so simple a relationship with the heat of reaction and the energy of activation. If, for example, the value of the field potential at a certain point near to one of these molecules was taken as this parameter then, since this potential enters into the corresponding wave equation as a function of the coordinates, the resulting relation between the characteristic energy of the system and χ will be, generally speaking, a complex one.*

The attempt is made below to give a derivation of Equation (1) which would be free of the indicated objections.

For the sake of definiteness, we will carry out the discussion as it would apply to the gaseous reaction of radical exchange. Let us consider an adiabatic reaction of the type:

$$RB + R' \longrightarrow R + BR', \qquad (2)$$

where B is an atom and R and R' are either atoms or radicals. As has been shown by experiment, relation (1) is obeyed with considerable accuracy for a series of reactions in which there is a variation of either R or R', the varied reactant being a radical. Specifically, it will be supposed that R in the series of reactions under consideration is varied and that R' remains unaltered. The entire line of reasoning can, without difficulty, also be carried over to the opposite case, as well as to that in which the atom B undergoes variation.

* Only in the theory of perturbations is it possible to obtain the linear dependence of the energy on χ by this method. The derivation of (1) which is outlined below is essentially equivalent to the application of this theory.

We will take a definite substitutent, R_0, as a standard and suppose that the change of the potential energy of the system R + B + R' during the passage from R_0 to an arbitrary R is determined by the alteration of a certain parameter, χ, the magnitude of which depends on the nature of R. The concrete physical nature of this parameter is not necessarily fixed and plays no role in what follows. For example, this could be that effective charge which, entering into the expression for the wave function, represents the charge with which the nucleus acts on the outer electrons of the atom or the radical, or it could be the potential of the electric field near to R, and so forth. In the general case, the transition from one radical R to another changes the depth of the potential well and the height of the potential barrier and also the values of the interatomic distances corresponding to them. However, as will be seen from the further development, the relationship between these distances and χ does not, in the first approximation, influence the position of the maxima and the minima.

We will designate by x_1, x_2 and x_3 the respective distances R–B, B–R' and R–R'* and by 1 the coordinates of the reaction. In the initial condition, (RB + R'), $x_1 = x_1^0$ represents the equilibrium distance in the molecule R–B; in the final condition, (R + BR'), $x_2 = x_2^0$ is the equilibrium distance in the molecule B–R'; in the activated state, (R.B.R'), $1 = 1^*$ is a definite combination of the corresponding values of the coordinates x_1^*, x_2^* and x_3^*. Near the point $\underline{1}$ corresponds to one of the normal coordinates of the activated complex; another two of these normal coordinates we will designate by l_1 and l_2 (in the case of a linear activated complex there is still a fourth normal coordinate). In conformity with what has been said, the potential energy surface for the reaction (2), $\epsilon(x_1, x_2, x_3\ \chi)$ has three extreme points:

I for $x_2 = x_3 = \infty$, $x_1 = x_1^0$, which is a minimum (RB + R')

II for $x_1 = x_3 = \infty$, $x_2 = x_2^0$, which is a minimum (R + BR')

III for $x_1 = x_1^*$, $x_2 = x_2^*$, $x_3 = x_3^*$, which is a maximum with respect to $\underline{1}$ and a mimimum with respect to l_1 and l_2 (R·B·R')

At these points the equations

$$(\partial\epsilon/\partial x_1)_I = (\partial\epsilon/\partial x_2)_{II} = (\partial\epsilon/\partial x_j)_{III} = 0,\ (j = 1, 2, 3), \qquad (3)$$

are valid, with the indicies I, II, III designating the sets of coordinates corresponding to the indicated extreme points. In view of these equations, the values x_1^0, x_1^*, x_2^* and x_3^* prove to be certain functions of χ, whereas x_2^0 obviously does not depend on χ.

We will now suppose that the parameter χ alters but little with a change in the nature of R, i.e., that $\Delta\chi << \chi$. This will be a valid supposition when R represents a radical YX and only Y is changed in the series of reactions under consideration, X remaining constant, as is the case, for instance, in a homologous series of radicals. We will introduce the symbol $\xi = \Delta\chi / \chi_0$ where χ_0 is the value of χ in the case of the reaction with that radical R_0 which has been accepted as the standard. Having expressed the energy ϵ and the coordinates x_1^0 and x_1^* ($i = 1, 2, 3$) as functions of ξ, we will, in the neighborhood of the indicated extreme points, write ϵ as a series in terms of ξ and will limit ourselves to linear members••

$$\epsilon_I = \epsilon_I^0 + \xi\left(\frac{\partial\epsilon_I}{\partial\xi}\right)_{\xi=0} + \xi\left(\frac{\partial\epsilon_I}{\partial x_1^0}\frac{\partial x_1^0}{\partial\xi}\right)_{\xi=0};$$

$$\epsilon_{II} = \epsilon_{II}^0;$$

$$\epsilon_{III} = \epsilon_{III}^0 + \xi\left(\frac{\partial\epsilon_{III}}{\partial\xi}\right)_{\xi=0} + \xi\sum_{i=1,2,3}\left(\frac{\partial\epsilon_{III}}{\partial x_i^*}\frac{\partial x_i^*}{\partial\xi}\right)_{\xi=0}.$$

• As the distances between the atoms and the radicals (x_1 or x_2) we will take the distance between B and those atoms of the radical with which B is directly connected in the molecule RB or BR'. By the term distance between two molecules of a radical (x_3) we will understand a corresponding quantity. We will suppose that the normal coordinates of the system R·B·R' depend only on x_1, x_2 and x_3.

•• In these equations ϵ_I^0, ϵ_{II}^0 and ϵ_{III}^0 represent the values of ϵ_I, ϵ_{II} and ϵ_{III} at $\xi = 0$.

Because of condition (3), only the first two terms on the right-hand sides of the first and the last equations are different from zero. In conformity with this, we find for the heat of reaction (exothermic) and the energy of activation (at the absolute zero of temperature and under neglect of differences in the null-point energies):

$$Q \equiv \varepsilon_I - \varepsilon_{II} = Q_0 + \xi G, \tag{4}$$

$$E \equiv \varepsilon_{III} - \varepsilon_I = E_0 - \xi G^*, \tag{5}$$

where $G_0 = \epsilon_I^0 - \epsilon_{II}^0$, $E_0 = \epsilon_{III}^0 - \epsilon_I^0$. are the heat of reaction and the energy of activation for that R^0, which has been accepted as the standard:

$$G = \left(\frac{\partial \varepsilon_I}{\partial \xi}\right)_{\xi=0}, \quad G^* = \left(\frac{\partial \varepsilon_I}{\partial \xi}\right)_{\xi=0} - \left(\frac{\partial \varepsilon_{III}}{\partial \xi}\right)_{\xi=0}. \tag{6}$$

Eliminating ξ from (4) and (5), we obtain Equation (1)

$$E = a - bQ,$$

in which

$$a = E_0 + Q_0 \frac{G^*}{G}, \quad b = \frac{G^*}{G}. \tag{7}$$

We will now suppose that the transition from the standard R^0 to the arbitrary R displaces in one and the same direction all of the points on the potential surface, or at least on that part of it lying between the original potential well and the barrier.* This supposition is rather natural in the case where in the sequence of radicals $\dot{R} = Y\dot{X}$ separate members differ from one another only in the nature of the substitutent Y. Under this supposition the derivatives $\left(\frac{\partial \epsilon_I}{\partial \xi}\right)_{\xi=0}$ and $\left(\frac{\partial \epsilon_{III}}{\partial \xi}\right)_{\xi=0}$ have the same sign. Further, since the influence of the change of R on the surface of the potential energy arises basically from the direct interaction of R with the atom B, whereby, $x_I^0 < x_I^*$, it is not difficult to see that $(\partial \epsilon_I/\partial \xi)_{\xi=0} > \partial \epsilon_{III}/\partial \xi)_{\xi=0}$. From what has been said, and taking Equations (6) and (7) into account, it follows that $0 < b < 1$ which corresponds to the experimental data.

For the above outlined derivation of the Relation (1) the supposition is essential that the influence of R on the potential energy surface is determined by the change in a single parameter, provided that this change is sufficiently small. This supposition, as has been noted above, is reasonable for a series of reactions of the type $RB + R' \rightarrow R + BR'$, in which the radicals $R \equiv Y\dot{X}$ differ only in the nature of Y. To a smaller degree is the indicated assumption a permissible one for a series in which the radicals R differ in the nature of the atom X or in which there is a change in the nature of the atom B, since with these changes the alteration of the parameter χ cannot be sufficiently small. From the derivation, it also follows that Relation (1) cannot be valid for a series of reactions in which there is a change in the nature of two of the components (for example, R and B or R and R') or in which certain of its members have a substitutent Y which is so highly branched that there arises a direct and strong interaction between B and Y ("steric repulsion"). Under such conditions the alteration of the potential surface will be, in general, determined by the change of more than one parameter.

* In other words, it is supposed that the potential curves corresponding to the various reactants do not intersect in the indicated region. For a discussion of this question see, for example, [8].

These conclusions are supported by the experimental data. Plotting the experimental energies of activation and heats of reaction of a graph, the points are found to lie rather close to a straight line in those cases where only the substitutent Y is varied in the radical R (or R') [6]. This regularity is observed to a lesser degree if in the series of reactions there is a variation of the atom of X or of B.* If in the graph there are introduced values of E and Q for reactions of the type $RB + R' \rightarrow R + BR'$ in which there are differences in the nature of two, or of all three, of the components (R,B,R'), then the points do not lie on this straight line but mostly fall into a band of approximately 3.5 kcal width and in certain instances even go beyond the limits of this field [6].

From the theoretical point of view it is to be expected that further refinements of the experimental data for E and Q will show that for reactions which differ in the nature of two of the radicals the values of a and b in Equation (1) will be somewhat different.

This reasoning is supported, for example, by the investigations of V. V. Voevodsky [5]. He found that for a series of reactions

$$RH + R' \rightarrow R + HR'$$

in which there is an alteration of R (R and R' were aliphatic radicals), it is possible to write the following relation:

$$E = a - 0.27Q.$$

It proves to be so that the quantity a, which is equal to the energy of activation when $Q = 0$, is related to the structure of R and can be determined for a series of radicals.

The dependence of a and b on the nature of the reacting molecules R is also well known for ions, in particular, in proteolytic reactions (for a review see [3]). At the present time, however, only in certain instances has the value of b been successfully related to the structural characteristics of the molecules, (see reference [9]).

LITERATURE CITED

[1] R. Ogg, M. Polanyi, Proc. Manchester Lit. Phil. Soc., 78, 41 (1933); Trans. Farad. Soc., 31, 604, 1375 (1935); P. Dimroth, Zs. angew. Chem., 46, 571 (1933); M. Evans, M. Polanyi, Trans. Farad. Soc., 31, 875 (1935); J. Horiuti, M. Polanyi, Acta Physicochim. URSS, 2, 505 (1935).

[2] M. Evans, M. Polanyi, Trans. Farad. Soc., 34, 11 (1938).

[3] L. P. Hammett, Physical Organic Chemistry, N. Y., 1940; R. P. Bell, Acid-Base Catalysis, Oxford, 1941; Teoriya absolyutnykh skorostei reaktsy (The Theory of Absolute Reaction Rates) Moscow, 1948.

[4] Kh. S. Bagdasaryan, ZhFKh (J. Phys. Chem.) 23, 1375, 1949.

[5] N. N. Tikhomirova, V. V. Voevodsky, DAN (Proc. Acad. Sci. USSR) 79, 933, 1951; V. V. Voevodsky, Sbom. Problemy mekhanizma organicheskikh reaktsy (Monograph, Problems of the Mechanism of Organic Reactions) Tr. Kievsk. soveshch. (Trans. Kiev Conference) Kiev, 1953, p. 58.

[6] N. N. Semenov, O nekotorykh problemakh khimicheskoy kinetiki i reaktsionnoi sposobnosti (Certain Problems of Chemical Kinetics and Reactivity) Izd. AN SSSR (Acad. Sci. USSR, Press) 1954.

[7] M. Evans, M. Polanyi, Trans. Farad. Soc., 32, 1333 (1936).

[8] R. D. Brown, Quart. Rev., 6, 63 (1952).

*The Relation (1) is not valid for the exchange of an atom of one halide, which is playing the role of the atom B, by another, a fact which is tied up with the intersection of the potential curves refering to the different reactants, [2] (see footnote on preceding page).

[9] N. D. Sokolov, Sborn. Katalizˇ (Monograph, Catalysis) Kiev, 1950; Usp. fiz. nauk (Progress of Phys. Sci.) 57, 205, 1955, DAN (Proc. Acad. Sci. USSR) 60, 825, 1948.

The Institute of Chemical Physics of the
Academy of Sciences of the USSR

Received August 11, 1956

CONCERNING THE EQUATIONS OF THE LIQUIDUS AND THE SOLIDUS FOR IDEAL SYSTEMS

M. Usanovich

(Presented by Academician V. A. Kargin August 31, 1956)

From the Clausius-Clapeyron equation, written in the form:

$$\ln \frac{P_1}{P_2} = \frac{L(T_1 - T_2)}{RT_1T_2},$$

and the equation of the vapor tension isotherm for a binary system (Raoult's Law), there follows:

$$\ln \frac{Y_A}{X_A} = \frac{L_A(T_A - T)}{RT_AT}; \tag{1}$$

$$\ln \frac{Y_B}{X_B} = \frac{L_B(T_B - T)}{RT_BT}, \tag{1a}$$

where Y_A is the mole fraction of the component A in the solid phase; X_A is the mole fraction of A in that liquid phase which is in equilibrium with this solid phase at the temperature T; T_A, and L_A are, respectively, the temperature and the heat of fusion of A; R is the universal gas constant and Y_B, X_B and L_B and T_B are the corresponding quantities for the component B.

Equations (1) and (1a) were introduced by van Laar [1] for a continuous series of solid solutions. In actuality, as we now see, they are not limited to the case of the continuous series of solid solutions, but rather they represent that equation of state for ideal systems which unites, in the most general form, the Clausius-Clapeyron equation and Raoult's Law. They are not, however, the equations of the liquidus $f(x,T)=0$ or the solidus $f(y,T)=0$.

The latter can be deduced from Equations (1) and (1a) through the variation of additional conditions. In the case where A and B do not form solid solutions, i.e., where $Y_A=1$ and $Y_B=1$, each of these two equations passes over into the well-known logarithmic form of Shreder (equation of the liquidus)

$$-\ln X_A = \frac{L_A(T_A - T)}{RT_AT}; \tag{2}$$

$$-\ln X_B = \frac{L_B(T_B - T)}{RT_BT}. \tag{2a}$$

Solving Equations (2) and (2a) simultaneously at the eutectic point ($T = T_E$), for which $X_A + Y_B = 1$, we obtain:

$$\exp\left(-\frac{L_A(T_A - T_E)}{RT_AT_E}\right) + \exp\left(-\frac{L_B(T_B - T_E)}{RT_BT_E}\right) = 1 \qquad (3)$$

At the point of intersection of those curves which express the dependence of

$$1 - \exp\left(-\frac{L_A(T_A - T)}{RT_AT}\right) \text{ and } \exp\left(-\frac{L_B(T_B - T)}{RT_BT}\right)$$

on T, we find T_E. Knowing T_E we can readily determine the composition of the eutectic.

Equation (3) is the equation of the solidus for an ideal system with a eutectic.

In the case where A and B form a continuous series of solid solutions without maxima or minima,* $X_A + X_B = 1$ and $Y_A + Y_B = 1$. Combining these conditions with Equations (1) and (1a), we obtain:

$$X = \frac{1 - \exp\frac{L_B(T_B - T)}{RT_BT}}{\exp\frac{L_A(T_A - T)}{RT_AT} - \exp\frac{L_B(T_B - T)}{RT_BT}}. \qquad (4)$$

This equation has been derived in a rather complicated fashion by Seltz [2]. It is the equation of the liquidus for a continuous series of solid solutions which obey Raoult's Law.

The equation of the solidus, which was also obtained by Seltz, can be written in the form:

$$Y_A = \frac{1 - \exp\frac{L_B(T_B - T)}{RT_BT}}{1 - \exp\left(\frac{L_B(T_B - T)}{RT_BT} - \frac{L_A(T_A - T)}{RT_AT}\right)}. \qquad (5)$$

Thus, to an ideal system (one which obeys Raoult's Law) there correspond two types of diagrams: the eutectic type and the diagram of Rozeboom's type I. They are described by Equations (2), (2a), (3), (4), and (5).

LITERATURE CITED

[1] V. Ya. Anosov, S. A. Pogodin, Osnovnye nachala fiziko-khimicheskogo analiza (The Basic Principles of Physicochemical Analysis) Moscow-Leningrad, 1947, pages 319-320.

[2] H. Seltz, J. Am. Chem. Soc., 56, 307 (1934).

The Institute of Chemical Science
of the Academy of Sciences of the
Kazakh SSR

Received August 31, 1956

*Maxima and minima are in contradiction to the law of Raoult.

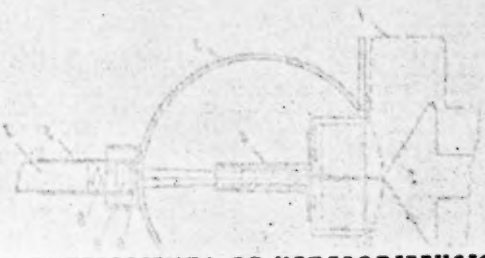

CERTAIN DATA ON THE COEFFICIENTS OF HETERODIFFUSION IN Cu – Ni, Fe – Ni AND Fe – Cr ALLOYS WITH DEFORMED AND UNDEFORMED CRYSTAL LATTICES

E. F. Chaikovsky

(Presented by Academician G. V. Kurdyumov July 3, 1956)

In this investigation there has been carried out an x-ray determination of coefficients of heterodiffusion using the method which has been described in [1]. The prepared samples were in the form of flat disks, 7 mm in diameter, of the one component metal on which the other metal was electrolytically plated as a film of the desired thickness. For x-ray analysis the composite samples were inserted in a cylindrical camera which had a cross-sectional diameter of 72 mm and was attached to the cathode of a sharp-focusing tube (Figure 1). During exposure the sample was rotated around an axis perpendicular to its surface. The small inherent width of the lines assured sharp focusing on the focusing circle where there were placed the film and the samples. The linear dimensions of the focal spot usually did not exceed 70-80 μ. Radiation of the various wavelengths obtained from different anodes (Fe in the case of the system Cu – Ni, V for investigating the system Fe – Cr, Cr for obtaining the x-ray diagrams of the system Fe – Ni; the Fe anode was used with an Mn filter; with the vadadium anode only the β_1 line was employed) was used in the study of the several systems. Because of the small thermal conductivity of the materials used in the anodes, the current through the tube usually did not exceed 0.25-0.5 ma at a potential of 30-40 kilovolts. The tube was fed from the customary high-voltage system in which the heating circuit for the tube filament was stabilized. A comparison of the intensities of the lines in the various diagrams, which was useful for purposes of control, was obtained by including in them as a standard a substance capable of giving interference lines over a certain suitable angular interval, this standard being employed in the form of a superposed flat sector of a disk of small (0.2-0.3 mm) diameter.

In the investigations of the systems Cu – Ni, Fe – Ni and Fe – Cr the samples used consisted of disks of the one component covered by a film of the other. Films of Ni, Cu and Fe which had been detached from the underlying base were also prepared, and, prior to diffusional annealing, these were subjected to a separate heating with a view to removing lattice distortions, thereby bringing the metal into a condition close to that of equilibrium.

A preliminary x-ray investigation showed that immediately after electrolysis the films obtained displayed a broadening of the lines in the x-ray diagrams. A calculation of the photometric curves for the broadened lines was carried out by the method of harmonic analysis [2] and it was thus possible to determine the magnitude of the "microdeformations" and the size of the mosaic regions in the film. After a preliminary annealing, even at comparatively low temperatures (400-500°) this initial broadening of the lines was practically eliminated. Diffusional annealing was carried out for samples in which: 1) an electrolytic film had been deposited on a massive disk; 2) two electrolytic films had been successively plated out, and 3) an electrolytic film prepared in the free condition and previously annealed to a sufficiently high temperature (the Cu film to 1060°, the films of Ni and Fe to 1100°) had subsequently been so pressed to a massive equilibrated disk of the second component as to obtain the desired contact. Thus, heterogeneous diffusion took place in samples wherein: a) both components were in a condition close to that of equilibrium; b) neither component was, in the initial state, at equilibrium and c) one component was at equilibrium and the other was not. Unfortunately diffusional annealing for the samples with an impressed Cr film could not be successfully carried out, and accordingly data could not be obtained in the Fe – Cr system on diffusion in a sample with both components in the equilibrium condition.

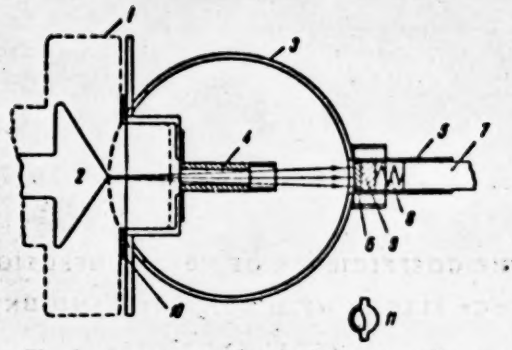

Fig. 1. Arrangement for obtaining x-ray diagrams : 1) body of tube; 2) anode of tube ;3) body of camera ;4) diaphragm 5) holder for sample and standard; 6) sample and standard ;7) motor shaft; 8) spring ;9) packing; 10) adjusting plate; 11) form of standard.

Diffusional annealing of the samples and preliminary annealing of the films was carried out in a furnace either under vacuum (Fe−Cr) of in an atmosphere of H_2. Optimum thicknesses of the electrolytic films were calculated on the basis of the depth of the half-adsorption layer and were checked experimentally (Ni film on Cu, 3 μ ; Cu film on Ni, 3.5 μ ; Fe film on Cr, 4.5 μ ; Cr film on Fe, 2.5 μ ; Ni film on Fe, 5.3 μ ; Fe film on Ni, 1.3 μ. The figures presented are correct for the x-ray radiations which have been indicated above).

Diffusional annealings of one hour duration were carried out on each sample, first at 400° and then at successively higher temperatures spaced 100° apart. The change in the concentration distribution was recorded after each diffusional annealing, comparison being made with the result obtained after heating at the preceding lower temperature. The possibility of handling the data according to the well-known method of Matano [3] was thus lost but, on the other hand, there was obtained the advantage of greater accuracy in the determination of the temperature dependence of D, since all of the values of D at the various temperatures were established from the results of experiments on a single sample. The procedure for calculating the magnitude of D and its dependence on the concentration is described in [1].

In Figures 2 and 3 there are shown the x-ray diagrams of samples from the Fe−Ni and Fe−Cr systems after diffusional annealing of these samples at various temperatures. In the Fe−Cr system the sample consisted of an electrolytic Fe film deposited on nonequilibrated Cr and in the Fe−Ni system it consisted of an Ni film on nonequilibrated Fe.

In Figure 4 there is shown the experimentally determined distribution of concentrations in these same samples after their annealing at the various temperatures. The curves in the Fe−Ni system reveal a plateau at 600° in that region in which there is formed the phase $Fe-Ni_3$. From the data of the curves of Figure 4 and analogous data applying to the other samples, values of D were calculated at various concentrations and temperatures (Table 1). From the log D, 1/T relation there was determined the energy of activation, Q, values of which are also presented in Table 1.

It follows from the data which have been obtained here that the coefficients of heterodiffusion for the nonequilibrated and for the pre-annealed samples markedly differ from one another (for example, in the Cu−Ni system by a factor of 20). This detail sometimes escapes attention in the determination of coefficients of diffusion by certain methods employing radioactive isotopes where the time needed for diffusional annealing amounts to scores of hours and the initial differences in the behavior of the samples have the opportunity to level out.

In this connection, it should be noted that the x-ray technique of determing D rests on the registration of the diffusional processes over a distance $x \approx 5 \cdot 10^{-4}$ cm which, for times ranging from 10 to 10^4 seconds, permits the determination of coefficients of diffusion within the interval $\sim 10^{-8} - 10^{-12}$ cm²/sec. The possibility of utilizing short annealings opens the way in x-ray investigations for establishing differences in the coefficients of

TABLE 1

A. System Cu—Ni. $D \cdot 10^{11}$ cm²/sec.

t, °C	Neither component at equilibrium					Cu at equilibrium, Ni not at equilibrium					Both components at equilibrium				
	Concentration Cu (or Ni or Cr) at. %					Concentration Cu (or Ni or Cr) at. %					Concentration Cu (or Ni or Cr) at. %				
	17	33	50	72	90	17	33	50	72	90	17	33	50	72	90
600	2.0	—	—	—	6.3	0.5	—	—	—	0.6	—	—	—	—	—
700	4.6	5.0	5.5	6.7	10	1.5	1.6	1.6	1.7	2.0	—	—	—	—	0.1
800	—	9.6	10.2	11.0	20.1	4.4	4.5	4.6	4.8	5.5	0.4	—	—	0.6	1.0
900	—	—	—	—	—	—	10.2	10.3	11.0	12.2	3.2	3.4	3.6	4.0	—
1000	—	—	—	—	—	—	—	—	—	—	19.0	21.2	23	—	—
Q, kcal / g-atom	—	13	—	—	11	—	21	—	—	20	53.6	—	—	48.4	—

B. System Fe—Ni. $D \cdot 10^{11}$ cm²/sec.

°C	Neither component at equilibrium					Both components at equilibrium				
	Concentration Cu (or Ni or Cr) at. %					Concentration Cu (or Ni or Cr) at %				
	31	46	62	77	92	31	41	62	77	92
600	1.7	—	—	2.5	2.6	—	—	—	—	—
700	6.6	8.0	9.5	11.6	—	1.3	—	—	—	2.6
800	—	28.1	—	—	—	11.1	—	—	21	20
900	—	—	—	—	—	70.0	92	122	—	—
Q, kcal/ g-atom	25	25	—	—	—	—	46	—	46	—

C. System Fe—Cr. $D \cdot 10^{11}$ cm²/sec.

°C	Neither component at equilibrium				
	Concentration Cu(or Ni or Cr) at.%				
	44	62	81	94	
800	1.0	1.1	1.4	2.1	
900	2.0	2.3	2.9	6.3	
1000	—	3.3	4.0	9.3	
Q, kcal/ g-atom	—	13.5	13.5	—	

diffusion in samples with equilibrated and with deformed lattices [4], which differences play a definite role in those various processes of crystallization which are tied up with diffusion over small distances of the order of microns.

The earlier described error in the determination of the coefficients of heterodiffusion by the x-ray method is additively composed of the relative error in the value of the concentration gradient dc/dx and the area

[1]. Taking into account the error resulting from the simplifications introduced into the calculations, the over-all error in the determination of D amounts to from 40 to 60% for a total width of the interference line (doublet) equal to 0.1 of the entire interval of concentrations. If the width of the interference line amounts to a larger part of the total interval of concentrations, the error of calculation increases, and with a line width of $^1/_3$ of the entire interval of concentrations it goes up to 200% of the measured quantity.

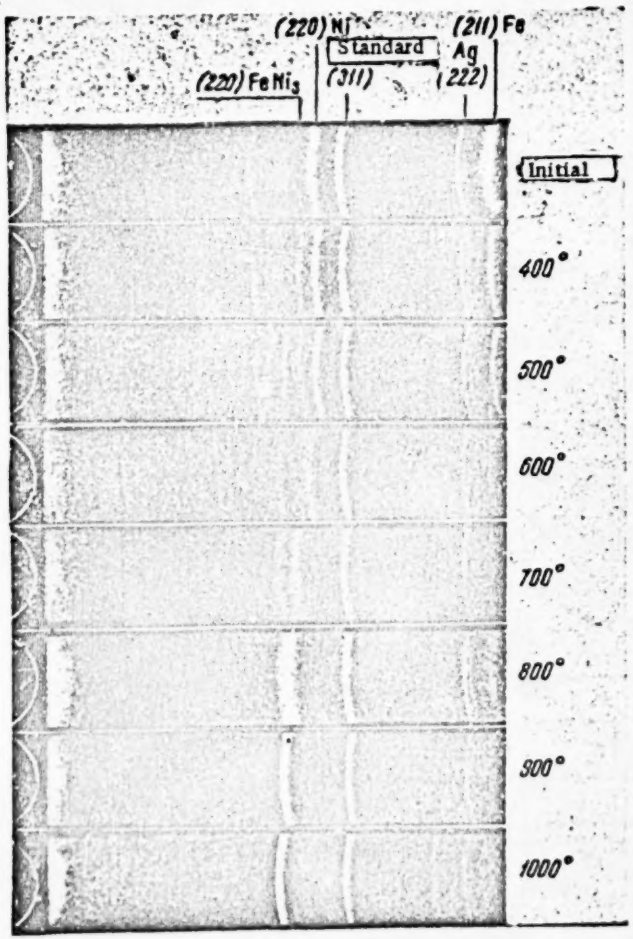

Fig. 2. x-Ray diagram of a diffusion sample from the Fe–Ni system. Neither component at equilbirum, Ni above. Kα) radiation from Cr.

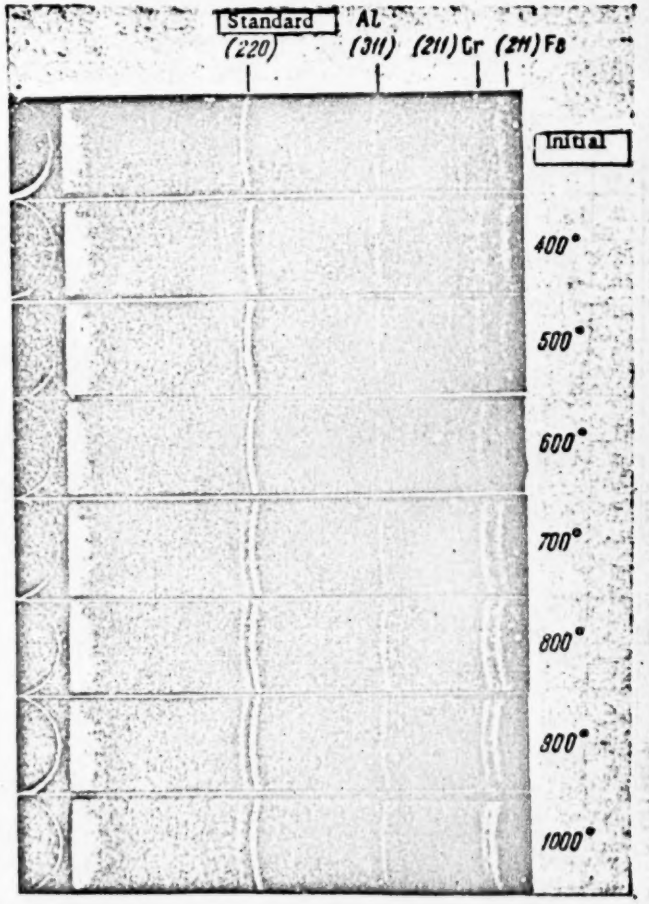

Fig. 3. x-Ray diagram of a diffusion sample from the Fe–Cr system. Neither component at equilibrium, Fe above. K_β) radiation from V.

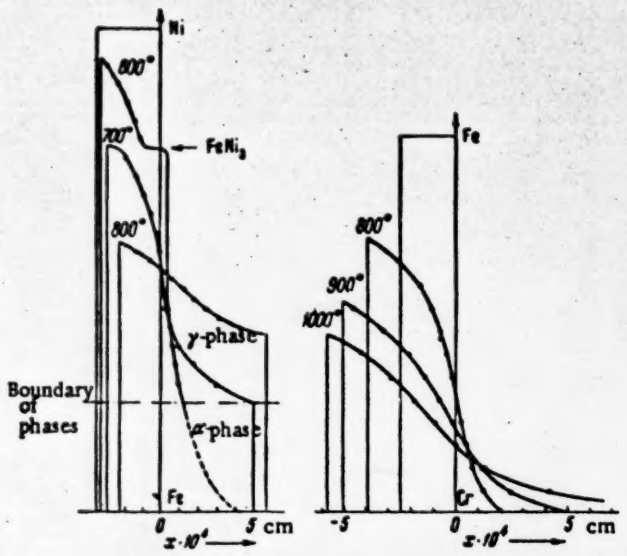

Fig. 4. Examples of concentration distribution curves; construction carried out by the method described in [1] using the data of the x-ray diagrams in Figures 2 and 3.

LITERATURE CITED

[1] B. Ya. Pines and E. F. Chaikovsky, Proc. Acad. Sci., USSR, 111, No. 6 (1956).

[2] B. Ya. Pines, Sharp-focusing X-ray Tubes and Applied X-ray Analysis (1955).

[3] V. Z. Bugakov, Diffusion in Metals and Alloys (1949).

[4] S. T. Konobeevsky, Bull. Acad. Sci. USSR, No. 5 (1937).

The A. M. Gorky State University
in Kharkov

Received August 29, 1956

THE INFLUENCE OF ADDITIVES ON THE VELOCITY OF SELF-DIFFUSION

M. E. Yanitskaya, A. A. Zhukhovitsky and S. Z. Bokshtein

(Presented by Academician G. V. Kurdyumov September 8, 1956)

The question of the influence of small concentrations of alloying elements on the diffusional mobility of the atoms of the solvent in a solid solution has much practical importance in connection with the problem of obtaining alloys with predetermined properties, especially ones which would be stable at high temperatures. A distinction should be made between the action of additives on the volume and on the boundary diffusion.

The theory, according to which the effect of additives is to be explained in terms of their influence on such thermodynamic properties as the heat of sublimation, is useless for elucidating the action at small concentrations. In actuality, additives essentially increase the coefficient of self-diffusion of the solvent even at such low concentrations that the heat of vaporization of the solvent and its other partial thermodynamic properties are practically unaltered.

For illustrating this state of affairs we have determined the parameters of self-diffusion and the thermodynamic characteristics of the solvent in two systems, one of which (Ag–Cu) has positive and the other (Ag–Sn) negative deviations from Raoult's Law.

Self-diffusion was investigated by the method of the thin layer [1]. The values which were found for the parameters of self-diffusion are presented in Tables 1 and 2.

It is to be seen from these tables that small percentages of alloying copper and tin considerably decrease the energy of activation of silver.

TABLE 1

The Parameters of the Self-diffusion of Silver in Silver-Copper Alloys

Number of alloy	Cu, atom %	D_0, cm²/sec.	E, kcal/mole	Temperature interval, °C
1	0.00	0.62	45200	690—906
2	0.17	0.65	45200	780—906
2	0.17	1.06	41000	690—780
3	0.84	0.68	45200	780—906
3	0.84	0.08	39000	690—906
4	1.68	0.07	40600	725—906
5	5.00	0.06	39900	725—880
6	8.15	0.04	38300	725—830

Additions in the amount 0.17 and 0.84% Cu and 0.18% Sn affect the energy of activation only at relatively low temperatures.

The thermodynamic characteristics of silver in the investigated systems were determined by us experimentally, using the method of isotopic exchange [2]. In addition, the heat of dilution for the silver-copper system was calculated according to the semi-empirical formula which has been proposed by Krupkovsky [3].

The heats of dilution obtained for silver in solutions containing up to 1.68 at. % of copper and 2.8 at. % of tin are practically equal to zero. Values referring to alloys of higher concentrations are presented in Table 3. From them it is to be seen that the diffusional characteristics of alloys are more sensitive to additions than are the thermodynamic.

It is obvious that small additions cannot essentially change the heat of vaporization, which is a mean value. The energy of the transition state for self-diffusion can be sharply decreased near atoms of an additive, which, in turn, will affect the velocity of self-diffusion, particularly at relatively low temperatures. We note that small

admixtures cannot give a significant decrease in the rate of diffusion since experiments in which the conductivity of the basic mass of crystals would not be influential cannot be realized.

TABLE 2

The Parameters of the Self-diffusion of Silver in Silver-Tin Alloys

Number of alloy	Sn, atom %	D_0, cm²/sec.	E, kcal/mole	Temperature interval, °C
7	0.18	0.622	45200	830—900
7	0.18	0.132	41700	700—830
8	0.48	0.128	40900	700—850
9	0.91	0.170	40500	700—850
10	2.80	0.200	40250	700—850
11	4.56	0.225	39700	700—830

TABLE 3

Heats of Dilution of Silver

System	Atom % second component	Heat of dilution of silver, cal/mole	
		Experimental values	Calculated values
Ag—Cu	5	— 40	—16
Ag—Cu	8.15	—100	—46
Ag—Sn	4.56	+130	—

The cause of the alteration of the diffusional characteristics of the diluted solutions is to be found in the formation of regions around the atoms of the dissolved substance these regions having enhanced mobility or the so-called "short paths of diffusion" [4]. Independently of the concrete cause of the appearance of these "short diffusional paths," there arises the problem of describing their influence on the mean mobility of the atoms in the alloy.

We will consider the following simple model. Let it be so that the additives create, in a part ρ of the volume, an increased coefficient of self-diffusion D_1, at the same time as the coefficient of self-diffusion of the pure solvent is equal to D_0 and the effective coefficient of self-diffusion is D.

The diffusional resistance of the medium under combination of its sections in series is approximately equal to the sum of the diffusional resistances of these parts (this is strictly true for the stationary regime) i.e., it is equal to a sum of magnitudes which are reciprocals to the coefficients of diffusion, $1/D_i$.

The approximation, which is suitable for the description of the diffusion along linear trajectories, is also applicable, as will be shown later, to boundary diffusion, but completely neglects volume diffusion.

Actually, it is so that if the coefficient of diffusion were equal to zero in one of these sections, then the whole process would cease ($D = 0$), which, of course, cannot be true for volume diffusion. Summation over the conductivities (D_i), which would correspond to a supposition of parallel flow of currents, would be just as incorrect. This may be made clearer by supposing one of the partial coefficients of diffusion to be equal to infinity.

It is clear that the existence of regions showing an alteration in mobility does not correspond to combination either in series or in parallel.

For a stationary process of diffusion this question can be considered in its general form. Since the Poisson Equation is, in the absence of charges, equivalent to the stationary diffusional problem, the action of such a region is completely analogous to the influence on the electric field of a sphere within a dielectric differing from it in the value of the dielectric constant.

For the case of spherical regions this problem is considered in connection with the derivation of the Equations of Clausius-Mosotti and Lorentz-Lorentz, the theory of magnetic susceptibility, and so forth. For ellipsoidal regions a solution has been given by Fricke [5] in the course of an investigation of the electrical conductivity of suspensions.

For spherical regions and small concentrations the solution can be written in the following form:

$$\frac{D - D_0}{D_0} = 3\rho \frac{D_1 - D_0}{D_1 + 2D_0}. \qquad (1)$$

When $\frac{D_0}{D_1} \ll 1$, this equation goes over into the following:

$$\frac{D-D_0}{D_0} = 3\rho\left(1-\frac{3D_0}{D_1}\right). \tag{2}$$

Thus, if $D \to \infty$, then:

$$\frac{D-D_0}{D_0} = 3\rho. \tag{3}$$

This indicates that there is to be cut out, not the ρ-part of the volume, as in a series combination, but rather a quantity three times as large.

From Equation (2), making use of that expression through which the energy of activation is defined

$$\frac{\partial \ln D}{\partial T} = \frac{E}{RT^2},$$

it is not difficult to derive the effective value of the energy of activation and the multiple of the exponential

$$E = E_0 - 9\rho\frac{D_0}{D_1}(E_0 - E_1), \tag{4}$$

$$A = A_0\left\{1 + 3\rho - 9\rho\frac{D_0}{D_1}\left(1 - \frac{E_0 - E_1}{RT}\right)\right\}, \tag{5}$$

where E_0 and D_0 are the energy of activation and the coefficient of diffusion of the pure solvent and E_1 and D_1 are the similar quantities referring to the region of enhanced mobility.

We see that when $D_1 \to \infty$, $E = E_0$, which is natural since under these conditions diffusion proceeds outside of the regions possessing increased mobility. Since with $E_1 = E_0$ there once more arises the equality $E = E_0$, E must pass through a maximum.

The linear relationship between the change in the coefficient of self-diffusion and the concentration is valid for alloys of silver with copper and with tin under concentrations not exceeding 2 at. % and 1 at. % respectively.

The slopes of the curves in Figure 1 are related to the characteristics ρ and D_1, which cannot be determined from experimentation alone.

There is however, the possibility of the two following evaluations.

1. Supposing that $D_1 = \infty$, from the magnitude of ρ we obtain a radius for the disturbed region. This quantity, which is equal in the Ag–Cu system to $4 \cdot 10^{-8}$ cm and in the Ag–Sn system to $7 \cdot 10^{-8}$ cm, will be the lower limit of the radius, as is clear from Equation (2).

2. From the temperature dependence of $(D - D_0)/D_0$, supposing that ρ does not depend on temperature and adopting an exponential relation for D_1, it is possible to obtain a value of D_1. Calculations show that in the investigated systems the magnitude of this last is expressed by the equations:

$$D_1 = 1.1 \cdot 10^{-3} \exp\left(\frac{17000}{RT}\right) \quad (Ag - Cu),$$

$$D_1 = 1.6 \cdot 10^{-3} \exp\left(\frac{18000}{RT}\right) \quad (Ag - Sn).$$

The question arises as to the applicability of Equation (1) for the description of the processes involved in the superposition of the volume diffusion and the diffusion along the boundaries of grains and blocks. Since the "short paths" are here united with one another, it is clear that the concept of resistances connected in parallel will be a closer approximation for the larger paths of diffusion.

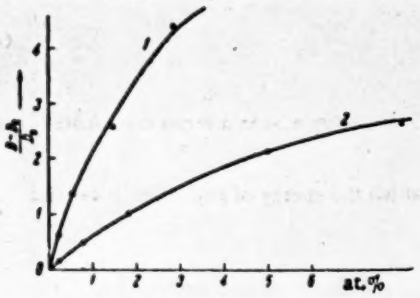

Fig. 1. The dependence on concentration of the change in the coefficient of self-diffusion of silver at 1000° K:
1) Ag–Sn, 2) Ag–Cu.

We will consider from an analogous point of view the influence of the additives on boundary diffusion. Inasmuch as boundary diffusion can be considered as a combination of resistances in series, small quantities of additives can sharply change the effective coefficient of resistance. From Equation (1) for the volume diffusion it follows that if $D_1 = 0$, i.e, if diffusion ceases in a certain sphere, then $(D - D_0)/D_0 = \frac{3}{2}\rho$.

Thus, the effect of the action of a region with zero mobility is 1.5 times greater than that effect which would be observed under parallel combination.

In addition, it has been shown [6], that 0.1% of boron decreases the coefficient of diffusion of tin on the grain boundaries of Nickel almost by a factor of ten. Obviously, this effect is related, not only to the presence of an increased concentration of boron on the grain boundaries, but also to the increased influence of retarding additives in a system of series-connected resistances. The accelerating action of the short paths of diffusion must be less in boundary diffusion than it is in volume diffusion.

Thus, with uniform intensity of action the retarding effect will act more strongly on the boundaries than in the volume and the accelerating effect will act less strongly.

We count it a pleasant duty to express our thanks to Ya. V. Shevlev and R. N. Rubinshtein for discussion of the results and for having pointed out to us certain references in the literature.

LITERATURE CITED

[1] S. N. Kryukov, A. A. Zhukhovitsky, DAN (Proc. Acad. Sci., USSR) 15, 3, 1953.

[2] A. A. Zhukhovitsky, M. E. Yanitskaya, S. N. Kryukov ZhFKh (J. Phys. Chem.) 29, 7, 1955.

[3] W. Ptak, Bull. Polon. Acad. Sci., 2, 3, 139 (1954).

[4] C. Zener, J. Appl. Phys., 22, 372 (1951).

[5] C. Frike, Phys. Rev., 24, 575 (1924).

[6] S. Z. Bokshtein, T. T. Gudkova, S. T. Kishkin, E. L. Moroz, Zavod. Lab. (Fact. Lab.) No. 4, 1955.

The I. V. Stalin Institute of Steel in Moscow

Received August 29, 1956

MEASUREMENT OF SATURATED VAPOR PRESSURES OF SOLID BISMUTH BY THE METHOD OF ISOTOPIC EXCHANGE

A. N. Nesmeyanov, B. Z. Iofa and B. V. Karasev

(Presented by Academician V. N. Kondratyev on July 31, 1956)

This work is the first measurement of saturated vapor pressure of solid bismuth. Results of measurements of saturated vapor pressure over a solid metal allow the calculation of a number of thermodynamic functions, knowledge of which is, at present, indispensable for thermal calculations on atomic electric plants, where bismuth can be used to transfer heat.

The saturated vapor pressure of liquid bismuth has been measured by a number of authors [1-5], but there is no accord between the values given by different experimentalists. Apparently among the low temperature measurements the most reliable are those of A. Granovskaya and A. Lyubimov [3]. Literature values for liquid bismuth do not allow exact calculations of saturated vapor pressure over solid bismuth. However it can be assumed that near the melting point the saturated vapor pressure of solid bismuth must be 10^{-8} to 10^{-11} mm mercury at STP (see Fig. 3). Such low saturated vapor pressures can apparently be measured only by using Langmuir's method [6] or the isotopic exchange method [7,8].

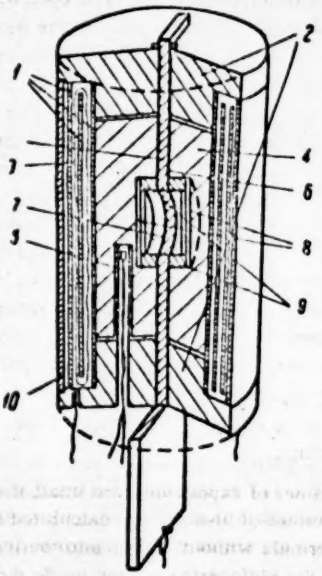

Fig. 1. Exchange chamber and heating oven.

Measurements of the saturated vapor pressure of solid bismuth were performed using Bi^{210}(RaE) as the radioactive indicator.

The RaE was extracted from old emission tubes (3 curies of radon) and purified of RaD and polonium.

The measurements were performed in a vacuum apparatus containing an exchange chamber heated by a special oven.

The exchange chamber 2 (Fig. 1) consisted of a steel cylinder divided into two halves kept together with the help of four screws. Both halves had cylindrical cavities where two discs 8 coated with a layer of metallic bismuth, were placed. The discs were solidly fixed within the chamber by means of two molybdenum rings 9. The chamber had a longitudinal through groove along which a molybdenum plug 6 could move freely. The plug could be fixed and also had an opening whose diameter coincided exactly with the internal diameter of the molybdenum rings. The exchange chamber was heated by means of an oven.

The oven (Fig. 1) made of brass consisted of a base and cover 2 which were connected by means of the outer cylinder 10. The base and the cover had through openings allowing free movement of the plug 6.

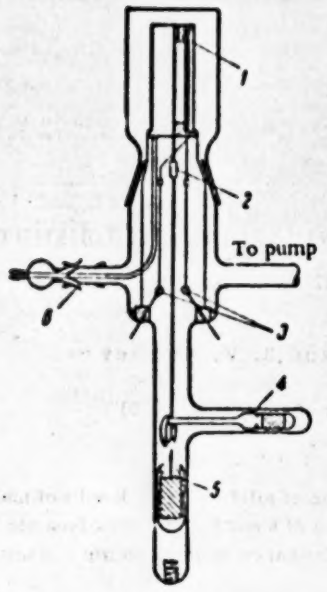

Fig. 2. Vacuum apparatus for measurement of small vapor pressures.

The oven was heated by a nichrome spiral 3 which was insulated from the metallic parts by quartz cylinders 1. The temperature of the chamber and of the exchanging samples was measured by a chromal-alumel thermocouple to 0.5°.

The vacuum apparatus (Fig. 2) was constructed of molybdenum glass and consisted of a base and a detachable part. The oven 1 with the exchange chamber was fixed within the base and the system 2-4-5 was set up allowing the plug to move with the help of external magnets, without affecting the vacuum in the apparatus. The oven was heated through molybdenum wires 3. The thermocouple was fixed with the help of picein in the detachable part 6.

The samples for exchange were prepared by electrolytic deposition on nickel discs of active or inactive bismuth. The depositions were performed from hydrochloric acid solutions with a current density of 10 milliamperes/cm^2 and a bath potential of 2 volts. The samples prepared always had equal thicknesses of metallic bismuth.

In performing the experiment with two nickel discs with a deposited layer of metallic bismuth, one of which contained RaE, were placed in the corresponding cylindrical cavities in the exchange chamber. The samples were preheated in vacuum in order to produce a metallic surface in equilibrium relative to the vapor. The exchange chamber was assembled and the plug placed in the position where it separated the samples. The detachable part was put on the base and the apparatus evacuated to a high vacuum ($5 \cdot 10^{-6}$ to 10^{-5} mm of mercury at STP). The oven was heated to the given temperature and the plug was lowered with the help of an external magnet. Simultaneously a timer was started. The opening in the plug coincided with the inner openings of the molybdenum rings and contact between the samples occurred. After a certain time lapse the plug was raised and the timer stopped. Special experiments showed that with the cover closed no radioactive bismuth vapors penetrated into the space containing the nonradioactive bismuth during the heating and the cooling of the chamber. At the end of the experiment the sample that was inactive before was placed into a special container and its activity measured by a surface counter. The activity of each sample was measured over a period of several weeks and the absence of RaD in the samples was confirmed. The activity of the samples was compared to specific activity determined from the activities of standards containing a known amount of the initial radioactive bismuth.

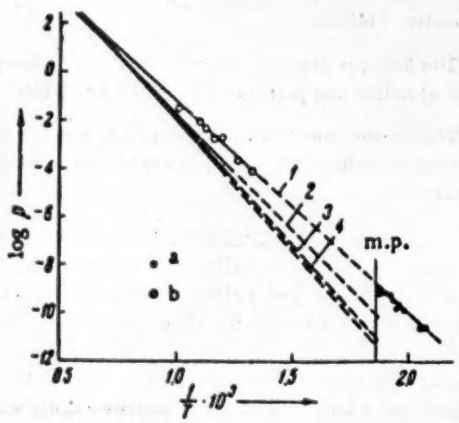

Fig. 3. Saturated vapor pressures of liquid and solid bismuth: 1) according to the data of [3], 2) according to the data of [2], 4) according to the data of [4]; a) our data, b) data of [3].

Since the times of exposition were small the saturated vapor pressure of bismuth was calculated from the following formula without taking into consideration the diffusion of the radioactive isotope inside the sample.

(1)

where I is the activity of the earlier inactive sample (impulses/min, α - is the specific activity of the initially active bismuth sample (impulses/min), S is the sample area participating in the exchange (0.785 cm^2), k is Clausing's factor, in our case equal to 0.826. M is the molecular weight of bismuth in the vapor state and τ is the time of the exposition (sec).

In using equation (1) it was assumed that the bismuth vapors consist only of diatomic molecules [2,9].

The results of the experiments are given in Table 1 and Fig. 3.

TABLE 1

Saturated Vapor Pressures of Solid Bismuth and the Standard Heat of Sublimation at Absolute Zero

T° K	p (mm of mercury at STP)	Deviation of p from the value calculated from eq(2), in %	−Rlnp (atm), cal	Φ'_{solid} cal	Φ' gas cal	ΔH_0^0 kcal/mole	$\Delta H_0^0 - \Delta H_{0\,av}^0$
479	$5.50 \cdot 10^{-11}$	+17.7	60.128	11.004	60.977	52.74	−1.23
485	$5.25 \cdot 10^{-11}$	−32.8	60.218	11.074	61.083	53.46	−0.51
502	$3.07 \cdot 10^{-10}$	+3.2	58.710	11.270	61.344	53.74	−0.24
507	$5.79 \cdot 10^{-10}$	+28.6	55 449	11.326	61.423	54.04	+1.07
512	$3.89 \cdot 10^{-10}$	−40.3	58.245	11.383	61.491	54.95	+0.48
515	$8.87 \cdot 10^{-10}$	+11.3	53.887	11.416	61.531	53.56	−0.41
516	$1.98 \cdot 10^{-9}$	+96	52.814	11 427	61.554	53.12	−0.85
525	$1.55 \cdot 10^{-9}$	+11.4	53.497	11.526	61.736	54.45	+0.48
528	$2.35 \cdot 10^{-9}$	+16.7	52.667	11.558	61.794	54.33	+0.36
530	$1.94 \cdot 10^{-9}$	−15.9	53.044	11.581	61.831	54.74	+0.77
532	$1.81 \cdot 10^{-9}$	−31.6	53.179	11 602	61.867	55 03	+1.06

Least squares treatment of the experimental results showed them to be well described by the following equation:

$$\log (\text{mm Hg}) = \frac{8397,0}{T} + 7,213 \qquad (2)$$

where T is the temperature of the exchange chamber and of the samples.

As can be seen from Fig. 3, our results agree well with the results of A. Granovskaya and A. Lyubimov [3] and the results of work performed at high temperatures and pressures.

Starting with the saturated vapor pressures of solid bismuth, we calculated the standard heat of sublimation at absolute zero ΔH_0^0 from the equation $\Delta H_0^0 = T[\Phi_{gas} - \Phi_{solid} - R\ln p\ (atm)]$.

According to general equations of thermodynamics and using the heat capacity of solid bismuth [10-12] and the results of spectroscopic investigations [12,13] ($I = 1.4 \cdot 10^{-37}$ g · cm^2, $\omega = 172\ cm^{-1}$), the following equations were constructed for the calculation of the Φ'-potentials:

$$\Phi_{solid} = 23,896 - 12,6411 \log T - 1,22 \cdot 10^{-3} - \frac{207,8}{T} \qquad (3)$$

$$\Phi'_{gas} = 16,222 + 16,015 \log T + R\ln Q_{vib.} \qquad (4)$$

where $Q_{vib.} = \left(1 - e^{-\theta/T}\right)^{-1}$ and $\theta = 247,2°$.

The calculated values of ΔH_0^0 are given in Table 1. The average value of ΔH_0^0 is 54.0 ± 0.7 kcal/mole.

The criterion for the reliability of the results obtained was a satisfactory spread in the values of ΔH_0° about the average value. The absence of a systematic trend in the values of ΔH_0° with temperature also indicated the reliability of the obtained magnitudes for the saturated vapor pressures of solid bismuth.

Received on July 6, 1956

LITERATURE CITED

[1] K. K. Kelley, US Bur. Min. Bull. 383 (1935).

[2] M. Yosiyama, J. Chem. Soc. Japan 62, 204 (1941).

[3] A. Granovskaya and A. Lyubimov Zhur. Fiz. Khim. 22, 103 (1948).

[4] A. H. Weber and S. C. Kirsch, Phys. Rev. 57, 1042 (1940).

[5] O. Kubashevsky and E. Evans, Thermochemistry in Metallurgy (Foreign Lit. Press, 1954).

[6] I. Langmuir, Phys. Rev. 14, 1273 (1913).

[7] A. N. Nesmeyanov, V. I. Lozgachev and I. F. Lebedev, Doklady Akad. Nauk SSSR 102, 307 (1955).

[8] A. N. Nesmeyanov, I. F. Lebedev, V. I. Lozgachev and E. G. Chudinov, Session of the Acad. of Sciences of USSR on the peaceful uses of atomic energy, July 1-5, 1955. Proceedings of the Comittee of Technical Sciences, Aca. Sci. USSR Press, 1955).

[9] I. F. Zartman, Phys. Rev. 37, 383 (1931).

[10] W. H. Keesom and J. N. Van den Ende, Proc. Acad. Sci. 33, 243 (1930); 34, 210 (1931) Amsterdam.

[11] C. T. Anderson, J. Am. Chem. Soc. 52, 2720 (1931).

[12] E. V. Britske, A. F. Kapustinsky et al., Thermodynamic Constants of Inorganic Compounds, Acad. Sci. USSR Press, 1949).

[13] C. M. Almy and F. M. Sparks, Phys. Rev. 44, 365 (1933).

THE ACTION OF γ-RADIATION ON THE OXIDATION OF HEXADECANE

M. A. Proskurnin, Yu. L. Khmelnitsky, E. V. Barelko, A. T. Slepneva and I. I. Melekhonova

(Presented by Academician A. N. Frumkin on September 28, 1956)

The action of ionizing radiations on the course of chemical reactions can be of a contradictory nature: on one hand it is possible to cause processes which practically can not be realized by any other means, e.g., it is possible to obtain phenol from a mixture of water and benzene in the presence of oxygen [1]; on the other hand, the radiation can strongly accelerate a number of slowly occurring processes. The latter effect must be particularly evident in the case of a reaction occurring through a chain mechanism. This is indicated by the well-known facts of photochemical action on chain reactions, as well as direct experiments on the initiation of polymerization reactions by ionizing radiations [2].

In the case of absence of a chain mechanism the number of reaction products is equal to the number of initial particles, formed by the action of secondary electrons on the molecule. However, to obtain this maximum yield it may be found necessary to have recourse to the action of catalytic additives which would increase the "utilization coefficient" of the initial chemically-active particles, as was shown by two of the authors of the present article for the case of radiolytic oxidation of benzene [3]. N. A. Bakh [4] has also pointed out the possibility of initiating short chains by radiation, in the oxidation of hydrocarbons.

However, particulary complicated and interesting relations between the various factors can occur in the case of reactions with branching or degenerate branching [5]. Reactions of this type are,e.g., the practically important case of oxidation of paraffinic hydrocarbons by molecular oxygen.

The works of V. K. Tsyskovsky[6], D. N. Chemyaev [7] and particularly of N. M. Emanuel [8] have uncovered the role of catalytic additives in the oxidation reactions of paraffinic hydrocarbons. Mainly, this role reduces to the fact that the catalyst is the initiator of the reaction, i.e., causes the formation of some active chemical substances which then lead the reaction. At this stage the catalyst itself can be removed from the reaction mixture. The role of such an initiator can also be played by an ionizing radiation as has been pointed out by us in several articles on the theory of chain reactions [5] and has been demonstrated experimentally for the case of a polymerization process [2]. Lately the expediency of using an ionizing radiation for the initiation of the oxidation of high-molecular weight hydrocarbons has been pointed out by N. M. Emanuel.

We performed experiments on the oxidation of hexadecane by molecular oxygen under the action of γ-radiation of Co^{60}.

The experiments were performed on a specially constructed source of activity 300 gm-equiv. [9]. The construction allowed the source to be removed behind a shield and the investigation of the kinetics of accumulation of oxidation products by removal of samples from the liquid during irradiation as well as in the post-irradiation periods.

Fig. 1. shows a diagram of the apparatus, the reaction vessel and its position relative to the radiation source. The temperature of the oven was kept constant to ± 1°C with the help of a contact galvanometer H connected to the thermocouple I built into the oven. The temperature of the reaction mixture was determined with the help of another thermocouple (in the well B), whose readings were recorded by the automatic potentiometer K.

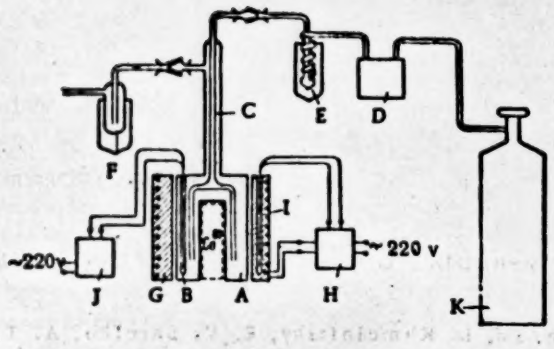

Fig. 1. Diagram of the apparatus: A) is the vessel where irradiation occurred, B) is the thermocouple well, C) are tubes through which oxygen was continuously circulated, D) is the apparatus for purifying of oxygen, E) and F) are liquid oxygen traps, G) is the oven for heating the reaction vessel, H) is the galvanometer, I) is the thermocouple, J) is an automatic potentiometer and K) is a bulb with oxygen.

Fig. 2 shows as an example a curve obtained from such a recording during one experiment. The arrow indicates the time of stopping the irradiation. Small decreases in the temperature for short periods of time correspond to the removal of samples.

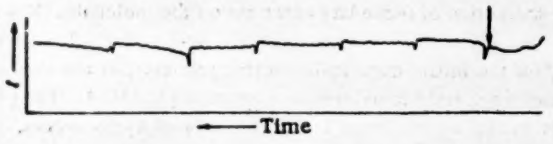

Fig. 2. Stability of the temperature during an experiment (on the ordinate axis 1 mm corresponds to 1° C).

The volume of the hexadecane put into the reaction vessel was 100 cm^3. For experiments the fraction of technical hexadecane was used, b.p. 120°-125° C at a pressure of 1-2 mm, $n_D^{20} = 1.4374$, $\rho_4^{20} = 0.7783$, iodine number = 0.2. The strength of the dose was determined by the ferrosulfate method in a calibrating experiment where a solution of Mohr's salt (10^{-3} N) in 0.8 Normal H_2SO_4 was placed instead of the hexadecane into the reaction vessel. The yield of this reaction was considered to be 15.6 molecules per 100 ev. [10]. The average strength of the dose was 80 r/sec. The analysis was performed mainly for total nonvolatile carboxylic acids by the method of titration with a base [11]. The experiments were conducted at 130° and at atmospheric pressure of oxygen. The samples of hexadecane were placed in the previously heated reaction vessel and then oxygen was passed with simultaneous irradiation. Samples were taken by changing the oxygen pressure and thus transferring a few cubic centimeters of the reaction mixture from the reaction vessel. Such a method allowed the conservation of a stationary state inside the vessel.

Fig. 3 gives the kinetic curves for the nonvolatile carboxylic acids obtained during the oxidation. The parts of the curves corresponding to the irradiation period are represented by dotted lines. The vertical lines indicate the cessation of irradiation. Curves 1-5 were obtained for varying periods of irradiation (from 0.25 to 3 hours). Curve b corresponds to no irradiation.

It is seen from the curves presented that irradiation of the reaction mixture increased considerably the rate of oxidation of the hexadecane. However, if the period of irradiation became longer than about 30 min, the rate of the reaction no longer depended on the time of irradiation. In other words, increase in the time of irradiation any further did not increase the rate of oxidation.

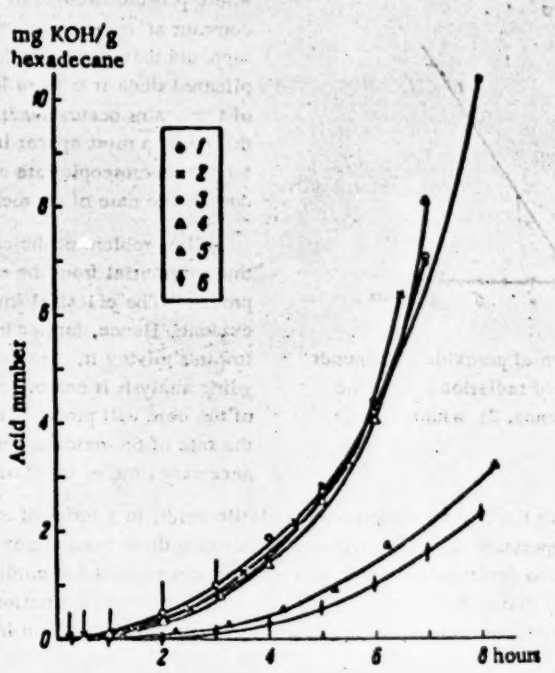

Fig. 3. Formation of nonvolatile carboxylic acids as a function of time under the action of different radiation doses (integral doses, kiloroentgens); 1) 576; 2) 144; 3) 864; 4) 288; 5) 72; 6) without irradiation.

Thus, under the conditions of our experiments initiation of the oxidation of hexadecane is most rationally done by irradiating the reaction mixture for about 30 minutes and then stopping the irradiation. It seems evident that there exists a very close analogy between the phenomena described here and the phenomena occurring on catalytic oxidation of hydrocarbons where the catalytic additive can be removed from the reaction mixture a certain time after the beginning of the reaction with the reaction still proceeding at the same rate.

An explanation of this phenomenon has been given by N. M. Emanuel from the standpoint of degenerate branching [8]. Assuming that degenerate branching occurs in the final product and that breaking of the chains follows a first-order law, he showed that after a certain time $\underline{t}$ the action of the catalyst does not increase the rate of the reaction. This time $\underline{t}$ is given by the relationship:

$$t >> k \ln\left(1 - \frac{\omega_0}{\omega_{0c}}\right),$$

where ω_0 is the rate of initiation of the chains in the absence of the catalyst, ω_{0c} is the rate of initiation of the chains in the presence of the catalyst and k is a coefficient being a combination of elementary reaction constants.

If a similar scheme is at least formally correct for reactions initiated by irradiation, then since ω_{0c} can be considered to be approximately proportional to the dose strength, the expression for $\underline{t}$ will be:

$$t >> k \ln\left(1 - \frac{a}{p}\right),$$

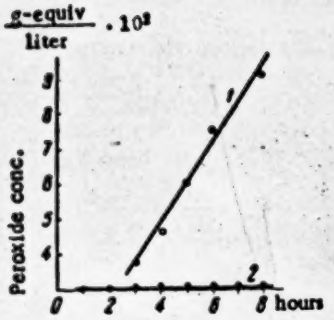

Fig. 4. Formation of peroxide compounds under the action of radiation; 1) time of irradiation 3 hours, 2) without irradiation.

where p is the strength of the dose and a is a magnitude constant at constant temperature. However, it can be supposed that the expression for t must be more complicated since it is more logical to assume that breaking of the chains occurs quadratically and not linearly. In this case $\sqrt{p}$ must appear instead of p in the expressions for the macroscopic rate of the reaction, as it often does in the case of photochemical reaction.

The problem of the connection between t and p is thus substantial from the standpoint of the theory of the process. The practical importance of this problem is evident. Hence, further investigations must be directed towards solving it. Let us only note that from the foregoing analysis it can be seen that increase in the strength of the dose will probably lead not only to an increase in the rate of the oxidation but also to a decrease in the necessary time of irradiation.

Simultaneously with the determination of nonvolatile acids, in a series of experiments we determined the acids volatile at the temperature of the experiment by freezing them from the oxygen stream coming out of the reaction vessel and also determined the amount of peroxides produced according to the method of K. I. Ivanov [12]. It was found that under the action of irradiation the rate of formation of the peroxides also increased. The kinetic curves for the formation of peroxide compounds are given in Fig. 4.

The L. Ya. Karpov Physicochemical Institute of Scientific Investigations.

Received on November 15, 1956

LITERATURE CITED

[1] Y. Stein and J. Weus, J. Chem. Soc. 1949,3245.

[2] J. C. Hayward, Nucl Sci. Abstr. 10, No.2, 80 (1956).

[3] M. A. Proskurnin and E. V. Barelko, Collection of papers on radiation chemistry (Acad. Sci. USSR Press, 1955) p. 99.

[4] N. A. Bakh, ibid., p. 145.

[5] N. N. Semenov, Collection, Problems of oxidation of hydrocarbons, Acad. Sci. USSR, Press, 1951) . p. 13.

[6] V. K. Tsyskovsky. ibid., p. 177.

[7] D. N. Chernyaev, N. S. Makushinskaya and G. P. Dobrovolsky, ibid., p. 184.

[8] N. M. Emanuel, Zhur. Fiz. Khim. 845 (1956).

[9] A. Kh. Breger, V. A. Belynsky and S. D. Prokudin, Atomic Energy, 1956, No. 4.*

[10] C. Hochanadel and J. Ghormly, J. Chem. Phys. 21, 880 (1953).

[11] All-Union State Standard 6985-51.

[12] K. I. Ivanov, Intermediary Products and Intermediary Reactions in the Autooxidation of Hydrocarbons 1949, p. 73.

*Original Russian pagination. See C. B. Translation.

INFRARED SPECTRA OF SOME SECONDARY AROMATIC AMINES

M. A. Salimov and V. M. Tatevsky

(Presented by Academician P. A. Rebinder on September 11, 1956)

Secondary aromatic amines are very important in chemical industry as inhibitors and additives to rubbers in rubber mixtures.

However there has not been any systematic investigation of the relation between the structure of secondary amines and their vibrational spectra. In Colthup's review [1] fatty and fatty-aromatic amines are considered among other aromatic compounds and it is mentioned that secondary amines have intense absorption bands in the regions 1200-1300 cm^{-1} and 3600-3500 cm^{-1}, which are ascribed by the author to the valence vibrations of the C-N and N-H bonds respectively. In Bellamy's monograph [2] it is also mentioned that all secondary amines in dilute solution have only one band in the region 3200-3500 cm^{-1}. In concentrated solutions a second band appears due to hydrogen-bonding, on the long-wavelength side. The region of the valence vibration of the C-N bond is given to be 1280-1350 cm^{-1}. In these and other articles the position of the absorption band of the in-plane deformational vibration of the N-H bond is discussed. In secondary amines the absorption band of this vibration is weak; it is supposed that it must occur in the region 1480-1650 cm^{-1}, i.e., in the same region as the characteristic band for the in-plane deformational vibration of the C-H bond [3]. Separate parts of the spectrum of diphenylamine are considered in the remaining articles [4,5]. Thus there is not in the literature a complete investigation of the spectra of secondary aromatic amines or of their complete and infrared spectra. As for tetraphenylhydrazine the literature does not contain any information on its vibrational spectrum.

In the present work we studied the infrared absorption spectra of diphenylamine, dinaphthylamine, β-naphthyl-N-amine and tetraphenylhydrazine in the region 4000-3700 cm^{-1}.

The aromatic amines were purified by repeated recrystallization. The tetraphenylhydrazine was prepared from diphenylamine by the method described in the literature [9]. Infrared absorption spectra of all substances investigated were obtained in the solid phase by precipitation on a KBr plate from solution. The spectra of the amines and of tetraphenylhydrazine were taken on a spectrograph IKS-11. The infrared spectrum of tetraphenylhydrazine was also obtained at 100° in a thermostatted cell. The following slit widths were used:

Prism	Frequency interval, cm^{-1}	Spectral width, cm^{-1}	Prism	Frequency interval, cm^{-1}	Spectral width, cm^{-1}
KBr	450-500	6	NaCl	1300-1500	9
	500-700	5		1500-1600	11
NaCl	650-800	4		1600-1750	13
	760-1075	5		1700-3500	16
	990-1340	7	LiF	2300-3500	8

The frequencies of the infrared absorption bands obtained are given in Table 1. The spectra obtained contain the characteristic bands of the amines and also of the phenyl and β-naphthyl groups.

In the region of the valence vibration of the N-H bond all amines exhibit two absorption bands: dinaphthylamine 3425 and 3465 cm^{-1}, β-naphthyl-N-phenylamine 3430 and 3450 cm^{-1} and diphenylamine 3392 and 3430 cm^{-1}. In all amines the band on the short wavelength side is more intense than the other band. Apparently the long wavelength band is due to intermolecular hydrogen bonding through the amine hydrogen.

while the short wavelength band is due to the valence vibration of the N-H bond. Naturally tetraphenylhydrazine does not exhibit any absorption bands in that region. As could be expected all amines have intense absorption bands in the region 3050-3085 cm^{-1}, doubtless due to the valence vibrations of the aromatic C-H bonds. Diphenylamine and β-naphthyl-N-phenylamine have also another band on the long wavelength side, which perhaps can be explained by splitting of the frequency due to intermolecular interactions in the solid phase. Tetraphenylhydrazine and all the amines exhibit intense bands in the region 1200-1300 cm^{-1}, which apparently are related to the valence vibration of the C-N bonds. It must be noted that if dinaphthylamine has one band at 1280 cm^{-1}, then β-naphthyl-N-phenylamine and diphenylamine each have two bands (1260, 1276 and 1298, 1312 cm^{-1} correspondingly). Tetraphenylhydrazine has in this region three absorption bands (1250, 1275 and 1300 cm^{-1}). Probably one of these three bands is due to the valence vibration of the N-N bond even though in the case of hydrazine the band at 850 cm^{-1} is assigned to this mode [6]. As can be seen from Table 1 we do not have bands of this frequency. It is known that tetraphenylhydrazine easily decomposes at temperatures above 70°, giving diphenylnitrogen free radicals. Evidently on decomposition of the molecule the intensity of the absorption band of the valence vibration of the N-N bond must decrease. Indeed the infrared absorption spectrum of tetraphenylhydrazine obtained at 100° (Fig. 4, dotted line), shows a sharp decrease in intensity of the absorption band at 1300 cm^{-1}, while the bands at 1250 and 1275 cm^{-1} join together. Other parts of the spectrum do not exhibit any substantial changes. The bands at 1250 and 1275 cm^{-1} are apparently the symmetrical and antisymmetrical valence vibrations of the C-N bonds. Moreover, two of the three amines investigated have in the region 1200-1300 cm^{-1}, each two bands which could also be attributed to the symmetrical and antisymmetrical vibrations of the C-N bonds. It does not seem possible to attribute unequivocally any one band to the in-plane deformational vibration of the N-H bond. On comparing the absorption bands of diphenylamine and tetraphenylhydrazine it is easily seen that the bands 1459 and 1520 cm^{-1} of diphenylamine do not appear in the case of tetraphenylhydrazine. The frequencies 1450 cm^{-1} in dinaphthylamine and 1460 cm^{-1} in β-naphthyl-N-phenylamine are very near to one of the above-mentioned frequencies (1459 cm^{-1}) of diphenylamine. Supposedly these bands could be assigned to the in-plane deformational vibration of the N-H bond in amines. The out-of-plane deformational vibrations of the N-H and C-H bonds occur in the region 700-1000 cm^{-1}. From the data obtained it is easily seen that in this region, apart from the band due to the vibrations of the C-H bonds in phenyl and naphthyl groups, all amines exhibit intense bands (860-880 cm^{-1}). Tetraphenylhydrazine does not have any band in this region and this supports our assignment. These bands are apparently due to the out-of-plane deformational vibrations of the N-H bonds. In symmetrical amines (e.g., naphthylamine and diphenylamine) the frequencies of these bands are equal (880 cm^{-1}) while in β-naphthyl-N-phenylamine this band is somewhat lower (860 cm^{-1}). The remaining bands can be assigned to the various vibrations of the phenyl and β-naphthyl groups.

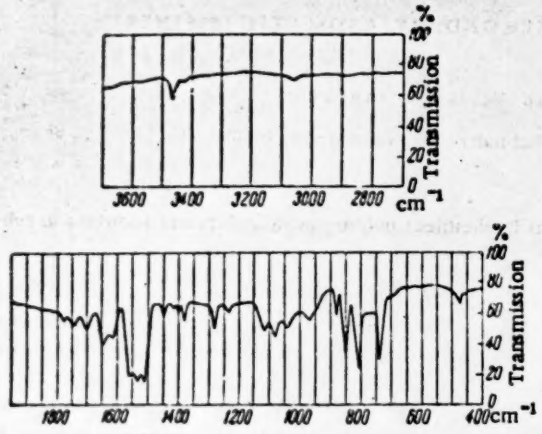

Fig. 1. The infrared spectrum of dinaphthylamine.

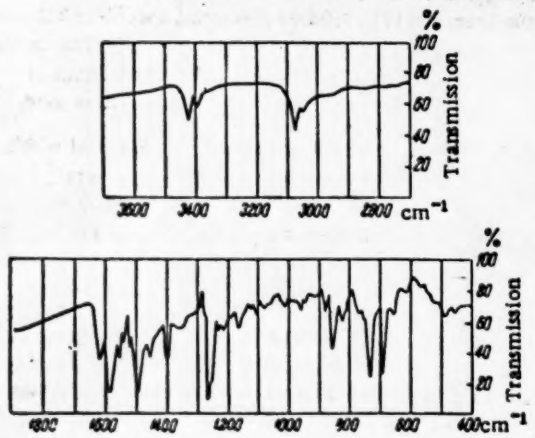

Fig. 2. The infrared spectrum of β-naphthyl-N-phenylamine.

TABLE 1

Dinaphthylamine		β-naphthyl-N-phenylamine		Diphenylamine		Tetraphenylhydrazine	
ν, cm^{-1}	Intensity*	ν, cm^{-1}	Intensity	ν, cm^{-1}	Intensity	ν, cm^{-1}	Intensity
		460	W	460	W		
475	W	485	W	485	W		
		615	W				
		658	W	645	W		
		690	VS	691	VS	690	VS
				701	aV		
736	VS	735	VS	735	VS	740	VS
806	VS	820	aV				
851	VS						
880	S	860	S	880	S		
		885	W				
		915	W				
968	W	960					
				1002	W	1008	W
1040	W	1020	W	1038	W	1040	W
1070	W	1080	W	1086	W	1080	W
1115	W	1115	W	1098	W		
		1130	W				
		1168	W	1162	W	1160	W
				1172	W	1178	W
				1188	W		
		1215	W	1225	W	1208	W
1235	W	1238	W	1240	VS		
		1260	VS	1258		1250	S
1280	S	1276	VS	1312	VS	1275	VS
						1300	S
1380	W						
1400	W	1400	W	1425	aV	1420	aV
1450	W	1460	aV	1459	aV		
				1496	S	1495	VS
1515	VS	1500	VS	1520	VS		
1535	VS	1535	W				
		1550	W				
1562	VS	1562	W				
		1598	VS	1599	VS	1598	VS
1615	aV	1620	S				
1650	W						
1700	W						
1750	W						
1775	W						
		3060	aV	3050	W		
3060	W	3085	S	3074	S	3085	W
3425	W	3430	W	3392	S		
6435	S	3450	S	3430	S		

* The intensity of the band: w-weak, av-average, s-strong, vs-very strong.

Fig. 3. The infrared spectrum of diphenylamine.

Fig. 4. The infrared spectrum of tetraphenylhydrazine.

The intense bands 690, 740, 1495 and 1598 cm^{-1} of tetraphenylhydrazine are doubtlessly due to the various vibrations of the phenyl group [1]. Bands similar in their frequencies and intensities (691, 735, 1495 and 1599 cm^{-1}) are found in diphenylamine. On examining the bands of dinaphthylamine it is easy to notice the characteristic absorption bands of the β-naphthyl group [7]: 736, 806 and 851 cm^{-1}. The other intense bands (1515, 1535, 1562, 1615 and 1650 cm^{-1}) are characteristic of the naphthalene ring [8]. The spectrum of β-naphthyl-N-phenylamine contains absorption bands characteristic of both the phenyl and the naphthyl groups.

Thus investigation of the infrared absorption spectra allows the establishment of a certain correspondence between the structure and the vibrational spectra of secondary aromatic amines.

The M. V. Lomonosov Moscow
State University

Received September 7, 1956

LITERATURE CITED

[1] B. Colthup, J. Opt. Soc. Amer. 40, 397 (1950).

[2] L. J. Bellamy, The Infrared Spectra of Complex Molecules (1955).

[3] D. A. Barr and R. N. Haszeldine, J. Chem. Soc. 4169 (1955).

[4] N. Fuson, M. Josien, R. L. Powell and E. Utterback, J. Chem. Phys. 20, 145 (1952).

[5] R. B. Barnes, R. C. Gore, U. Liddel and V. Z. Williams, Infrared Spectroscopy and its Industrial Application 1944, p. 88.

[6] V. M. Chulanovsky, Introduction to Molecular Spectral Analysis 1951, p. 394.

[7] R. L. Werner, W. Kennard and D. Rayson, Australian J. Chem. 8, 346 (1955).

[8] W. B. Person, G. G. Pimentel and O. Schnepp, J. Chem. Phys. 23, 230 (1955).

[9] L. Gaterman and G. Wieland, Practical Work in Organic Chemistry 1948, p. 397.

INFLUENCE OF AN EXTERNAL ELECTRIC FIELD ON A CHEMICAL REACTION IN A GAS

V. Timan

(Presented by Academician A. N. Frumkin on September 15, 1956)

In the previous article [1] in investigating the influence of ions on chemical reaction in a gas it was pointed out that in the case where the reaction products and the initial compounds interact differently with ions, the electrical field of the ions influences the equilibrium composition of the reaction. It is natural therefore, to investigate the effect of an external electric field on the equilibrium composition of the reaction where the initial compounds are nondipolar molecules and the products are dipolar molecules.

As a concrete case let us consider the reaction of the synthesis of ammonia $3H_2 + N_2 = 2NH_3$ which satisfies the above requirement.

The equilibrium composition of a reaction must be determined by the condition that in the equilibrium state the system has the minimum energy if the entropy and temperature are constant. In the presence of an external electric field a decrease in the total energy of the system must be realized at the expense of an increase in the gas of the number of NH_3 molecules, since these molecules interact with the external electric field stronger than N_2 and H_2 molecules and since the energy of this interaction is negative. Hence, the equilibrium composition of the reaction in the presence of an external electric field must shift to the side of increased amount of ammonia.

Actually the condition for the equilibrium is the equality:

$$\Sigma \mu_i \nu_i = 0. \tag{1}$$

For the reaction being considered this condition is written

$$3\mu_3 + \mu_2 = 2\mu_1. \tag{2}$$

where μ_3, μ_2 and μ_1 are, correspondingly, the chemical potentials of the hydrogen, nitrogen and ammonia molecules.

When an external field of intensity E is applied to the system, the chemical potentials can be written as:

$$\mu_1 = \mu_{1\,id} - E(d\overline{\cos v} + \beta_1 E),$$
$$\mu_2 = \mu_{2\,id} - E^2\beta_2,$$
$$\mu_3 = \mu_{3\,id} - E^2\beta_3.$$

Here μ_{1d} μ_{2d} μ_{3d} are, correspondingly, the chemical potentials of the ideal gases NH_3, N_2 and H_2 in the absence of any field; β_1, β_2, and β_3 are their polarizabilities; d is the dipole moment of the NH_3 molecule; $\overline{\cos v}$ is the well-known Langevin function

$$\overline{\cos v} = -\frac{1}{a} - \frac{e^a + e^{-a}}{e^a - e^{-a}}, \tag{4}$$

where a = Ed/kT.

The chemical potentials μ_{1d}, are expressed

$$\mu_{id} = kT \ln P_i + \chi_i(T), \tag{5}$$

where P_i is the partial pressure of the particles of the i-th type in the mixture and $\chi_i(T)$ is a certain function of the temperature

$$\chi_i(T) = -kT \ln \left\{ \left(\frac{m_i kT}{2\pi\hbar^2} \right)^{3/2} \sum_{k_i} \exp\left(-\frac{\epsilon^i_{k_i}}{kT} \right) \right\} - kT \ln kT. \tag{6}$$

Here ϵ^i_{ki} are the energy levels of a molecule of the i-th type (not including translational energy), m_i is the mass of the molecule of the i-th type.

The sum in equation (6) cannot be calculated in the general case without some assumptions on the properties of the molecule. The latter is unnecessary in evaluating the effect of the external field.

Substituting equations (5) and (3) into equation (2) and putting the concentrations C_i instead of the partial pressures P_i, we obtain after some transformations:

$$\frac{C_1 C_3^3}{C_2^2} = P^{-2} K_p(T) \exp\left\{ -\frac{2dE\overline{\cos v} + 2\beta_1 E^2 - 3\beta_3 E^2 - \beta_2 E^2}{kT} \right\}, \tag{7}$$

here $K_p(T) = \exp\left\{ -\frac{\sum_i \nu_i \chi_i(T)}{kT} \right\}$ is the equilibrium constant for the reaction of the synthesis of ammonia in the absence of an external field; C_1, C_2 and C_3 are the corresponding concentrations in the gas, of molecules of ammonia, nitrogen and hydrogen.

In practice it is always possible to choose the strength of the field and the temperature such as to fulfill the following inequality:

$$2dE\overline{\cos v} + 2\beta_1 E^2 > (3\beta_3 + \beta_2) E^2. \tag{8}$$

In the case of weak fields when it can be assumed that

$$\overline{\cos v} = \frac{Ed}{3kT}, \tag{9}$$

the inequality (8) can be written

$$\frac{2d^2}{3kT} + 2\beta_1 > 3\beta_2 + \beta_3.$$

In this case evaluation of the inequality shows that at $T = 10^{3°}$ the left part of the inequality is larger than the right part by more than ten times. This inequality will also be fulfilled at high field intensities when $\overline{\cos v}$ is given not by equation (9), but by the more accurate equation (4).

Thus, under these conditions, as can be seen from equation (7), the electric field shifts the equilibrium composition of the reaction to the side of a larger number of ammonia molecules. The shift will vary proportionally with the electric field.

Analogous considerations are applicable for any reaction where the initial compounds are nondipolar molecules and the products of the reaction are dipolar molecules.

The Artem Dnepropetrovsk Mining Institute

Received on March 23, 1956

LITERATURE CITED

[1] B. L. Timan, J. Exptl-Theoret. Phys. (USSR) 27, 5 (1954).

[2] L. Landau and E. Lifshits, Statistical Physics, 1951.*

* No reference to [2] appears in the original text – Publisher's note.

INVESTIGATION OF THE MECHANISM OF SYNTHESIS OF DIVINYL BY THE METHOD OF S. V. LEBEDEV USING RADIOACTIVE CARBON

Corresponding Member of the Academy of Sciences, USSR S. Z. Roginsky, O. M. Vinogradova, and N. P. Keier

Many different schemes have been proposed to explain the mechanism of the formation of divinyl from ethyl alcohol [1-6]. At present the scheme proposed by Yu. A. Gorin [4] and, independently of him, by M. Ya. Kagan et al [5] seems to be the best-grounded scheme yet. According to it the formation of divinyl from ethyl alcohol occurs in four stages:

1) $2C_2H_5OH \rightarrow 2CH_3CHO + 2H_2$

2) $2CH_3CHO \rightarrow CH_3 - CHOH - CH_2 - CHO \rightarrow CH_3 - CH = CH - CHO + H_2O$

3) $CH_3 - CH = CH - CHO + C_2H_5OH \rightarrow CH_3 - CH = CH - CH_2OH + CH_3CHO$

4) $CH_3 - CH = CH - CH_2OH \rightarrow CH_2 = CH - CH = CH_2 + H_2O$

The American scientists Quatlebaum, Toussaint and Dunn [6] also came to similar conclusions. However, they consider that divinyl is formed from the crotonic aldehyde in one stage through deoxygenation, which presupposes adsorption of the crotonic aldehyde in the enol form, redistribution of hydrogen among the adsorbed molecules of ethyl alcohol and crotonic aldehyde, and desorption of the latter as divinyl, leaving oxygen behind on the catalyst.

In the present work we attempted to clarify the stage mechanism of formation of divinyl from ethyl alcohol with the help of molecules labeled by radioactive carbon.

1. Reaction in the Adsorption Layer

First we studied the transformations of ethyl alcohol and aldehydes in the adsorption layer. For this purpose ethyl alcohol was adsorbed at room temperature on Lebedev's catalyst. Then after increasing the temperature to 500°, desorption of the volatile products of the reaction was performed. The volatile products were separated by vacuum distillation and identified by the dependence of their vapor pressure on temperature.

In this way it was shown that in the adsorption layer on Lebedev's catalyst, ethyl alcohol is transformed into ethylene and acetaldehyde and, in small quantities, into diethyl ether. Under the above conditions divinyl was not found.

An analogous investigation of the transformation of acetaldehyde showed that in the adsorption layer on Lebedev's catalyst, it transformed mainly into crotonic aldehyde and higher condensation products. Even at room temperatures formation of crotonic aldehyde could be observed. Simultaneously, ethylene and divinyl are produced in very small quantities.

Investigation of the transformation of crotonic aldehyde showed that it transformed into ethylene, divinyl and higher condensation products. Formation of an unimportant amount of acetaldehyde was also observed. Introduction into the adsorption layer of small amounts of ethyl alcohol during the investigation of the adsorption of the aldehydes, increased the yield of divinyl from acetaldehyde as well as from crotonic aldehyde.

The results given above point out the possibility of the following sequence of transformations in the adsorption layer: ethyl alcohol – acetaldehyde – crotonic aldehyde – divinyl. This substantiates the possibility that divinyl is formed according to the scheme of Gorin-Kagin, but does not prove that it is the only way.

2. Study of the Genetical Relations with the Help of Labeled Molecules

It is possible to determine the mutual transformations of various substances in the reaction and the degrees of their participation in the formation of divinyl by adding, during the synthesis to the initial ethyl alcohol, substances labeled with C^{14}, whose role in the process is of interest to us, and then studying the distribution of C^{14} among the reaction products. Such an approach allows us to determine the actual scheme for the formation of divinyl and to clarify the part played in its synthesis by other processes.

The investigation was performed in a small dynamical apparatus. The products of the synthesis: ethyl alcohol, acetaldehyde, ethylene, diethyl ether and divinyl were separated and analyzed for their C^{14} content.

3. Isotopic Exchange Between the Alcohol and the Aldehyde

Investigations using mixtures of labeled ethyl alcohol with acetaldehyde showed that in the condensate obtained as a result of the synthesis, ethyl alcohol, acetaldehyde and divinyl all had very nearly the same specific radioactivities. This value was considerably smaller than the specific radioactivity of the initial ethyl alcohol (Table 1).

In experiments performed using mixtures of labeled acetaldehyde with ethyl alcohol, we also obtained ethyl alcohol and acetaldehyde with similar specific radioactivities which were smaller than the specific radioactivity of the initial acetaldehyde.

The observed redistribution of radioactivity between the acetaldehyde and the ethyl alcohol on Lebedev's catalyst is a consequence of the redistribution of hydrogen between these two molecules. This redistribution leads to an apparent redistribution of radioactive carbon. This is an interesting example of intermolecular isotopic exchange of one element, as a direct consequence of a usual chemical reaction with displacement of another element.

TABLE 1

Initial radioactive substance and its specific radioactivity in impulses per 1 mg of $BaCO_3$	Specific radioactivity of the reaction products		Redistribution of H, %
	Ethyl alcohol	Acetaldehyde	
Ethyl alcohol 469	373	320	98
Ethyl alcohol 272	214	206	98
Acetaldehyde 280	47	45	100

The equality of the specific radioactivities of acetaldehyde, ethyl alcohol and divinyl obtained in the above experiments indicates that this process occurs at a far larger rate than the rate of formation of divinyl. Divinyl is formed from the mixture of ethyl alcohol and the aldehyde where the isotopic carbon exchange through redistribution of hydrogen has been already factually completed.

The rate of this process can be conditionally characterized by percent of redistribution of hydrogen, expressing the ratio of the specific radioactivity of the ethyl alcohol obtained to the specific radioactivity which would be obtained on uniform distribution of all radioactive carbon among all carbon-containing substances.

Investigation of the redistribution of hydrogen at different temperatures showed that its rate drops rather slightly with decrease in temperature, remaining considerable at room temperature (Table 2). To clarify the mechanism of this process we investigated it on typically dehydrogenating (ZnO) and dehydrating (Al_2O_3) catalysts. It was found that on Al_2O_3 the redistribution of hydrogen occurs practically completely in the time during which only 23% of exchange occurs on the dehydrogenating catalyst (Table 2). This makes probable the

supposition that the process of redistribution of hydrogen does not have common stages with the process of dehydrogenating of ethyl alcohol. The redistribution of hydrogen takes place also without a catalyst but at a very small rate. Thus, in two months of standing it reached only 58%. In other words, Lebedev's catalyst at 21° accelerates the isotopic exchange between ethyl alcohol and acetaldehyde by approximately 1500 times.

TABLE 2

Catalyst	Temperature, °C	Time of Contact	Redistribution of H,%
Lebedev's	300	4-8 seconds	90
	200	"	83
	21	1 hour	60
Al_2O_3	390	4-8 seconds	98
ZnO	390	"	23
Without catalyst	21	24 hours	0*
	21	2 months	58*

* In liquid mixture of ethyl alcohol with marked acetaldehyde (10%).

The interaction between acetaldehyde and ethyl alcohol can serve as a model reaction for the interaction between other alcohols and aldehydes in Lebedev's process. Applied to the system crotonic aldehyde – ethyl alcohol, redistribution of hydrogen must unavoidably lead to the formation crotyl alcohol. This speaks in favor of the Gorin-Kagan scheme for the transformation of crotonic aldehyde into divinyl and does not agree with the mechanism of deoxygenation of Quatlebaum, Toussaint and Dunn. It is natural to think that if deoxygenation does take place in the system crotonic aldehyde – ethyl alcohol, then it also should occur in the system marked acetaldehyde – ethyl alcohol. This would lead to the formation of radioactive ethylene from the marked acetaldehyde, i.e., the redistribution of C^{14} between the aldehyde and the ethyl alcohol, which we observed experimentally, would not occur.

4. Investigation of the Role of Crotonic Aldehyde

Synthesis of divinyl from a mixture of ethyl alcohol with labeled crotonic aldehyde on Lebedev's catalyst leads to the formation of divinyl whose specific radioactivity is considerably smaller than the specific radioactivity of the initial crotonic aldehyde. The presence of radioactivity in divinyl shows that during the synthesis the crotonic aldehyde transforms into divinyl.

The smaller specific radioactivity of divinyl relative to the specific radioactivity of the initial crotonic aldehyde is a consequence of its dilution by nonradioactive divinyl formed from ethyl alcohol. The role of the crotonic aldehyde in the formation of the nonradioactive divinyl from ethyl alcohol could be clarified from the specific radioactivity of crotonic aldehyde obtained from the reaction products. However, we were not able to find crotonic aldehyde among the reaction products. This indicated that crotonic aldehyde is easily transformed on Lebedev's catalyst. Considering the results of experiments on the transformation of acetaldehyde in the adsorption layer it can be concluded that formation of crotonic aldehyde from acetaldehyde occurs at a large rate. This and also the fact that the rate of transformation of crotonic aldehyde into divinyl, calculated from the radioactivities, exceeds the rate of transformation of ethyl alcohol into divinyl, speak in favor of intermediary formation of crotonic aldehyde in obtaining divinyl from ethanol.

The investigation performed has shown that fundamentally the formation of divinyl occurs through condensation of the acetaldehyde to crotonic aldehyde, which in the presence of an excess of ethyl alcohol and as a result of redistribution of hydrogen, transforms into crotyl alcohol. Dehydration of the latter leads to the formation of divinyl. Application of labeled carbon atoms allowed a more careful study of the redistribution of hydrogen. This process occurs, apparently, through the formation and decomposition of intermediary complexes of molecules of alcohol and aldehyde.

Thus, the basic sequence of stages in the transformation scheme of Gorin-Kagan is substantiated. The nature of the participation in the process of the ether and the ethylene found among the reaction products, remains unexplained. Results pertaining to this problem were briefly treated in reference [7].

LITERATURE CITED

[1] I. I. Ostromyslensky, J. Russ. Phys. Chem. Soc. 47, 1494 (1915).

[2] S. V. Lebedev, J. Gen. Chem. 3, No. 6, 698 (1933).

[3] A. A. Balandin, Progr. Chem. 4, 1004 (1935).

[4] Yu. A. Gorin, J. Gen. Chem. 16, 283 (1946).

[5] M. Ya. Kagan, G. D. Lyubarsky and O. M. Podurovskaya, Bull. Acad. Sci. USSR, Div. Chem. Sci. 1947, No. 2, 173.

[6] W. Quatlebaum, W. Toussaint and I. Dunn, J. Am. Chem. Soc. 69, 593 (1947); H. Jones, E. Stanly and B. Corson, ibid., 71, 1822 (1949).

[7] O. M. Vinogradova, N. P. Keier and S. Z. Roginsky, Paper presented at the All-Union Conference on Application of Isotopes to Catalysis (Moscow, 1956).

Physical Chemistry Institute of
the Academy of Sciences, USSR

Received September 20, 1956

PROCEEDINGS OF THE ACADEMY OF SCIENCES OF THE USSR

Section: PHYSICAL CHEMISTRY

Volume 112, Issues 1-6

January-February, 1957

TABLE OF CONTENTS

	Page	Russian Issue No.	Russian Page
1. The Limits of Stable Propagation of Flames in Gases Under Changing Pressures. D. I. Abugov	1	1	86
2. Dependence of Absorption Spectra of Solutions and Isomorphous Alum Crystals on Their Chromium Content. I. I. Antipova-Karataeva	7	1	90
3. The Role of Intermediates in Complex Chain Reactions. N. S. Enikolopyan	11	1	93
4. Determination of the Zero Potential of Lead Dioxide Electrodes by the Method of Measuring the Hardness. D. I. Leikis and E. K. Venstrem	17	1	97
5. Diffusion Precipitation of Aerosols on a Streamlined Cylinder with a Small Capture Coefficient. G. L. Natanson	21	1	100
6. The Influence of Sulfur on the Interphase Tension at the Metal–Slag Boundary. S. I. Popel, O. A. Esin, G. F. Konovalov and N. S. Smirnov	27	1	104
7. The Formation of Nitric Oxide by the Adiabatic Compression of Combustible Mixtures. Yu. N. Ryabinin, A. M. Markevich, and I. I. Tamm	31	2	283
8. The Mechanism of Vulcanization in the Presence of 2-Mercaptobenzothiazole. B. A. Dogadkin, I. A. Tutorsky and D. M. Pevzner	35	3	449
9. An Approximation Method for Calculating the Surface Tension of Metals. S. N. Zadumkin	39	3	453
10. The Energy of Activation of the Elementary Reaction RO_2 + RH in the Oxidation of n-Decane. D. G. Knorre, Z. K. Maizus and N. M. Emanuel	45	3	457
11. An Electron Microscopic Investigation of the Structure of the Spheroidal Graphite in Cast Iron. E. A. Leontyev, V. M. Lukyanovich and B. S. Milman	51	3	461
12. The Adsorption of Vapors on the Surface of Gold. A. I. Sarakhov	55	3	464
13. The Problem of the Polymorphism of Di-Calcium Silicate. N. A. Toropov, B. V. Volkonsky and V. I. Sadkov	59	3	467
14. The Energy of Adsorption of Hydrocarbons on Graphite. N. N. Avgul and A. V. Kiselev	63	4	673
15. A Dynamic Method for Studying the Structures and the Specific Surfaces of Adsorbents. V. T. Bykov and O. E. Presnyakova	69	4	677
16. The Thermoelectrical Properties of the Silicides of Chromium. L. N. Guseva and B. I. Ovechkin	73	4	681
17. A Radiometric Study of the Chromatography of Di- and Trivalent Ions over the Interval of Concentrations from 10^{-1} to 10^{-9} N. S. Yu. Elovich and V. N. Prusakov	77	4	684

(continued on inside back cover)